

NCDOT
2013-10



Final Report

Performance Evaluation and Placement Analysis of W-beam Guardrails behind Curbs

Prepared By

Howie Fang
David C. Weggel
Ning Li
Matthew Gutowski
Ryan Baker
Emre Palta
Daniil Kuvila

The University of North Carolina at Charlotte
Department of Mechanical Engineering & Engineering Science
Charlotte, NC 28223-0001

December 15, 2014

Technical Report Documentation Page

1. Report No. FHWA/NC/2013-10	2. Government Accession No.	3. Recipient's Catalog No.	
4. Title and Subtitle Performance Evaluation and Placement Analysis of W-beam Guardrails behind Curbs		5. Report Date December 15, 2014	
		6. Performing Organization Code	
7. Author(s) Howie Fang, David C. Weggel, Ning Li, Matthew Gutowski, Ryan Baker, Emre Palta, Daniil Kuvila		8. Performing Organization Report No.	
9. Performing Organization Name and Address The University of North Carolina at Charlotte 9201 University City Boulevard Charlotte, NC 28223-0001		10. Work Unit No. (TRAIS)	
		11. Contract or Grant No.	
12. Sponsoring Agency Name and Address North Carolina Department of Transportation Research and Analysis Group 104 Fayetteville Street Raleigh, North Carolina 27601		13. Type of Report and Period Covered Final Report 08/16/2012 – 10/31/2014	
		14. Sponsoring Agency Code NCDOT 2013-10	
Supplementary Notes:			
16. Abstract <p><i>This report summarizes the research efforts of using finite element modeling and simulations to evaluate the performance of NCDOT W-beam guardrails behind curbs under MASH TL-2 impact conditions. A literature review is included on performance evaluation of W-beam guardrails as well as applications of finite element modeling and simulations in roadside safety research.</i></p> <p><i>The modeling and simulation work was conducted on three NCDOT W-beam guardrails (with placement heights of 27, 29, and 31 inches) placed at the curb face and at 12 feet from the curb face. The 29-inch guardrail was also evaluated at 6 feet from the curb face. The guardrails with 27-, 29-, and 31-inch placement heights were impacted by a 1996 Dodge Neon and a 2006 Ford F250 at 44 mph (70 km/hour) and at two impact angles (25° and 15°). The guardrails performance was determined by evaluating the vehicular responses based on MASH exit box criterion, MASH evaluation criterion F, exit angles, yaw, pitch, and roll angles, transverse displacements, and transverse velocities.</i></p> <p><i>The simulation results demonstrated the effectiveness of the 29- and 31-inch guardrails placed at 12 feet from the curb face under MASH TL-2 impact conditions. Under small angle vehicular impacts (i.e., 15°), the guardrails with 27-, 29-, and 31-inch placement heights were shown to be effective at all three placement locations in relation to the curb face. Finite element modeling and simulations were shown to be both effective and efficient and can be used to study crash scenarios that are difficult and/or extremely expensive to conduct with physical crash testing.</i></p>			
17. Key Words <i>W-beam; Median barrier; Barrier height; 27-inch; 29-inch; 31-inch; Roadside safety; Highway safety; Finite element method</i>		18. Distribution Statement	
19. Security Classif. (of this report) Unclassified	20. Security Classif. (of this page) Unclassified	21. No. of Pages 98	22. Price

Form DOT F 1700.7 (8-72)

Reproduction of completed page authorized

DISCLAIMER

The contents of this report reflect the views of the authors and not necessarily the views of the university. The authors are responsible for the facts and the accuracy of the data presented herein. The contents do not necessarily reflect the official views or policies of either the North Carolina Department of Transportation or the Federal Highway Administration. This report does not constitute a standard, specification, or regulation.

ACKNOWLEDGMENTS

This study was supported by the North Carolina Department of Transportation (NCDOT) under Project No. 2013-10. The authors would like to thank NCDOT personnel from the *Roadway Design Unit*, *Transportation Mobility & Safety*, *Highway Division 5*, *Project Services Unit*, *FHWA – NC Division*, and *Research and Development Unit* for the support and cooperation during the grant period.

EXECUTIVE SUMMARY

This report summarizes the research efforts of using finite element modeling and simulations to evaluate the performance of NCDOT W-beam guardrails behind curbs under MASH TL-2 impact conditions. A literature review is included on performance evaluation of W-beam guardrails as well as applications of finite element modeling and simulations in roadside safety research.

The modeling and simulation work was conducted on three NCDOT W-beam guardrails (the 27-, 29-, and 31-inch guardrails) placed at the curb face and at 12 feet from the curb face. The 29-inch guardrail was also evaluated at 6 feet from the curb face. The guardrails with 27-, 29-, and 31-inch placement heights were impacted by a 1996 Dodge Neon and a 2006 Ford F250 at 44 mph (70 km/hour) and at two impact angles (25° and 15°). The guardrails performance was determined by evaluating the vehicular responses based on MASH exit box criterion, MASH evaluation criterion F, exit angles, yaw, pitch, and roll angles, transverse displacements, and transverse velocities.

The simulation results demonstrated the effectiveness of the 29- and 31-inch guardrails placed at 12 feet from the curb face under MASH TL-2 impact conditions. Under small angle vehicular impacts (i.e., 15°), the guardrails with 27-, 29-, and 31-inch placement heights were shown to be effective at all three placement locations in relation to the curb face. Finite element modeling and simulations were shown to be both effective and efficient and can be used to study crash scenarios that are difficult and/or extremely expensive to conduct with physical crash testing.

TABLE OF CONTENTS

Title Page	i
Technical Report Documentation Page	ii
Disclaimer	iii
Acknowledgments	iv
Executive Summary	v
Table of Contents	vi
List of Tables	vii
List of Figures	viii
1. Introduction	1
1.1 Background	1
1.2 Research Objectives and Tasks	3
2. Literature Review	7
2.1 Performance Evaluation of W-beam Guardrails	7
2.2 Performance of Safety Barriers behind Curbs	15
2.3 Crash Modeling and Simulations	16
3. Finite Element Modeling of Vehicles and W-beam Guardrails	23
3.1 FE Models of a Passenger Car and Pickup Truck	23
3.2 FE Model of the W-beam Guardrails	25
3.3 Simulation Setup	26
4. Simulation Results and Analysis	28
4.1 Case 1: Guardrails Placed at the Curb Face	29
4.2 Case 2: Guardrails Placed at 12-ft from the Curb Face	49
4.3 Case 3: Guardrails Placed at 6-ft from the Curb Face	68
4.4 Comparison of Guardrail Performance at Different Locations	75
5. Findings and Conclusions	78
6. Recommendations	80
7. Implementation and Technology Transfer Plan	81
References	82

List of Tables

Table 3.1: Specifications of the two test vehicles used in crash simulations

Table 3.2: Simulation conditions for all cases

Table 4.1: The exit box criterion defined in MASH

Table 4.2: Exit box dimensions for the test vehicles of this project

Table 4.3: Simulation results of Case 1 (guardrails placed at the curb face)

Table 4.4: Simulation results of Case 2 (guardrails placed at 12 feet from the curb face)

Table 4.5: Simulation results of Case 3 (guardrails placed at 6 feet from the curb face)

Table 4.6: Vehicle redirection characteristics of the 27-inch guardrail

Table 4.7: Vehicle redirection characteristics of the 29-inch guardrail

Table 4.8: Vehicle redirection characteristics of the 31-inch guardrail

List of Figures

Fig. 1.1: A W-beam guardrail behind a curb.

Fig. 1.2: NCDOT 2'-6" curb and gutter (NCDOT Standard Drawing 846.01).

Fig. 1.3: Placement of guardrail at face of curb (NCDOT Standard Drawing 862.01).

Fig. 1.4: Placement of guardrail at 12-*ft* offset from the curb face (NCDOT Standard Drawing 862.01).

Fig. 1.5: Evaluation of guardrails behind curbs at length-of-need sections.

Fig. 1.6: FE models of a G4(1S) guardrail, a small passenger car, and a large pickup truck.

Fig. 1.7: FE model of a W-beam guardrail placed at the curb face and impacted by a Ford F250.

Fig. 1.8: Performance evaluation of a guardrail at the curb face under MASH TL-2 conditions.

Fig. 1.9: Performance evaluation of a guardrail at 12 feet from the curb face under MASH TL-2 conditions.

Fig. 1.10: Definition of vehicle responses.

Fig. 3.1: FE models of the two vehicles used in crash simulations.

Fig. 3.2: FE models of the soil block around a post.

Fig. 3.3: Short-bolts on a guardrail splice.

Fig. 3.4: FE model of a W-beam guardrail placed at curb face and impacted by a Ford F250.

Fig. 3.5: FE model of a W-beam guardrail placed at 12 feet from curb face and impacted by a Ford F250.

Fig. 4.1: The exit-box criterion in MASH.

Fig. 4.2: A Dodge Neon impacting the 27-inch guardrail at the curb face.

Fig. 4.3: Yaw, pitch, and roll angles of Dodge Neon impacting the 27-inch guardrail at the curb face.

Fig. 4.4: Permanent deformation of the 27-inch guardrail at the curb face and impacted by a Dodge Neon.

Fig. 4.5: Simulations of Dodge Neon impacting the 27-inch guardrail at the curb face.

Fig. 4.6: Transverse displacements and velocities of the Dodge Neon impacting the 27-inch guardrail at the curb face at 44 mph (70 km/hour) and 25°.

Fig. 4.7: Transverse displacements and velocities of the Dodge Neon impacting the 27-inch guardrail at the curb face at 44 mph (70 km/hour) and 15°.

- Fig. 4.8: A Ford F250 impacting the 27-inch guardrail at the curb face.
- Fig. 4.9: Yaw, pitch, and roll angles of Ford F250 impacting the 27-inch guardrail at the curb face.
- Fig. 4.10: Permanent deformation of 27-inch guardrail at the curb face and impacted by a Ford F250.
- Fig. 4.11: Simulations of Ford F250 impacting the 27-inch guardrail at the curb face.
- Fig. 4.12: Transverse displacements and velocities of the Ford F250 impacting the 27-inch guardrail at the curb face at 44 mph (70 km/hour) and 25°.
- Fig. 4.13: Transverse displacements and velocities of the Ford F250 impacting the 27-inch guardrail at the curb face at 44 mph (70 km/hour) and 15°.
- Fig. 4.14: A Dodge Neon impacting the 29-inch guardrail at the curb face.
- Fig. 4.15: Yaw, pitch, and roll angles of Dodge Neon impacting the 29-inch guardrail at the curb face.
- Fig. 4.16: Permanent deformation of the 29-inch guardrail at the curb face and impacted by a Dodge Neon.
- Fig. 4.17: Simulations of Dodge Neon impacting the 29-inch guardrail at the curb face.
- Fig. 4.18: Transverse displacements and velocities of the Dodge Neon impacting the 29-inch guardrail at the curb face at 44 mph (70 km/hour) and 25°.
- Fig. 4.19: Transverse displacements and velocities of the Dodge Neon impacting the 29-inch guardrail at the curb face at 44 mph (70 km/hour) and 15°.
- Fig. 4.20: A Ford F250 impacting the 29-inch guardrail at face of curb.
- Fig. 4.21: Yaw, pitch, and roll angles of Ford F250 impacting the 29-inch guardrail at face of curb.
- Fig. 4.22: Permanent deformation of the 29-inch guardrail at the curb face and impacted by a Ford F250.
- Fig. 4.23: Simulations of Ford F250 impacting the 29-inch guardrail at the curb face.
- Fig. 4.24: Transverse displacements and velocities of the Ford F250 impacting the 29-inch guardrail at the curb face at 44 mph (70 km/hour) and 25°.
- Fig. 4.25: Transverse displacements and velocities of the Ford F250 impacting the 29-inch guardrail at the curb face at 44 mph (70 km/hour) and 15°.
- Fig. 4.26: A Dodge Neon impacting the 31-inch guardrail at face of curb.
- Fig. 4.27: Yaw, pitch, and roll angles of Dodge Neon impacting the 31-inch guardrail at the curb face.
- Fig. 4.28: Permanent deformation of the 31-inch guardrail at the curb face and impacted by a Dodge Neon.
- Fig. 4.29: Simulations of Dodge Neon impacting the 31-inch guardrail at the curb face.

- Fig. 4.30: Transverse displacements and velocities of the Dodge Neon impacting the 31-inch guardrail at the curb face at 44 mph (70 km/hour) and 25°.
- Fig. 4.31: Transverse displacements and velocities of the Dodge Neon impacting the 31-inch guardrail at the curb face at 44 mph (70 km/hour) and 15°.
- Fig. 4.32: A Ford F250 impacting the 31-inch guardrail at the curb face.
- Fig. 4.33: Yaw, pitch, and roll angles of Ford F250 impacting the 31-inch guardrail at the curb face.
- Fig. 4.34: Permanent deformation of the 31-inch guardrail at the curb face and impacted by a Ford F250.
- Fig. 4.35: Simulations of Ford F250 impacting the 31-inch guardrail at the curb face.
- Fig. 4.36: Transverse displacements and velocities of the Ford F250 impacting the 31-inch guardrail at the curb face at 44 mph (70 km/hour) and 25°.
- Fig. 4.37: Transverse displacements and velocities of the Ford F250 impacting the 31-inch guardrail at the curb face at 44 mph (70 km/hour) and 15°.
- Fig. 4.38: A Dodge Neon impacting the 27-inch guardrail at 12 feet from the curb face.
- Fig. 4.39: Yaw, pitch, and roll angles of Dodge Neon impacting 27-inch guardrail at 12 feet from the curb face.
- Fig. 4.40: Permanent deformation of the 27-inch guardrail at 12 feet from the curb face and impacted by a Dodge Neon.
- Fig. 4.41: Simulations of Dodge Neon impacting the 27-inch guardrail at 12 feet from the curb face.
- Fig. 4.42: Transverse displacements and velocities of the Dodge Neon impacting the 27-inch guardrail at 12 feet from the curb face at 44 mph (70 km/hour) and 25°.
- Fig. 4.43: Transverse displacements and velocities of the Dodge Neon impacting the 27-inch guardrail at 12 feet from the curb face at 44 mph (70 km/hour) and 15°.
- Fig. 4.44: A Ford F250 impacting the 27-inch guardrail at 12 feet from the curb face.
- Fig. 4.45: Yaw, pitch, and roll angles of Ford F250 impacting 27-inch guardrail at 12 feet from the curb face.
- Fig. 4.46: Permanent deformation of the 27-inch guardrail at 12 feet from the curb face and impacted by a Ford F250.
- Fig. 4.47: Simulations of Ford F250 impacting the 27-inch guardrail at 12 feet from the curb face.
- Fig. 4.48: Transverse displacements and velocities of the Ford F250 impacting the 27-inch guardrail at 12 feet from the curb face at 44 mph (70 km/hour) and 25°.
- Fig. 4.49: Transverse displacements and velocities of the Ford F250 impacting the 27-inch guardrail at 12 feet from the curb face at 44 mph (70 km/hour) and 15°.
- Fig. 4.50: A Dodge Neon impacting the 29-inch guardrail at 12 feet from the curb face.

- Fig. 4.51: Yaw, pitch, and roll angles of Dodge Neon impacting 29-inch guardrail at 12 feet from the curb face.
- Fig. 4.52: Permanent deformation of the 29-inch guardrail at 12 feet from the curb face and impacted by a Dodge Neon.
- Fig. 4.53: Simulations of Dodge Neon impacting the 29-inch guardrail at 12 feet from the curb face.
- Fig. 4.54: Transverse displacements and velocities of the Dodge Neon impacting the 29-inch guardrail at 12 feet from the curb face at 44 mph (70 km/hour) and 25°.
- Fig. 4.55: Transverse displacements and velocities of the Dodge Neon impacting the 29-inch guardrail at 12 feet from the curb face at 44 mph (70 km/hour) and 15°.
- Fig. 4.56: A Ford F250 impacting the 29-inch guardrail at 12 feet from the curb face.
- Fig. 4.57: Yaw, pitch, and roll angles of Ford F250 impacting 29-inch guardrail at 12 feet from the curb face.
- Fig. 4.58: Permanent deformation of the 29-inch guardrail at 12 feet from the curb face and impacted by a Ford F250.
- Fig. 4.59: Simulations of Ford F250 impacting the 29-inch guardrail at 12 feet from the curb face.
- Fig. 4.60: Transverse displacements and velocities of the Ford F250 impacting the 29-inch guardrail at 12 feet from the curb face at 44 mph (70 km/hour) and 25°.
- Fig. 4.61: Transverse displacements and velocities of the Ford F250 impacting the 29-inch guardrail at 12 feet from the curb face at 44 mph (70 km/hour) and 15°.
- Fig. 4.62: A Dodge Neon impacting the 31-inch guardrail at 12 feet from the curb face.
- Fig. 4.63: Yaw, pitch, and roll angles of Dodge Neon impacting 31-inch guardrail at 12 feet from the curb face.
- Fig. 4.64: Permanent deformation of the 31-inch guardrail at 12 feet from the curb face and impacted by a Dodge Neon.
- Fig. 4.65: Simulations of Dodge Neon impacting the 31-inch guardrail at 12 feet from the curb face.
- Fig. 4.66: Transverse displacements and velocities of the Dodge Neon impacting the 31-inch guardrail at 12 feet from the curb face at 44 mph (70 km/hour) and 25°.
- Fig. 4.67: Transverse displacements and velocities of the Dodge Neon impacting the 31-inch guardrail at 12 feet from the curb face at 44 mph (70 km/hour) and 15°.
- Fig. 4.68: A Ford F250 impacting the 31-inch guardrail at 12 feet from the curb face.
- Fig. 4.69: Yaw, pitch, and roll angles of Ford F250 impacting 31-inch guardrail at 12 feet from the curb face.
- Fig. 4.70: Permanent deformation of the 31-inch guardrail at 12 feet from the curb face and impacted by a Ford F250.

Fig. 4.71: Simulations of Ford F250 impacting the 31-inch guardrail at 12 feet from the curb face.

Fig. 4.72: Transverse displacements and velocities of the Ford F250 impacting the 31-inch guardrail at 12 feet from the curb face at 44 mph (70 km/hour) and 25°.

Fig. 4.73: Transverse displacements and velocities of the Ford F250 impacting the 31-inch guardrail at 12 feet from the curb face at 44 mph (70 km/hour) and 15°.

Fig. 4.74: A Dodge Neon impacting the 29-inch guardrail at 6 feet from the curb face.

Fig. 4.75: Yaw, pitch, and roll angles of Dodge Neon impacting 29-inch guardrail at 6 feet from the curb face.

Fig. 4.76: Permanent deformation of the 29-inch guardrail at 6 feet from the curb face and impacted by a Dodge Neon.

Fig. 4.77: Simulations of Dodge Neon impacting the 29-inch guardrail at 6 feet from the curb face.

Fig. 4.78: Transverse displacements and velocities of the Dodge Neon impacting the 29-inch guardrail at 6 feet from the curb face at 44 mph (70 km/hour) and 25°.

Fig. 4.79: Transverse displacements and velocities of the Dodge Neon impacting the 29-inch guardrail at 6 feet from the curb face at 44 mph (70 km/hour) and 15°.

Fig. 4.80: A Ford F250 impacting the 29-inch guardrail at 12 feet from the curb face.

Fig. 4.81: Yaw, pitch, and roll angles of Ford F250 impacting 29-inch guardrail at 6 feet from the curb face.

Fig. 4.82: Permanent deformation of the 29-inch guardrail at 6 feet from the curb face and impacted by a Ford F250.

Fig. 4.83: Simulations of Ford F250 impacting the 29-inch guardrail at 6 feet from the curb face.

Fig. 4.84: Transverse displacements and velocities of the Ford F250 impacting the 29-inch guardrail at 6 feet from the curb face at 44 mph (70 km/hour) and 25°.

Fig. 4.85: Transverse displacements and velocities of the Ford F250 impacting the 29-inch guardrail at 6 feet from the curb face at 44 mph (70 km/hour) and 15°.

1. Introduction

Curbs are essentially obstructive structures that may cause vehicles to lose control upon striking and result in tripped rollovers. The use of curbs on high-speed highways is discouraged by the highway design policy of the American Association of State Highway and Transportation Officials (AASHTO). Despite the discouragement of their usage, curbs are often required or needed for restricted rights-of-way, drainage considerations, access control, delineation, etc. In many places, a barrier is installed in combination with a curb, with W-beam guardrail being one of the most commonly used barriers. Figure 1.1 shows an example of a W-beam guardrail placed behind a highway curb.

W-beam guardrails are widely-used safety devices on U.S. highways; they are typically comprised of a steel, W-shaped rail mounted on steel or wood posts. Although many W-beam guardrails satisfy the safety requirements of NCHRP Report 350 or Manual for Assessing Safety Hardware (MASH) on flat surfaces, their performance in relation to their placement behind curbs remains an open issue. Since curbs can cause the striking vehicle to vault and experience suspension compression, the vehicle may override or under-ride the guardrail, depending on the guardrail's location and height as well as the (bumper) height of the vehicle. Appropriate design and installation of the guardrail should account for the curb's geometry and vehicle sizes in order to reduce the potentially hazardous results of curb crashes.



Fig. 1.1: A W-beam guardrail behind a curb.

1.1 Background

All barriers used on U.S. highways are designed according to the AASHTO Roadside Design Guide and must be tested to satisfy the safety criteria specified by MASH, which specifies more severe impact conditions than those in the old standard, NCHRP Report 350. For example, the two test vehicles in MASH Test Level 2 (TL-2) and Test Level 3 (TL-3) are changed to 1100C (1,100 kg or 2,420 *lb*) and 2270P (2,270 kg or 5,000 *lb*), representing 34% and 13.5% mass increases over those of NCHRP Report 350. In addition, the TL-2 impact angle, which was 20° in NCHRP Report 350, was changed to 25° in MASH. Although all in-service guardrails that passed the NCHRP Report 350 tests are allowed to continue to use, it is important to evaluate guardrail performance under MASH test conditions for retrofit projects and/or practical safety concerns.

The performance of W-beam guardrails behind curbs is different from those placed on flat terrain. First, curbs elevate the height of the W-beam rail relative to the impacting vehicle. Second, curbs change the height of the impacting vehicle due to suspension compression and vaulting. Furthermore, the location (or offset) of the guardrail relative to the curb face significantly affects the guardrail's performance, particularly when considering different vehicle sizes. To this end, performance evaluation of W-beam guardrails based on flat-terrain testing cannot be used directly to guide guardrail installation involving curbs.

North Carolina has two designs for guardrail placement at curbs and gutters. In both placements, a 6-inch curb (AASHTO Type B curb) is used along with a 2-foot gutter, as illustrated in Fig. 1.2. Figure 1.3 shows the first design of guardrail placement in which the face of the W-beam guardrail is flush with the curb face. In the second placement, the guardrail face has a 12-foot offset from the curb face, as shown in Fig. 1.4. To address some of the known issues of the 27-inch G4(1S) W-beam guardrail, NCDOT designed and investigated the use of 29- and 31-inch guardrails (with rail heights or placement heights of 29 and 31 inches, respectively, measured from grade to the rail top). Recently, NCDOT upgraded the design standard to adopt the 29-inch guardrail replacing the 27-inch guardrail in North Carolina. The performance of these guardrails placed behind curbs (see Figs. 3 and 4) has not been fully investigated and determined under MASH TL-2 conditions.

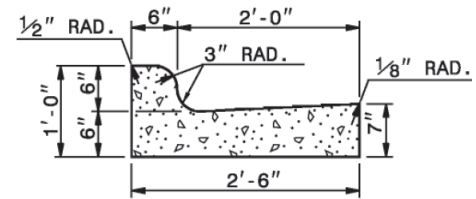


Fig. 1.2: NCDOT 2'-6" curb and gutter (NCDOT Standard Drawing 846.01).

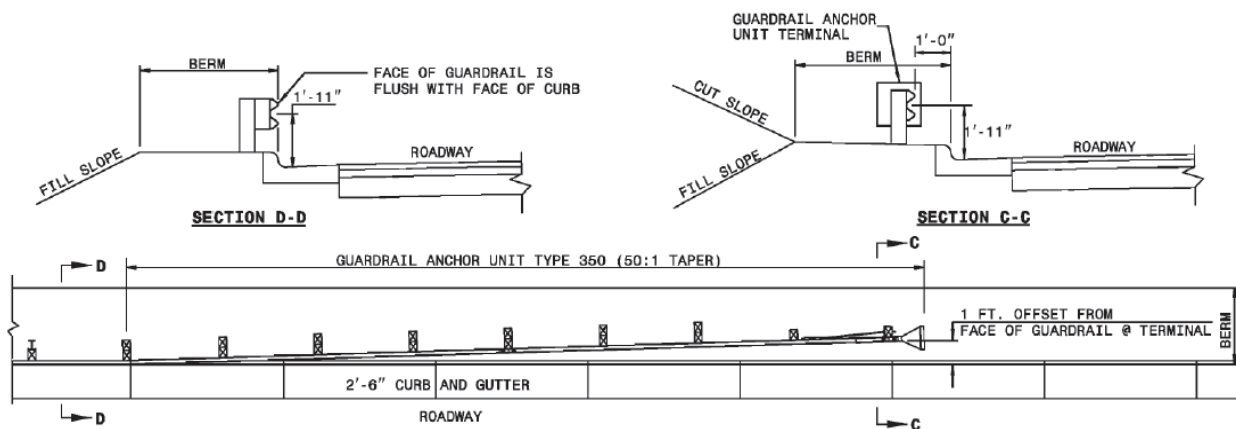


Fig. 1.3: Placement of guardrail at face of curb (NCDOT Standard Drawing 862.01).

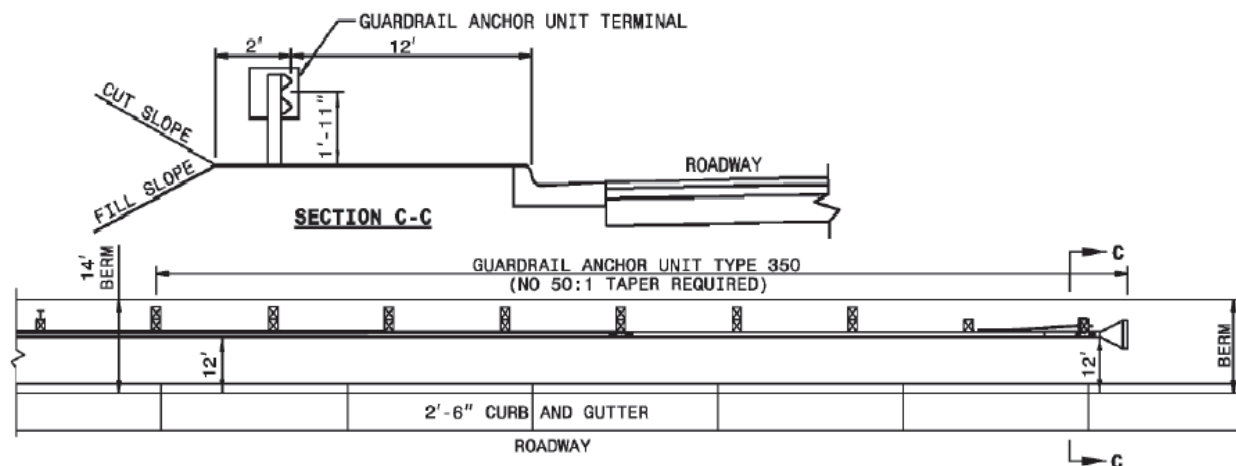
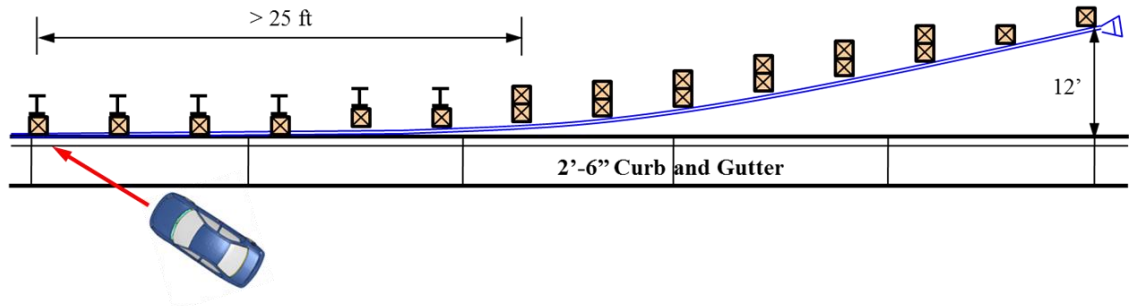
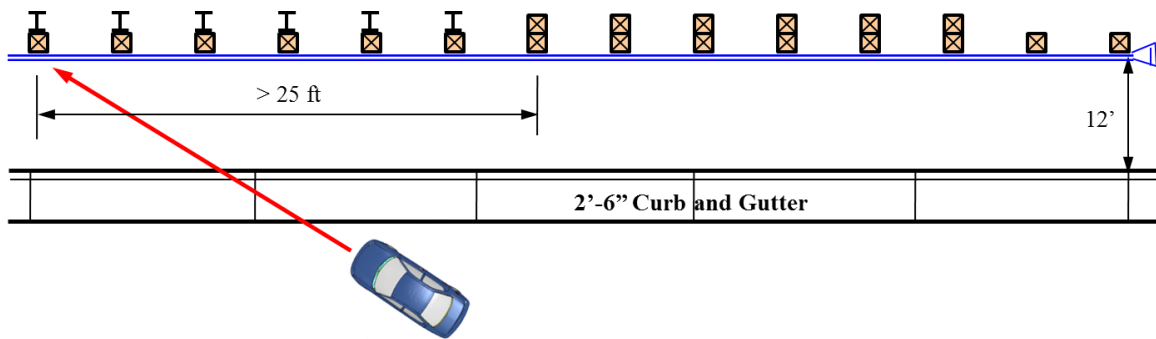


Fig. 1.4: Placement of guardrail at 12-ft offset from the curb face (NCDOT Standard Drawing 862.01).

The guardrail offset from the curb face for guardrails at placement heights of 27, 29, and 31 inches needs to be tested to provide guidance for new and retrofit installations. The length-of-need section of a guardrail is typically supported by steel posts, which are different from the wood posts at the terminals. Depending on the guardrail locations behind curb, the terminals are different (see Fig. 1.5). To minimize the effects of terminals on the length-of-need sections in the performance evaluation of guardrails at different locations, the initial impact point on the guardrail was set at least 25 feet (7.62 m) from the first wood post nearest to the steel post section, as schematically shown in Fig. 1.5.



a. Guardrail at the curb face



b. Guardrail at 12 feet from the curb face

Fig. 1.5: Evaluation of guardrails behind curbs at length-of-need sections.

1.2 Research Objectives and Tasks

In this study, full-scale finite element (FE) simulations were employed to evaluate the performance of W-beam guardrails at 27-, 29- and 31-inch placement heights behind the NCDOT 2'-6" curb and gutter with zero and 12-foot offsets. Simulations were performed to evaluate the NCDOT 29-inch guardrail at 6 feet from the curb face. The impact conditions were the same as those of MASH TL-2 conditions, except that the MASH TL-2 tests were conducted on flat terrain. Additionally, the guardrails with 27-, 29- and 31-inch placement heights were also evaluated at 15° angle impact, with all other test parameters the same as those of the 25° angle impacts. The simulation results were analyzed and compared to determine the effectiveness of guardrails at 27-, 29- and 31-inch placement heights and their optimum installation offsets. The research project had six major tasks as stated below.

Task 1: Literature Review and Data Collection

A comprehensive literature review was conducted on crash testing and modeling and simulations that were related, in particular, to guardrails and curbs to assist with model validation and crash simulations.

Task 2: FE Model Development and Validation

In this task, the FE models of the three W-beam guardrails (rail heights: 27, 29 and 31 inches) were created for crash simulations. The model of the 27-inch G4(1S) guardrail was available from a previous project and the models of the 29- and 31-inch guardrails were created based on the 27-inch guardrail model. Figure 1.6 shows the FE models of a G4(1S) guardrail, a small passenger car (1,090 kg or 2,400 lb), and a pickup truck (2,499 kg or 5,504 lb). These models will be used in the simulation work of this project.

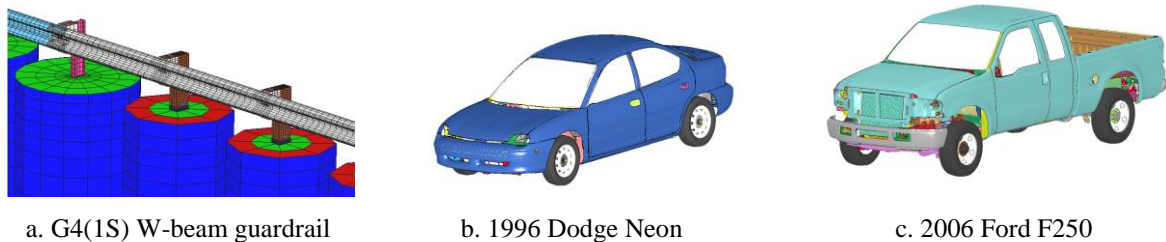


Fig. 1.6: FE models of a G4(1S) guardrail, a small passenger car, and a large pickup truck.

The FE model of the 6-inch curb along with fill slope, berm, gutter, and roadway were created based on NCDOT standard designs. Figure 1.7 shows one of the simulation models in which the W-beam guardrail was placed at the curb face and impacted by a 2006 Ford F250. All of the FE models were verified based on NCDOT designs and validated using available simulation results and/or test data from literature.

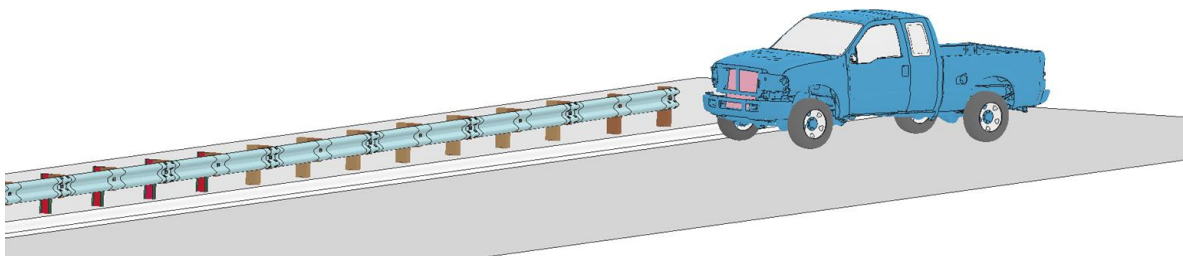


Fig. 1.7: FE model of a W-beam guardrail placed at the curb face and impacted by a Ford F250.

Task 3: Performance Evaluation of 27-inch W-beam Guardrail

In this task, the 27-inch W-beam guardrail was evaluated at two locations, at the curb face and at 12 feet from the curb face, under impacts of a small passenger car and a large pickup truck. The impact speed was 44 mph (70 km/hr) and the impact angle was 25° for both vehicles, same as the MASH TL-2 conditions. In addition, the guardrail was also evaluated at

an impact speed of 44 mph (70 km/hr) and an impact angle of 15° for both vehicles. Figures 1.8 and 1.9 illustrate the simulation configurations for the guardrail placed at the curb face and at 12 feet from the curb face, respectively. In all of these simulations, the vehicle started on the roadway and ran off the travel lane at the prescribed speed and angle towards the curb.

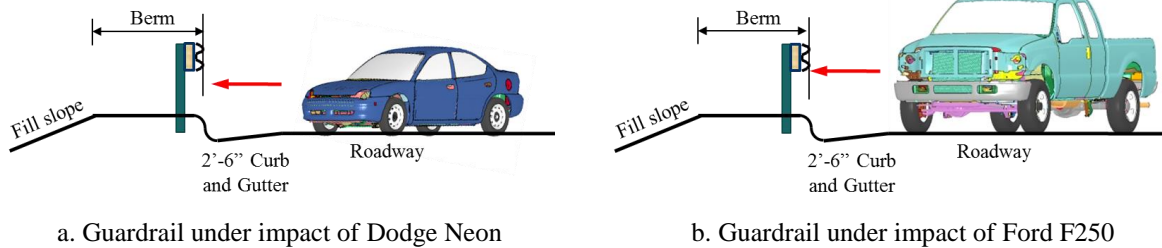


Fig. 1.8: Performance evaluation of a guardrail at the curb face under MASH TL-2 conditions.

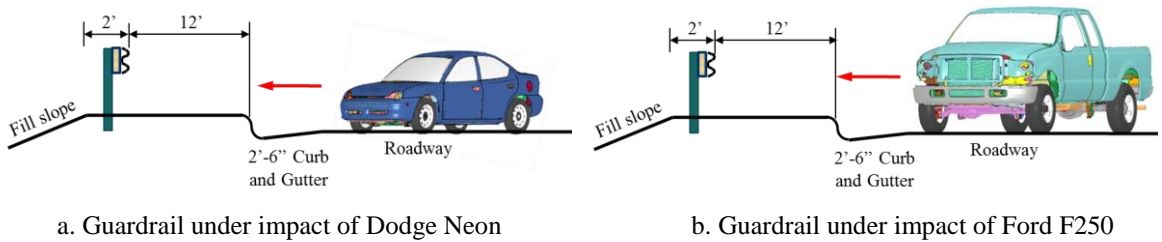


Fig. 1.9: Performance evaluation of a guardrail at 12 feet from the curb face under MASH TL-2 conditions.

The vehicle's responses in terms of redirection, rollover, lateral displacements, and velocities were analyzed to determine the effectiveness of the 27-inch guardrail at the curb face and at a 12-foot offset. In evaluating the vehicle's responses, the exit box criterion specified by MASH was adopted. For the guardrail to pass the crash tests, MASH also requires that the maximum roll and pitch angles of the impacting vehicle do not exceed 75 degrees. Figure 1.10 shows the definition of the three rotational responses (roll, pitch, and yaw) along with the corresponding translational responses (surge, sway, and heave). The time histories of the three response parameters, i.e., roll, pitch, and yaw angles, were recorded for the entire period of simulations. The maximum roll and pitch angles were extracted and compared with the MASH threshold values. In addition to the above mentioned MASH evaluation criteria, the time histories of the vehicle's lateral displacements and velocities were also examined for performance evaluation. The effectiveness of the 27-in guardrail was determined based on analyses of simulation results for both small and large vehicles. The performance of the 27-inch guardrail was compared at different locations and also compared with guardrails with 29- and 31-inch placement heights at the same locations.

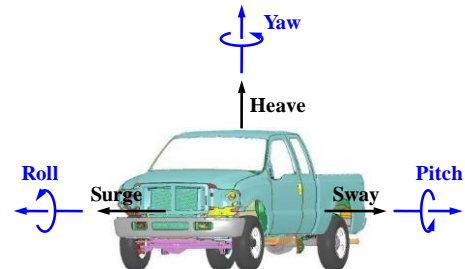


Fig. 1.10: Definition of vehicle responses.

Task 4: Performance Evaluation of 29-inch W-beam Guardrail

In this task, the 29-inch W-beam guardrail at the face of curb and at 12-foot offset from the curb face was evaluated under the same conditions as those for the 27-inch guardrail in Task 3. In addition, the 29-inch guardrail was also evaluated when placed at 6 feet from the curb face and under the same impacts as those at 12 feet from the curb face. The performance of the 29-inch guardrail was compared at different locations and also compared with guardrails at 27- and 31-inch placement heights at the same locations.

Task 5: Performance Evaluation of 31-inch W-beam Guardrails

The 31-inch W-beam guardrail was evaluated at two locations, at the curb face and at 12 feet from the curb face. The impact conditions and evaluations were the same as those for the 27-inch guardrail in Task 3. The performance of the 31-inch guardrail was compared at different locations and also compared with guardrails at 27- and 29-inch placement heights at the same locations.

Task 6: Recommended Guideline for Guardrail Installation behind Curbs

In this task, the FE simulation results of the three guardrails at the face of curb, at 6-foot offset, and at 12-foot offset behind the curb were analyzed. Based on the analyses, the offset from the curb face where the guardrail had the best performance at each of the three placement heights (i.e., 27, 29, and 31 inches) was determined and recommended as guidance for new and retrofit installations.

Task 7: Final Report

This final report provides a comprehensive summary of research activities, findings, and outcomes for this project. It synthesizes literature review, FE modeling efforts, simulation results, and the performance evaluation of the 27-, 29- and 31-inch W-beam guardrails behind curbs. The final report also includes recommended guidance on guardrail offsets from the face of curb for installing the guardrails at 27-, 29- and 31-inch placement heights.

2. Literature Review

Median barriers have been developed and used on U.S. highway for decades. Presently, the W-beam guardrails and cable barriers are widely used across the U.S. In this section, we provide a comprehensive summary of studies related to W-beams guardrail, CMBs, and other barrier systems. The topics cover performance evaluation (in-service and crash testing) and the application of FE modeling and simulations to highway safety research.

2.1 Performance Evaluation of Median Barriers

In the early 1960's, New York State pioneered the development of weak-post barrier systems through analytical models and full-scale vehicle crash testing. In 1965 the state guardrail and median barrier standards were changed to include only weak-post barriers. In the early 1970's, a study by Zweden and Bryden (1977) was performed to evaluate the field performance of the older strong-post barriers and newly-developed weak-post barriers based on New York State accident data collected from 1967 to 1970. Statistical analysis was performed to compare the performance of the investigated barriers based on occupant injury, vehicular responses, and after impact maintenance. This study generated a number of significant conclusions on the performance of weak- and strong-post barriers. Although there was no significant difference in fatality rates between the two barriers, weak-post barriers exhibited a combined fatality/serious injury rate significantly lower than that for strong-post barriers. The resulting occupant injury appeared to be linked to barrier stiffness since the two barriers (both strong and weak post versions) had lower injury severity rates, while the stiffer median barriers had the highest injury rates. With respect to barrier penetration, the weak-post barriers demonstrated a lower penetration rate than the strong-post barriers (with the exception of the W-beam), which may be due to the lack of consistency between early strong-post barrier designs. The study also indicated that barrier penetrations for the weak-post systems typically resulted from a low rail height. Barrier end terminals (first or last 50 feet of the barrier) were observed to have higher penetration rates than their midsection counterparts and resulted in higher serious injury rates. Barrier damage was linked to their stiffness; however, weak-post barriers on average were less expensive to repair than strong-post barriers despite the former's longer damage lengths.

An analysis performed in the 1970s indicated that most guardrails do not perform well when placed on 1:6 or steeper slopes. Since that time, the vehicle fleet has changed dramatically with a significant increase in the popularity of light trucks and sport utility vehicles. In addition, there has been a significant change in the design of roadside barriers in recent decades. It is unclear how these changes affect the behavior of longitudinal barriers placed on slopes. Information from the Fatality Analysis Reporting System (FARS) database of the National Highway Traffic Safety Administration (NHTSA) indicated that some cross-median crashes have occurred where median barriers were in place. A full-scale crash test also showed that a passenger vehicle could penetrate a cable barrier on the backside of a depressed median.

In the early 1980's, significant changes in vehicle designs led to a large increase in the number of smaller and lighter vehicles on highways. A study (Hiss and Bryden 1992) was initiated in 1983 by the New York State DOT to determine how impact severity on traffic

barriers was affected by vehicle sizes and weights, barrier types and mounting heights, and roadway features. Several conclusions were drawn regarding the performance of cable, W-beam, and box-beam guardrails. For cable and W-beam median barriers, however, the sample sizes were too small to assess their performance due to their limited use and exposure to possible accidents.

Ross et al. (1984) investigated the impact performance of longitudinal barriers when placed on sloped terrain using both crash tests and the highway vehicle object simulation model (HVOSM) computer program. In the study, they determined typical conditions to place longitudinal barriers on sloped terrain and evaluated the impact behavior of widely used barrier systems. Guidelines were developed for the selection and placement of barriers on sloped terrain. It was found from the study that W-beam and Thrie-beam barriers were more sensitive to the effects of sloped terrain than cable barriers.

In the study conducted by Ross et al. (1993), uniform procedures were developed for evaluating the safety performance of candidate roadside hardware, including longitudinal barriers, crash cushions, breakaway supports, truck-mounted attenuators, and work zone traffic control devices. The report from this study, the NCHRP Report 350, has been adopted as the standard guideline for evaluating the safety performance of roadside safety devices. The evaluation of devices is facilitated through three main criteria: 1) structural adequacy; 2) occupant risk; and 3) post-impact trajectory. Structural adequacy refers to how well the device performs its intended task (i.e. a guardrail preventing a vehicle from striking a shielded object). The occupant risk criteria attempts to quantify the potential for severe occupant injury. The post-impact vehicle trajectory ensures that the device will not cause subsequent harm (i.e. a vehicle being redirected back into traffic). The guideline recognizes the infinite number of roadside hardware installations and crash configurations; therefore, standardized installation configurations and practical worst-case impact scenarios are used to provide a basis of comparing the performance of similar devices. Of particular note is the multi-service level concept that provides six different test levels to allow for more or less stringent performance evaluation (ideally depending on the ultimate usage/placement of the hardware).

With respect to cross-median crashes, the NCHRP Report 350 is the standard by which median barriers are tested. Although the report specifies six different test levels, the warrants for devices meeting an individual test level is outside the scope of the document and left to the judgment of the transportation agency implementing the hardware. Generally, however, devices tested to the lower test levels (1 and 2) are used on lower volume, lower speed roadways, while devices tested to higher levels (3 to 6) are typically used on larger volume, higher speed roadways. Note that the 2000P, 2000-kg (4,409-pound), test vehicle is used to evaluate the strength and redirecting capabilities of longitudinal barriers up to and including test level 3. All impacts are performed at 25° and at 50, 70, and 100 km/hour for test levels 1, 2 and 3, respectively.

In the NCHRP Project 22-14, "Improvement of the Procedures for the Safety Performance Evaluation of Roadside Features," updates were incorporated to the NCHRP Report 350 based on assessments at TL-3 conditions, which was the basic level used for devices on the

National Highway System (NHS). In the report published by Mak and Bligh (2002), the effects of higher impact speeds and additional impact angles were considered for Test Level 3. These additional parameters were considered due to the fact that a number of states have changed maximum speed limits on some of their highways to 121 km/hour (75 mph) and most crashes occurring at an impact angle of 25° often cause an evaluation of the stability of the test vehicle instead of containment capability. The report determined that increasing the test impact speed to 110 km/hour (68.4 mph) would have significant effects on many of the existing roadside safety devices. Although some barriers could be modified to accommodate the higher impact speeds with minor modifications, other barriers would require major modifications. Due to other design constraints, some barriers may not be able to accommodate the higher impact speed regardless. Increasing the impact speed could result in a whole new generation of roadside safety hardware. In return, the higher impact speed would only cover an additional 2.84% of the crashes, increasing the percentage of crashes with impact speeds equal to or less than the design test speed from about 90% to 92.7%. The reduction of the impact angle to 20° from 25° poses a number of arguments including the possibility for existing W-beam guardrail systems having difficulty containing vehicles at the higher impact speeds. However, it should be emphasized that the selection on impact conditions is more of a policy decision than a technical issue to be resolved in the update of NCHRP Report 350 guidelines.

In the early 1990's, the Traffic Engineering Branch of NCDOT conducted a study (Lynch et al. 1993) of accidents on North Carolina's interstate highways in which vehicles crossed the median and entered the opposing travel lanes. The study analyzed accidents that occurred during the time period from April 1, 1988 through October 31, 1991. The objectives of this study were to identify interstate locations with unusually high cross-median accidents, to determine possible safety improvements, to develop a priority listing of these locations with recommended improvements, and to develop a model for identifying potentially dangerous locations on North Carolina interstate highways. Data collected in the study showed that 751 cross-median crashes took place in North Carolina, resulting in 105 fatalities. These crashes represented three percent of total crashes but 32% of total fatalities on interstate highways during the study period. One of the outcomes of this study was the recommendation to construct median barriers at 24 sections of interstate highways in North Carolina.

From observation of cross-median collisions (CMCs) that happened where median barriers were not warranted by the Pennsylvania DOT design policy, Donnell et al. (2002) reviewed the methods used to assess median safety on interstates and expressways in Pennsylvania. A critical literature review and assessment of median safety practices in various state DOTs were conducted, and qualitatively assessed median safety practices were used to provide input for quantitative data collection. Negative binomial regression models were used to model CMC frequencies on median-divided highways. The qualitative results from the study suggested that three-strand cable barriers, strong-post W-beam guardrail, or concrete barriers were recommended median barriers in appropriate site conditions. Quantitative results showed that CMCs were rare events and that nearly 15% involved fatalities and 72% involved nonfatal injuries. Additional findings included that CMC rates at earth-divided highways decreased as the median width increased, that CMCs appeared more likely to occur downstream of interchange entrance ramps, and that CMCs were more likely to involve

adverse pavement surface conditions (wet or icy) than other crashes.

In a project funded by the New Jersey DOT, Gabler et al. (2005) evaluated the post-impact performance of two median barrier systems in New Jersey: a three-strand cable median barrier system and a modified Thrie-beam median barrier system. FE modeling was adopted as a major means for the investigation. The project also included field investigation of crashes into the subject barriers and a survey of the median barrier experience of other state DOTs. This study concluded that three-strand cable barriers were capable of containing and redirecting passenger vehicles, that cable barriers were effective at reducing the incidence of cross-median collisions in wider medians, and that cable barriers reduced the overall collision severity despite typically increasing the total number of accidents.

Ray and McGinnis (1997) provided a synthesis of information regarding the use of guardrails and median barriers in the U.S. and their performance with respect to the testing standards specified by the NCHRP Report 350. Comprehensive background information is provided for the evolution of testing procedures, selection and placement procedures, and in-service evaluation of longitudinal and median barriers. The notable advantages of steel-post cable guiderails/median barriers, as indicated in the report, are their compliance to test level 3 of the NCHRP Report 350, inexpensive installation, minimized sight distance problems, reduced occupant forces in the event of a collision, and reduced snow drifting/accumulation. Disadvantages of this system include periodic monitoring of cable tension, a large clear area for barrier deflection, and increased barrier damage in the event of a collision.

Using data collected from Connecticut, Iowa, and North Carolina from 1997 to 1999, Ray and Weir (2001) performed an in-service performance evaluation of four guardrail systems: the G1 cable guiderail, G2 weak-post W-beam guardrail, and the G4(1S) and G4(1W) strong-post W-beam guardrails. The study particularly focused on estimating the number of unreported collisions and the true distribution of vehicle occupant injuries. The collision performance was measured in terms of collision characteristics, occupant injury, and barrier damage. Within the sample size limitations of the data collected in the study, no statistically significant difference was found on the performance of the guardrails in the three states, and there was no difference between the performance of G1 and G2 and between G1 and G4(1W). However, occupant injuries were found less common in collisions with a G1 cable guardrail than in collisions with G4(1S) or both G4 types combined.

Ray et al. (2003) reviewed literature on in-service evaluation studies and identified previously effective methods. The in-service performance of common barriers and terminals was examined by collecting data in the following three areas: crash, maintenance, and inventory information. A procedure manual for planning and conducting in-service evaluations of roadside hardware was developed based on the methods used and the lessons learned in the evaluation study. The manual was subsequently used as a guide for an in-service evaluation project performed in Washington State by a different research team and modified based on their experiences and recommendations.

The evaluation the crashworthiness of roadside features across vehicle platforms was

analyzed by Bligh and Mak (1999). The impact performances of roadside safety features are typically evaluated through full-scale crash testing with two vehicles selected from the extremes of the passenger vehicle fleet in terms of weight and size. The implicit assumption was that if a roadside safety device successfully passed the test requirements for vehicles at the extremes for the fleet, it would perform satisfactorily for all other vehicles in between. Since many vehicle parameters could influence the performance during impacts, this assumption may or may not be valid. The safety performances of roadside features for various passenger car platforms and light-truck subclasses were evaluated in the study, which consisted of evaluations of the frequency and severity of roadside crashes for these generic platforms and subclasses by using recent crash data from the Fatal Accident Report System, the General Estimates System, and the Highway Safety Information System.

A new median barrier guideline (Miaou et al. 2005; Bligh et al. 2006) for Texas was developed to assist highway engineers evaluating median barrier needs with the intention of achieving the highest practical level of median safety. In this work, statistical crash models for various types of median-related crashes were developed based on an analysis of crash data in Texas. Based on the estimates from the frequency and severity models and crash costs used by Texas Department of Transportation (TxDOT), an economic analysis of the median barrier need was performed. Guidelines for installing median barriers on divided, access-controlled freeways were developed as a function of average annual daily traffic (AADT) and median width. Guidance to assist engineers evaluating median barriers needed on existing highway facilities was also developed based on the mean cross-median crash rate.

Mak and Sicking (2003) created the NCHRP Report 492: Roadside Safety Analysis Program (ASAP) which was developed under the guidelines of NCHRP Project 22-9, "Improved Methods for the Cost-Effectiveness Evaluation of Roadside Safety Features." Project 22-9 was started to make an improved cost effective analysis procedure for assessing roadside safety improvements. This was achieved by the development of RSAP. The RSAP incorporates two integrated programs, the Main Analysis Program, which contains the cost-effectiveness procedure and algorithms; and the User Interface Program, which provides a user friendly environment for data input and review of program results. The cost-effectiveness procedure incorporated into RSAP is based on the concept of incremental benefit/cost analysis. In 2009, NCHRP project 22-27 "Roadside Safety Analysis Program (RSAP) Update" (currently ongoing) is using AASHTO Technical Committee on Roadside Safety to develop the next edition of the Roadside Design Guide (RDG). The objective of this project was to rewrite the software, update the manuals, improve the user interface, and update the embedded default data tables of the Roadside Safety Analysis Program (RSAP). (NCHRP 22-27 (Active))

In the NCHRP Project 17-14, "Improved Guidelines for Median Safety," researchers attempted to develop guidelines for using median barrier and selecting median widths and slopes (BMI-SG 2004). Unfortunately, collection of data needed for this project proved to be very expensive, and the data limitations hampered the strength of the recommendations. The project results have not been incorporated into practice, but should be very beneficial to future research.

The placement of median barriers on sloped median also imposes a significant challenge to retaining the same performance as when placed on flat terrain. The performance tests specified by the NCHRP Report 350 are all based on flat terrain conditions. Terrain conditions can have a significant effect on the barrier's impact performance (AASHTO 2006). The slopes in the median can affect the performance of the barrier as the location of the vehicle impacting the barrier may be significantly different from those on flat terrain.

To avoid some of the obstacles that NCHRP Project 17-14 faced, the NCHRP Project 22-21 focused on typical cross-section designs for a construction or reconstruction projects rather than the exact cross-section design at a particular point. The typical cross-section designs are determined fairly early in the design process before adjustments are made to account for variations along the alignment (e.g., horizontal and vertical curves, interchanges and intersections, and special drainage requirements). Project 22-21 was started on January 24, 2006 and the project was completed in April 2011. However, the Midwest Research Institute panel is reviewing the final rough draft of the research findings making them unavailable at the time of writing. The project report should contain guidance that practitioners can use to evaluate the safety implications of various median cross-section designs, including barrier type and placement guidelines (based on NCHRP Project 22-22), so that a cost-effective design can be achieved. NCHRP Project 22-22, "Placement of Traffic Barriers on Roadside and Median Slopes," (NCHRP 22-22 (Pending)) has been planned and the project results are to be incorporated into the final product of NCHRP Project 22-21.

In 2009, the Manual for Assessing Safety Hardware (MASH) was published (MASH 2009). This report superseded the 17 year old NCHRP Report 350. MASH presents uniform guidelines for crash testing permanent and temporary highway safety features and recommends evaluation criteria to assess test results. MASH does not supersede any guidelines for the design of roadside safety hardware, which are contained within the AASHTO *Roadside Design Guide*. A few of the significant changes between NCHRP Report 350 and MASH include:

- The small car test vehicle weight was increased from 820C (1,800-lbs) to 1100C (2,420-lbs)
- The small car impact angle was increased from 20° to 25°
- The light truck test vehicle weight was increased from 2000P (4,400-lbs) to 2270P (5,000-lbs)
- TL-4 single unit truck test was revised; mass was increased from 8,000-kg (18,000-lbs) to 10,000-kg (22,000-lbs) and speed was increased from 80 km/hour (50 mph) to 90 km/hour (56 mph).

As of January 1, 2011, the FHWA has required that all new products must be tested using MASH crash test criteria for use on the National Highway System (NHS).

A study was conducted to analyze median barrier crash severity using 5 years of data from rural divided highways in North Carolina. (Hu et al. 2010) The criteria that was used for the analysis includes, median barrier type, the barrier offset distance from the edge of the traveled way, roadway segment characteristics, roadway surface conditions, driver and vehicle characteristics, the use of median barrier placement, and median cross-slope data. The major findings from this study include the conclusion that less severe crash outcomes

pertain to cable median barriers crashes when compared to concrete and guardrail barrier systems. Also, the barrier offset distance from the road is associated with a lower probability of severe crash outcomes and cable barrier systems that were installed on the steeper slope medians were associated with an increase in crash probabilities.

In 2010, Hampton et al. (2010a) conducted crash tests and finite element validation on already damaged G4(1S) W-beam section. The finite element validation will be discussed in depth in subsequent sections. The testing of already damaged barrier systems had not previously been conducted. Two crash tests were performed by the MGA Research Corporation for NCHRP Project 22-23 “Criteria for Restoration of Longitudinal Barriers” to evaluate the performance of guardrails with pre-prescribed rail and post deflections. The first crash test was conducted at 48.28 km/hour (30 mph) at an impact angle of 25° and resulted in 10.97 meters (36ft) damaged section of barrier with a maximum deflection of 0.37 meters (1.21 feet). The second crash test was performed in the damaged location; however, the results were undesirable. The barrier provided little to no resistance and the vehicle was vaulted over the barrier. These results were due to the fact that there was a failure present that separated the post from the rail. These tests concluded that post and rail deflection of 0.279 meters (0.92 feet) or more would result in the vehicle vaulting over the median barrier.

Ochoa et al. (2011) completed a study to optimize guardrail barriers for rural roadways in the United States, Europe, and other developing countries. In order to optimize the W-beam guardrail, the main methods of failure had to be defined and considered. In conventional strong post W-beam guardrails, the relatively high release load varies by around 360% and is further compounded by another 40% because of variations in guardrail panel yield strength. A physics-based guardrail analysis has determined that the solution is to optimize the release load in relation to post section properties. This optimization is accomplished by introducing an improved fastening system that incorporates a separate deformable release member to consistently provide a predefined release load of around 7,565-N (1,700-lbs) with a maximum variation of around 20%. The versatile W-beam guardrail incorporating these improvements has been successfully crash tested and accepted by FHWA at NCHRP Report 350 test levels and Test Level 3 of the AASHTO Manual for Assessing Safety Hardware.

In 2011, the AASHTO *Roadside Design Guide* presented a synthesis of current information and operating practices related to roadside safety. The guide was intended to be used as a resource document from which individual highway agencies could develop standards and policies. It included a synthesis of current information and operating practices related to roadside safety and focused on safety treatments that can minimize the likelihood of serious injuries when a motorist leaves the roadway. The 2011 edition has been updated to include hardware that has met the evaluation criteria contained in the NCHRP Report 350 and includes an outline of the most current evaluation criteria contained under the MASH.

For decades, the W-beam guardrails have been used on U.S. highways to prevent errant vehicles from entering unsafe areas or impacting fixed objects. The W-beam guardrails have become commonly used barrier systems and have had good safety performance for many years. Although the original W-beam guardrails were found to be able to safely contain or redirect small and full-size vehicles, a research study conducted at the Texas Transportation

Institute (TTI) in 1983 indicated their design weakness for large vehicle impacts. The major safety concern came from the observation of vehicle rollover due to snagging of the front wheel on the posts.

In the late 1990's, following the implementation of safety standards of NCHRP Report 350, researchers from TTI and the Midwest Roadside Safety Facility (MwRSF) conducted several studies using crash testing to determine whether the strong post G4(1S) W-beam guardrail would meet the requirements of NCHRP Report 350 under TL-3 impact conditions. The research results showed that the strong post W-beam guardrails, both with steel and wood blockouts, caused vehicle rollovers. The studies also evaluated the performance of the modified G4(1S) guardrail with a rail height of 27¾ inches. Despite the satisfactory barrier performance showed in most of the crash tests, it was concluded that this system “may not have sufficient reserve capacity to safely contain and redirect higher center-of-mass vehicles during high-speed and high-angle collisions.”

In 2000, researchers at MwRSF developed a new guardrail system in cooperation with the Midwest States' Regional Pooled Fund Program. This new W-beam guardrail system, known as the Midwest Guardrail System (MGS), included a nominal mounting height of 31 inches measured to the rail top. The MGS was tested under TL-3 impact conditions of NCHRP Report 350 and found to be capable of safely contain and redirect both pickup trucks and small cars. The research work suggested that the MGS could “improve the barrier performance for vehicles with higher center-of-mass, provide reasonable barrier height tolerances, and reduce the potential for W-beam rupture.” Later in 2009, the MGS was tested using a 2270P vehicle under MASH TL-3 conditions and found to pass the safety requirements.

The above mentioned studies, along with other research works, resulted in the recommendation of increasing rail heights of the G4(1S) W-beam guardrails to 27¾ and 31 inches, as shown in the USDOT memorandum issued in May 2010. Concerns of the safety performance of the standard G4(1S) W-beam guardrail were mainly based on the TL-3 impact conditions of both NCHRP Report 350 and MASH. However, their performance under MASH TL-2 conditions has not been studied and deserves investigation to provide practical guidance for their usage on non-national highways where lower-speed impacts prevail.

Historically, the safety performance of vehicles and roadside safety devices has been evaluated through full-scale crash testing. Physical crash testing is a valid means to examine the safety performance of barrier systems; however, it is very expensive, time-consuming, and difficult to perform. Consequently, only a limited number of representative crash scenarios can be evaluated using regulations and/or guidelines given by FMVSS for vehicle crashworthiness and by MASH or NCHRP Report 350 for roadside safety hardware designs.

With the rapid development of computing hardware and commercial software for high performance computing, computer simulations have been used more and more in highway safety designs. Over the recent decades, various FE models of vehicles and roadside safety devices have been developed; a library of these FE models is available from the National

Highway Traffic Safety Administration (NHTSA) and National Crash Analysis Center (NCAC). NHTSA also maintains a comprehensive database of crash testing data and reports.

2.2 Performance of Safety Barriers behind Curbs

The performance of longitudinal barriers of all kinds is influenced by curbs. Curbs are essentially obstructive structures that may cause vehicles to lose control upon striking and result in tripped rollovers. Therefore, the use of curbs on high-speed highways is discouraged by the AASHTO highway design policy. Despite the discouragement of their usage, curbs are often required or needed in many places, with W-beam guardrail being one of the most commonly used barriers.

Early studies of barrier performance behind curbs can be found in the works of Dunlap (1973) and Olson et al. (1974). In the work by Olson et al. (1974), the Type B, Type D, and Type G curbs were studied using simulations of vehicular impacts at various speeds (30 to 75 mph) and angles (5° to 20°). The study showed that the distance from the curb face to the maximum rise point was increased with the increase of impact speed and/or impact angles. For example, the distances to the maximum rise points for Type B curb were 5, 8, and 10 feet for impacts at 30, 45, and 60 mph, respectively, all at a 25° impact angle. This observation was also true for Type D and Type G curbs.

Plexico (2002) studied common types of curbs to identify those that could be used safely and effectively on high-speed roadways, i.e., with operating speeds greater than 37 mph (60 km/hour). The results of the study led to the development of guidelines for curb and curb-barrier installations (Plexico et al. 2005). Using both computer simulations with validated vehicle model by full-scale crash tests, Plexico et al. (2005) studied the bumper heights of a C2500 pickup truck at various distances from the curb face after striking a curb. The simulation results showed that the G4(1S) W-beam guardrail at the face of a Type B curb could safely redirect a C2500 pickup truck, and that the curb would cause the vehicle's bumper to ride above the guardrail if placed at 8 feet (2.5 m) from the curb face. For the case of guardrail at 13 feet (4 m) from the curb face, their simulations were prematurely terminated and no results were available.

Using both vehicle dynamics simulations and finite element simulations, Marzougui et al. (2009) studied the effects of curbs on cable median barriers installed behind curbs. In the study, different vehicle sizes, impact speeds, and impact angles were used to determine the vehicle trajectories behind the curbs that were used to determine the impact points relative to cable heights. It should be noted that the study was focused on the effectiveness of cable barriers based on cable heights and impact points, and that vehicle redirection characteristics and post-impact responses were not used to determine the barrier performance. One useful observation from the study was that the distance of vehicle vaulting after hitting the curb was larger at a large impact angle than that at a small impact angle.

In 2009, researchers at MwRSF started an investigation on the performance of the MGS (i.e., the MwRSF 31-inch W-beam guardrail) behind the AASHTO Type B 6-inch curb (Zhu et al.

2009; Thiele et al. 2009; Thiele et al. 2010). Their study involved both computer simulations (Zhu et al. 2009) and full-scale crash tests at MASH TL-3 (Thiele et al. 2009) and TL-2 (Thiele et al. 2010) conditions. Computer simulations were first employed to study vehicle trajectory after impacting the curb and to determine the vehicle's impact heights at different lateral locations from the curb face. The major assumption was that as long as the impact heights were within certain range, the curb-MGS combination would perform satisfactory. Followed their computer simulation work, full-scale crash testing was conducted at MASH TL-3 conditions on the MGS installed at 8 feet (2.44 m) from the curb face. The test results showed that the MGS did not meet the safety criteria by MASH due to multiple occurrences of vehicle snagging followed by a rollover. Finally, full-scale crash testing was conducted at MASH TL-2 conditions on the MGS at 6 feet from the curb face. The test results showed that the MGS met the MASH safety criteria. This conclusion, however, was not in agreement with the researchers' simulation results that showed the vehicle overriding the guardrail. The results of this study indicated that the 31-inch MGS could be installed at 4-12 feet from the curb face under MASH TL-2 conditions. The research, however, did not indicate if this range of offset would also work for other W-beam guardrail systems.

Recently, Ohio DOT issued a Roadside Safety Field Guide (Ohio DOT 2013) that gave guidelines on installing W-beam or Thrie-beam guardrails behind curb. In this guide, the guardrails were not suggested for installation behind curbs if the curb height is more than 6 inches and the impact speed is higher than 50 mph. Other recommendations include that the guardrail should not be closer than 8 feet from the curb face if installed behind curb and impacted by vehicles at 45 mph or lower speeds. For vehicular impacts at 45-50 mph, the recommended distance from the rail face to the curb face is at least 13 feet. These impact speeds are close to and slightly higher than the impact speed specified by MASH TL-2; however, no impact angles are specified in this guide.

2.3 Crash Modeling and Simulations

Mackerle (2003) provided a bibliography that had 271 references published between 1998 and 2002 on crash simulations using FE analysis (FEA) and impact-induced injuries. This bibliography categorized the references into four different topic areas: 1) Crash and impact simulations where occupants are not included; 2) Impact-induced injuries; 3) Human surrogates; and 4) Injury protection. Topics in the first area include crashworthiness of aircrafts and helicopters, automobiles, and vehicle rail structures. The second area of research utilizes two major types of models for humans, the crash dummy and real human body models. Research topics in this area are mainly on biomechanics and impact analyses for various human injuries. Topics on human surrogates focus on the development FE models of hybrid and other types of human dummies. These dummy models are used to obtain dynamic responses of the whole human bodies during impacts, which are difficult to measure experimentally. In the area of injury protection, FE techniques are utilized to analyze and simulate injury protection systems such as seat belt, air bags, and collapsible structures to reduce serious or fatal injuries. The references included in Mackerle's bibliography are generally useful to the work on FE crash simulations; however, only a few references under injury protection are related to roadside safety and none is related to CMB simulations.

Most publicly available FE models of vehicles and roadside safety structures were developed

at the FHWA National Crash Analysis Center (NCAC) at George Washington University. Since the 1990's, significant efforts have been put on the development of FE crash models that are available as LS-DYNA input files from NCAC's website (NCAC web1). A list of references on these modeling efforts and simulation work performed at NCAC is also available from NCAC's website (NCAC web2).

The modeling and simulation efforts at NCAC can be found in several representative works. Marzougui et al. (2000) developed the FE model of an F-shaped portable concrete barrier (PCB) and validated the model with full-scale crash test data. With the proven fidelity and accuracy of the modeling methodology, the models of two modified PCB designs were created and used in FE simulations to evaluate their safety performance. A third design was then developed based on the simulation results and its performance was analyzed. In the work by Zaouk et al. (2000a, 2000b), a detailed FE model of a 1996 Plymouth Neon was developed. The three dimensional geometric data of each component was obtained by using a passive digitizing arm and then imported into a preprocessor for mesh generation, parts connection, and material properties. Tensile tests were conducted on the specimen to obtain the material properties of the various sheet metal components. The body-in-white model was used in the simulation of a frontal impact and the results were compared with test data to evaluate the accuracy and validity of the model. Kan et al. (2001) developed an integrated FE model that included the vehicular structure, interior components, an occupant (Hybrid III dummy), and an airbag for crashworthiness evaluation. The integrated model was then used in a case study to demonstrate the potential benefit of the integrated simulation and analysis approach, which would further improve the engineering practice with cost savings and producing more accurate and consistent analysis results.

Marzougui et al. (2004) developed a detailed suspension model and incorporated it into the previously developed FE model of a Chevrolet C2500 pickup truck (Zaouk et al. 1997). Pendulum tests were conducted at the Federal Outdoor Impact Laboratory (FOIL) of FHWA and compared with simulation results of deformations, displacements, and accelerations at various locations. Crash simulations were performed using the upgraded vehicle model and the results were compared with crash data from previously conducted full-scale tests.

To facilitate the use of FE simulation to evaluate roadside safety structures at higher test levels specified by the NCHRP Report 350, Mohan et al. (2007) improved and validated a previously developed model of a 1996 Ford F800 single unit truck. This 8172-kg (18,000-lbs) truck was used in the NCHRP Report 350 as the standard vehicle for test level 4. Simulations were performed using the improved model and the results were compared with those from a full-scale crash test. The global kinematics and acceleration time histories of the truck from simulation correlated well with the crash test. Mohan et al. also suggested further improving the normal forces on non-impacted tires so as to correlate well on the vehicle's yaw by considering frictions between the tire and barrier and between the tires and ground.

In a study by Marzougui et al. (2007), a FE W-beam model was developed and was validated by using full-scale crash testing. The model was shown to give an accurate representation of the real system by comparing the roll and yaw angles. Using the validated model, they performed four simulations of a passenger truck impacting the W-beam with different rail

heights. The simulation results showed that the effectiveness of the barrier to redirect a vehicle could be compromised when the rail height was lower than recommended.

Researchers from the roadside safety group at Worcester Polytechnic Institute (WPI) utilized FE models in a number of roadside safety studies. Ray (1996a) analyzed data of full-scale crash tests and developed a criterion using statistical parameters to assess the repeatability of full-scale crash test and to evaluate simulation results compared to crash data. Ray (1996b) reviewed the history of using FEA in roadside safety research, and presented the vehicle, occupant, and roadside hardware models that had been developed to date. Ray and Patzner (1997) developed a nonlinear FE model of a modified eccentric loader breakaway cable terminal (MELT) and used it in simulating a full-scale crash test involving a small passenger car. Simulation results were analyzed and compared to crash data, and the FE model were recommended to be used in the evaluation of new design alternatives. Plaxico et al. (1997) developed a 3D FE model of a modified Thrie-beam and simulated the impact of a compact automobile on this guardrail. The computational model was then calibrated with data from an actual field test that was previously conducted as part of a full-scale crash test program carried out under the auspices of FHWA. Plaxico et al. (1998) developed the FE model of a breakaway timber post and soil system used in the breakaway cable terminal (BCT) and the modified eccentric loader BCT. Simulation results were compared and found to correlate well to data from physical tests. Patzner et al. (1999) examined the effects of post strength and soil strength on the overall performance of the MELT terminal system using a nonlinear FE model. A matrix of twelve simulations of particular full-scale crash test scenarios was used to establish the combinations of post and soil strengths that produce favorable results. The parametric study showed that certain combinations of soil and post strengths increased the hazardous possibilities of wheel snagging, pocketing, or rail penetration, while other combinations produced more favorable results.

In the work of Plaxico et al. (2000), the impact performance of two strong-post W-beam guardrails, the G4(2W) and G4(1W), were compared. After validating the FE model of the G4(W2) guardrail with data of a full-scale crash test, the FE model of the G4(1W) guardrail was developed. The two guardrails were compared with respect to deflection, vehicle redirection, and occupant risk factors. The two systems were found to perform similarly in collisions and both to satisfy the requirements of the NCHRP Report 350 for the test 3-11 conditions. Using LS-DYNA simulations and laboratory experiments, Plaxico et al. (2003) investigated the failure mechanism of the bolted connection of a W-beam rail to a guardrail post, which could have a significant effect on the performance of a guardrail system. A computationally efficient and accurate FE model of the rail-to-post connection was developed to be used in analysis of guardrail system performance using LS-DYNA. Orengo et al. (2003) presented a method to model tire deflation in LS-DYNA simulations along with examples to use the model. Deflated tires have significantly different behaviors from those of inflated tires, as observed in real world crashes and in full-scale crash tests. Vehicles' kinematics is strongly coupled to the behaviors of deflated tires; therefore, modeling such behaviors is critical to roadside hardware simulations. Ray et al. (2004) used LS-DYNA simulations to determine if an extruded aluminum bridge rail would pass the full-scale crash tests for test levels three and four conditions of the NCHRP Report 350. The simulation results, which were supported by a subsequent AASHTO LRFD analysis, indicated a high

likelihood of passing the crash tests.

FE simulations have also been used by researchers at the Midwest Roadside Safety Facility (MwRSF). Reid (1996) utilized FEA in the study of material property influence on automobile crash structures and attempted to develop crashworthiness guidelines for design engineers. In one of his later works, Reid (1998) demonstrated through two simple examples the potential modeling issues that could be easily overlooked in FE impact simulations: contact definition and damping. He also suggested ways to check for modeling errors and to make improvements. In the work of Reid and Bielenberg (1999), FE simulations were performed for a bullnose median barrier crashed by a 2000-kg (4405-lbs) pickup truck to determine the cause of failure and to evaluate a potential solution to the problem. In a collaborative work to improve the FE model of a Chevrolet C2500 pickup truck (Reid and Marzougui 2002; Tiso et al. 2002), structural modeling methods were introduced for model improvement through refining meshes, using better material models, adding details to simplified components, and improving connections between components. Suspension modeling, which is critical to the correct vehicle dynamic responses, was also investigated in this collaborative work and a new model was successfully developed with significant improvements.

To educate roadside safety engineers and promote the use of simulations, Reid (2004) summarized ten years of the simulation efforts at MwRSF on the development of new roadside safety appurtenances. More recently, Reid and Hiser (2004) studied the friction effects, particularly between solid elements, on component connections and interactions in crash modeling and analysis. In their work on modeling bolted connections that allowed for slippage, Reid and Hiser (2005) investigated two modeling techniques that are based on discrete-spring clamping and stressed clamping model with deformable elements, respectively. The simulation results for both models compared well with test data, with the stressed clamping model with deformable mesh having better accuracy accompanied by significantly increased computational cost. Hiser and Reid (2005) also investigated improved FE modeling methods for slip base structures, which could have a considerable potential for reducing the amount of crash resistance and thus occupant injury when struck by errant vehicles. They developed and evaluated two bolt preloading methods, with one using discrete spring elements and the other using pre-stressed solid elements. Similar to their findings in the work of modeling hook-bolts, they found that the method using solid elements was more accurate than that using discrete spring elements when the impact conditions became more severe. As a result, the model using pre-stressed solid elements was incorporated into the FE model of a cable guardrail system. The results showed that the slip base model was acceptable in both end-on impact and length-of-need impact simulations.

In 2009, Reid et al. (2009) investigated the potential of increasing the suggested flare rates for strong post W-beams to reduce guardrail installation lengths, which would result in decreased guardrail construction and maintenance costs, and reduce the impact frequency. Both computer simulation and full-scale crash tests were used in the evaluation of increased flare rates up to, and including, 5:1. Simulation results indicated that the conventional G4(1S) guardrail modified to incorporate a routed wood block could not successfully meet NCHRP Report 350 crash test criteria when installed at any steeper flare rates than the 15:1

recommended in the Roadside Design Guide. Their study also showed that the Midwest Guardrail System (MGS) could meet NCHRP Report 350 impact criteria when installed at a 5:1 flare rate, yet with greater impact severities during testing than anticipated. Reid et al. also indicated that whenever roadside or median slopes are relatively flat (10:1 or flatter), increasing the flare rate on guardrail installations becomes practical and has some major advantages including significantly reducing guardrail lengths and associated costs. The study, however, did not give any indications of W-beam performance on steeper slopes.

FE simulations were also found in the work of other researchers in roadside safety Research. Whitworth et al. (2004) evaluated the crashworthiness of a modified W-beam guardrail using detailed FE models of the guardrail and a Chevrolet C2500 pickup truck. The simulation results were compared and found in good agreement with crash test data in terms of roll and yaw angles. Simulations were also performed to evaluate the effect of certain guardrail design parameters, such as rail mounting height and routed/non-routed blockouts, on the crashworthiness and safety performance of the system. In the work of Bligh et al. (2004), FEA was utilized to develop new roadside features to address three roadside safety issues. An alternative to the popular T6 tubular W-beam bridge rail was developed to address problems with vehicle instability observed in full-scale crash testing. A retrofit connection to TxDOT's grid-slot portable concrete barrier was developed to limit dynamic barrier deflections to levels that are more practical for work zone deployment. Finally, crashworthy mow strip configurations were developed for use when vegetation control around guard fence systems is desired to reduce the cost and risk associated with hand mowing. In a project funded by the New Jersey DOT, Gabler et al. (2005) evaluated the post-impact performance of two median barrier systems in New Jersey: a three-strand cable median barrier system and a modified Thrie-beam median barrier system. FE modeling was adopted as a major means for the investigation. The project also included field investigation of crashes into the subject barriers and a survey of the median barrier experience of other state DOTs. This study concluded that the three-strand cable barriers were capable of containing and redirecting passenger vehicles, that cable barriers were effective at reducing the incidence of cross-median collisions in wider medians, and that cable barriers reduced the overall collision severity despite typically increasing the total number of accidents.

Computer simulations are also used by international researchers on roadside safety research. Using LS-DYNA simulations, Atahan (2002) analyzed a strong-post W-beam system that was failed in a previously conducted full-scale crash test. After identifying the cause of failure and incorporating necessary improvements, a new W-beam system was developed and showed improved performance based on simulation results. Atahan (2003) studied the impact performance of G2 steel weak-post W-beams installed at the slope-break point on non-level terrains using LS-DYNA simulations. His results showed that there was a risk of increased vehicle instability when the roadside slope adjacent to the W-beam guardrail became steeper than 6:1. Atahan and Cansiz (2005) investigated the failure of a bridge rail-to-guardrail transition design in a full-scale crash test in which the vehicle rolled over the guardrail. They used full-scale LS-DYNA simulations to replicate the crash tests and identified the cause of the failure attributed to the low height of the W-beam rails. In the work by Atahan (2007), LS-DYNA simulation was used to study the crashworthiness behavior of a bridge rail-to-guardrail transition structure under 8,000 kg of impact load. This work demonstrated the

effectiveness of FE simulations for its replications of the actual dynamic interactions and mechanics of the crash. Atahan also pointed out that the use of a real soil model other than the simplified spring soil model could improve the accuracy of FE simulations but would significantly increase the computational costs.

Using LS-DYNA, Fang et al. (2010) conducted a study evaluating the performance of three types of barriers on sloped medians. Single-face W-beam, two designs of a double-face W-beam, and low-tension cable barriers were used in an analysis evaluating multiple impact speeds and impact angles. The simulation results suggested that the effectiveness of the W-beam guardrail and CMB could be reduced on sloped medians compared to their performance on flat terrain as specified in the NCHRP Report 350. It was observed that the tendency and severity of vehicle rollover increased with the increase of impact angles while holding other conditions constant. This was shown to be true for the single-face W-beam, double-face W-beam, and CMB. The performance of the barriers investigated in this project exceeded the TL-3 requirements of the NCHRP Report 350.

Hampton et al. (2010a) also performed a finite element validation of the two crash tests that were performed by the MGA Research Corporation for NCHRP Project 22-23 “Criteria for Restoration of Longitudinal Barriers.” The FE simulations were comparable to the crash tests that were performed and additional FE simulations were performed with reduced deflections on the barrier to determine where the effective guardrail performance cutoff occurs. The finite element models determined that repairs are recommended for strong-post W-beam guardrail with combined rail-and-post deflection exceeding 152.4 mm (6 inches) in the lateral direction.

A similar simulation to evaluate the performance of strong-post W-beam guardrails with missing posts in accordance with NCHRP Report 350 was performed by Hampton et al. (2010b). The effect of missing posts on the guardrail crash performance was quantitatively evaluated using finite element models of crash tests using a 2000-kg (4409-lbs) pickup truck. Simulations in which one, two, or three posts were removed from the guardrail were conducted with varying points of impact to evaluate the effect of missing posts. The finite element model results demonstrated that guardrail missing even one post can show markedly decreased vehicle performance due to wheel snagging. Both maximum deflection and maximum rail tension greatly increased as more posts were removed from the guardrail and it was determined that if even one post was missing, the guardrail performance is significantly reduced and post replacement should be a high consideration.

Vehicle impact height is one of the most important parameters in evaluating the performance of barrier systems. The vehicle impact height can vary depending on the trajectory of the vehicle along the median and the lateral offset of the barrier. The performances of the modified G4(1S) W-beam guardrail, modified Thrie-beam guardrail, Midwest guardrail system, and modified weak post W-beam guardrail were analyzed by Ferdous et al. (2011) using LS-DYNA. Each model was validated based on the results obtained from existing crash tests. Using vehicle models from NCHRP Report 350, the override and under-ride limits for each guardrail model were identified. The performance limit of each barrier was determined by parametrically varying the vehicle impact height to determine at what point

the override or rollover for the pickup truck and under-ride for the small passenger car occurs.

FE simulation, particularly with LS-DYNA, has been increasingly used in roadside safety research. In addition to the abovementioned references, FHWA recently published several manuals on using LS-DYNA material models and evaluation of these models (Lewis 2004; Murray et al. 2005; Murray 2007; Reid et al. 2004). These references can also be useful in the crash modeling work using LS-DYNA.

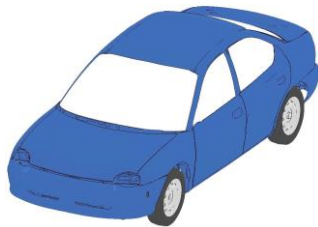
3. Finite Element Modeling of Vehicles and W-beam Guardrails

The simulation work of this project involved finite element (FE) models of two vehicles (a 1996 Dodge Neon and a 2006 Ford F250) and three NCDOT W-beam guardrails with 27-, 29-, and 31-inch placement heights. The three guardrails were placed behind a 6-inch AASHTO Type B curb at two locations: 1) flush with the curb face; and 2) at 12 feet from the curb face. Additionally, the 29-inch guardrail was also evaluated when placed at 6 feet from the curb face. All crash simulations were conducted with the two vehicles impacting the guardrails at 44 mph (70 km/hour) and at impact angles of 25° and 15°. The impact speed of 44 mph (70 km/hour) and the 25° impact angle are the same as MASH TL-2 conditions, except that MASH TL-2 tests are conducted on a flat terrain.

In all simulation cases, the vehicle left the travel lane at the prescribed speed and angle, passed the gutter, and ran against the curb before hitting the guardrail. The impact speed was defined in the vehicle's travel direction, and the impact angle was defined as one between the vehicle's travel direction and the guardrail's longitudinal direction.

3.1 FE Models of a Passenger Car and Pickup Truck

The FE models of the two vehicles used in this project were a 1996 Dodge Neon passenger car and a 2006 Ford F250 pickup truck, as shown in Figure 3.1. Table 3.1 gives the specifications of the two vehicles relevant to this project.



a. A 1996 Dodge Neon passenger car



b. A 2006 Ford F250 pickup truck

Fig. 3.1: FE models of the two vehicles used in crash simulations.

Table 3.1: Specifications of the two test vehicles used in crash simulations

Specification	Vehicle	
	1996 Dodge Neon	2006 Ford F250
Curb weight *	2,403 lbs. (1,090 kg)	5,504 lbs. (2,499 kg)
Overall length	171.8 in (4.36 m)	226.4 in (5.75 m)
Overall width	67.5 in (1.71 m)	79.9 in (2.03 m)
Overall height	52.8 in (1.34 m)	76.5 in (1.94 m)
Ground clearance	5.7 in (145 mm)	8.3 in (211 mm)

* The curb weight is the weight of the vehicle with all standard equipment and amenities, but without any passengers, cargo or any other separately loaded items in it.

The FE model of the 1996 Dodge Neon had a total of 339 parts that were discretized into 283,683 nodes and 270,727 elements (2,852 solid, 92 beam, 267,775 shell, and 8 other elements). Ten different constitutive models were used, including the piecewise linear plasticity model defined for most steel components, the elastic model for the tires and a few other components, the viscous damping model for the shock absorbers, the low-density foam model for the radiator core, the spot-weld model for sheet metal connections, the Blatz-Ko rubber model for nearly incompressible rubber cushions, the rigid model for most mounting hardware, and the null material model defined for contact purposes. Hourglass control was used on components that could potentially experience large deformations. The FE model of the Dodge Neon was originally developed at NCAC and validated with the NHTSA's Frontal New Car Assessment Program (NCAP) tests.

The FE model of the 2006 Ford F250 was composed of a total of 746 parts that were discretized into 737,990 nodes and 736,407 elements (25,905 solid, 2,305 beam, 707,656 shell, and 541 other elements). Eleven different constitutive models were used, including the piecewise linear plasticity model defined for most steel components, the linear and nonlinear elastic spring model for the suspension springs, the viscous damping model for the shock absorbers, the low-density foam model for the radiator core, the spot-weld model for sheet metal connections, the viscos-elastic model for rubber cushions, and the null material model defined for 48 parts for contact purposes. Hourglass control was used on various components that could potentially experience large deformations. The FE model of the F250 was originally developed at NCAC and validated using frontal-impact tests that were conducted on flat terrain according to the Federal Motor Vehicle Safety Standards and Regulations (FMVSS).

Simulations of the vehicles crashing into roadside barriers imposed significant challenges to the numerical models due to the large, nonlinear deformations and the large numbers of components being in contact. For example, in the simulations of the Ford F250 crashing into the W-beam guardrail, the W-beam rails and the vehicle's fender experienced severe deformations. The vehicle's wheel, fender, bumper cover, suspension, and a number of other parts were in contact with the guardrail post, rail, and bolts. These contacts needed to be handled by selecting the appropriate contact algorithms to eliminate the unrealistic penetrations of the elements. Otherwise, the simulations would encounter great numerical difficulties, resulting in premature termination and unrealistic behaviors of the vehicle and/or guardrail (e.g., the vehicle being entangled with the guardrail components). The Ford F250 initially experienced contact issues that was caused by the tow hook elements (on the front of the vehicle) impacting and penetrating the guardrail and becoming entangled. The contact definition between these two parts was investigated and modified to ensure a proper handling of the contact. The FE model of the Dodge Neon experienced a similar issue with elements on the bumper cover penetrating the guardrail and becoming entangled due to a contact definition that was used in the original model but inappropriate for the simulations of this project. The contact definition between the vehicle's bumper and the guardrail was changed to resolve this contact issue. Before running simulations for this project, simulations were conducted using the Ford F250 and the Dodge Neon to ensure appropriate contacts being defined for all parts in the guardrail and the vehicles.

3.2 FE Models of the W-beam Guardrails

The FE model of the G4(1S) W-beam guardrail was originally developed at NCAC. It contained six different constitutive models: the piecewise linear plasticity model for most steel components, the elastic model for the wood block-outs and terminal posts, the soil and foam for the soils around posts, the rigid model for the bolts and road surface, the nonlinear elastic spring model for the bolt-tensioning spring in the long-bolts (used to attach the rails and wood block-outs to the posts), and the null material model used for contact purposes.

In the original NCAC model, the soil around each post was a cylindrical block that was suitable for flat-terrain conditions. For W-beam guardrails installed on the shoulder of sloped median and/or behind curbs, the boundary of the cylindrical soil blocks would not match to the borderlines. In this project, the guardrail model including the soil foundations was obtained from a previous NCDOT research project (Fang et al., 2010) in which an FE model of a square soil foundation was developed for use on both flat terrains and sloped medians (with minor modifications). The square soil model used the same material model and properties as the original NCAC soil model. The FE model of the square soil foundation was compared and found identical to the circular soil model using simulations of a vehicular crash test. For the model of guardrails placed at the curb face, the soil model was further modified to match the curb geometry. Figure 3.2 shows the original NCAC soil model, the square-shaped soil model, and the close-to-curb soil model developed for this project. Note that when the guardrails were not placed at the curb face, the FE model in Fig. 3.2b was used.

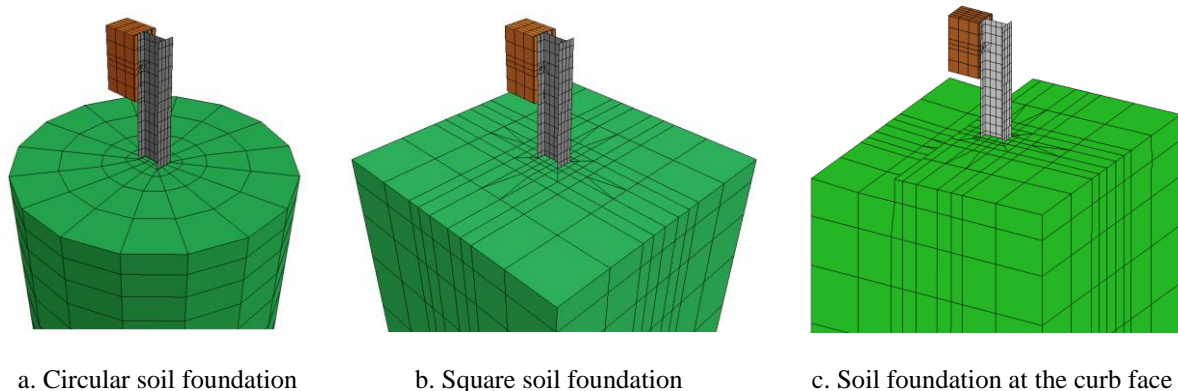


Fig. 3.2: FE models of the soil block around a post.

In addition to modifications on the soil model, modeling issues such as initial penetrations among the components were found in the original guardrail model and were resolved in the FE models of this project. The revised models were found to have improved numerical stability and accuracy of the simulations with the elimination of penetrations and the use of sophisticated contact algorithms. To reduce the computational cost of the simulations and further improve the numerical stability, the guardrail models were simplified on the bolt connections of the rail splices. Figure 3.3 illustrates the location of a guardrail splice where two W-beam rail sections are joined and secured by eight short-bolts. In the original guardrail model, these short-bolts incorporated a failure mechanism that could separate the bolt and nut upon reaching the failure point (defined by a threshold value of the force). While realistic and capable of emulating the bolt's behavior, these bolt connections were modeled

with their individual components and thus were computationally expensive. It was determined through simulation testing that these short-bolts would never reach their failure point under the impact conditions used in this project, i.e., MASH TL-2 impact conditions. Therefore, the failure mechanism was removed from these short-bolts to simplify these component models. It should be noted that contacts were defined between the short-bolts and the rails so the rails could still rip off at holes where the bolts were placed. The simplifications along with resolutions to other contact issues (e.g., initial penetrations due to mismatched geometries) were found to significantly improve the FE model's stability and efficiency.

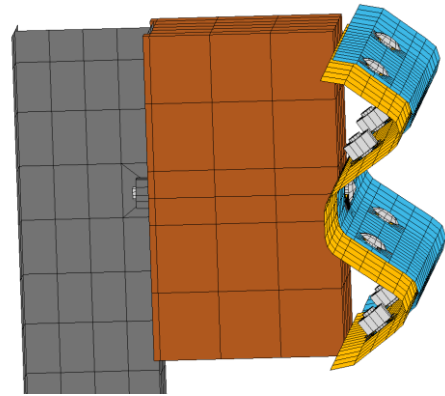


Fig. 3.3: Short-bolts on a guardrail splice.

The FE model of the guardrail segment, once effectively modified, was duplicated to create the entire 400-ft (122-m) section of the guardrails required for this project. This duplication of the guardrail section was done with an in-house code developed to replicate not only the parts, nodes, elements, and material properties, but also the contact definitions defined between each pair of parts. The program was also capable of merging the ends of adjacent segments with proper numbering and contact definitions. With this program, the guardrail model was generated by duplicating the length of need section and connecting to two terminal sections obtained from the original guardrail model.

3.3 Simulation Setup

The three guardrail models were combined with the two vehicle models to conduct the simulation work of this project, which was divided into three major categories based on guardrail locations:

- 1) Case 1: Guardrails placed flush with the curb face (or at the curb face)
The 27-, 29-, and 31-inch guardrails were evaluated.
- 2) Case 2: Guardrails placed at 12 feet from the curb face
The 27-, 29-, and 31-inch guardrails were evaluated.
- 3) Case 3: Guardrails placed at 6 feet from the curb face
Only the 29-inch guardrail was evaluated.

Figures 3.4 and 3.5 show the simulation models of the 29-inch guardrail placed at the curb face and 12 feet from the curb face, respectively, and impacted by a Ford F250.

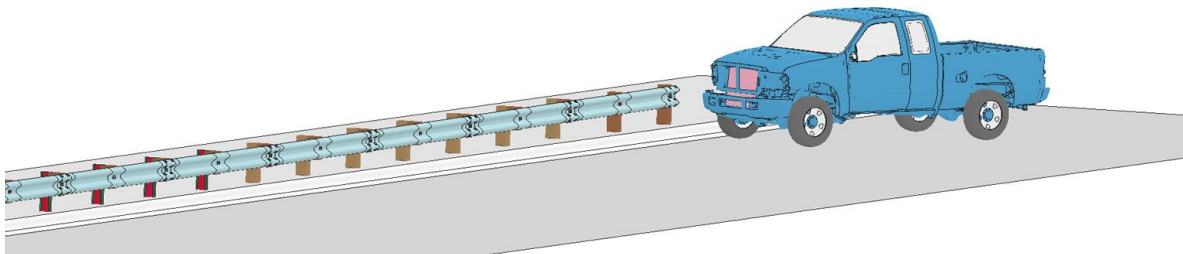


Fig. 3.4: FE model of a W-beam guardrail placed at curb face and impacted by a Ford F250.

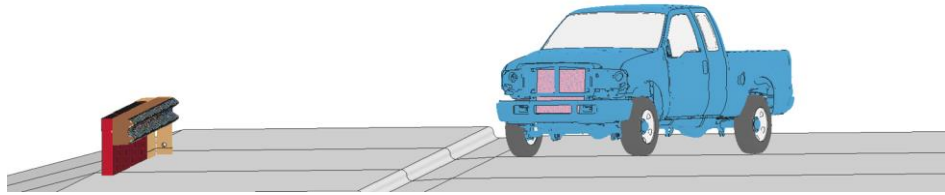


Fig. 3.5: FE model of a W-beam guardrail placed at 12 feet from curb face and impacted by a Ford F250.

Table 3.2 summarizes the simulation conditions for all the three cases. The impact speed was 44 mph (70 km/hour) for all of simulation cases.

Table 3.2: Simulation conditions for all cases

Case No.	Guardrail Location	Guardrail Height	Impacting Vehicle	Impact Angle
1	At the curb face	27, 29, and 31 inch	Ford F250 and Dodge Neon	25° and 15°
2	At 12 feet from the curb face	27, 29, and 31 inch	Ford F250 and Dodge Neon	25° and 15°
3	At 6 feet from the curb face	29 inch	Ford F250 and Dodge Neon	25° and 15°

Based on Table 3.2, Case 1 and Case 2 each required a total of 12 simulations (3 guardrail heights, two vehicles, and two impact angles), and Case 3 had a total of four simulations.

4. Simulation Results and Analysis

The FE simulation results for the three cases in Table 3.2 are presented in this section. The performance of guardrails under vehicular impacts was evaluated using vehicular responses that were classified by the MASH exit box criterion. The simulation results of the vehicles' yaw, pitch, and roll angles as well as transverse displacements and velocities were also examined to provide a comprehensive understanding of vehicular responses.

The exit box criterion was designed to determine vehicle redirection characteristics based on certain vehicular responses after impacting a longitudinal barrier. Figure 4.1 illustrates the definition of the exit box, which begins at the point of the vehicle's last contact point with the barrier's initial face location. The size of the exit box (i.e., the side lengths A and B of this rectangular area) is determined by the type and size of the impacting vehicle. Table 4.1 gives the definition of sizes A and B in MASH.

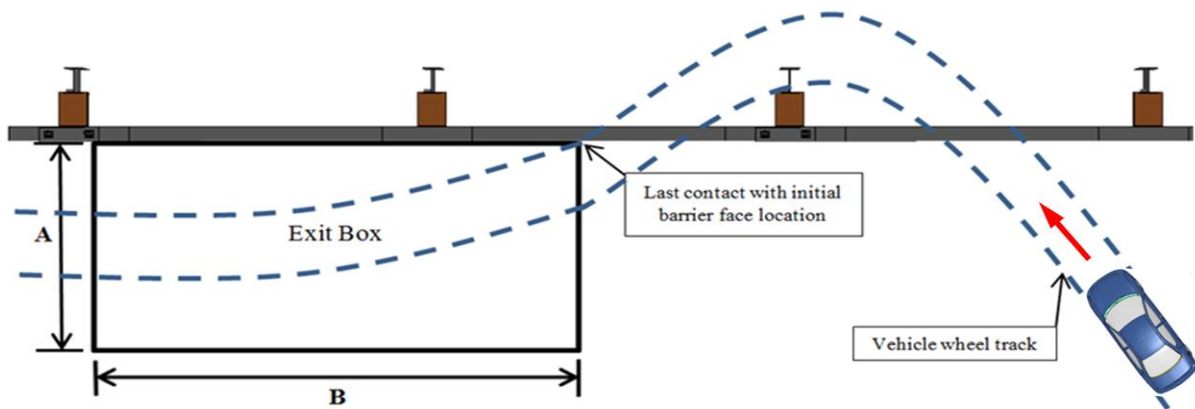


Fig. 4.1: The exit-box criterion in MASH.

Table 4.1: The exit box criterion defined in MASH

Vehicle Type	Exit Box Dimension	
	A	B
Cars or Pickup Trucks	$7.2 + V_W + 0.16V_L \text{ (ft)}$	32.8 ft (10 m)
Other Vehicles	$14.4 + V_W + 0.16V_L \text{ (ft)}$	65.6 ft (20 m)

In Table 4.1, V_W and V_L stand for the vehicle's width and length, respectively. According to the exit box criterion, if all four wheels of the vehicle remain inside the exit box for the distance B, the case is considered to be a safe redirect. Although the exit box criterion is a useful tool for determining the post-impact vehicular trajectories, use of this criterion alone is not sufficient to determine if the vehicle has been safely redirected. In addition, a large exit angle and/or spin-outs, which may be caused by pocketing and snagging of the vehicle on the guardrail posts, may still be present even for a case determined as a safe redirect by the exit box criterion.

The exit box dimensions for the Dodge Neon and Ford F250 were obtained using the formula in Table 4.1 and the vehicle data in Table 3.1. The exit box dimensions for both vehicles are given in Table 4.2. These two exit boxes were used to assess the post-impact vehicular responses from the simulation results.

Table 4.2: Exit box dimensions for the test vehicles of this project

Vehicle	Exit Box Dimension	
	A	B
1996 Dodge Neon	15.1 <i>ft</i> (4.6 <i>m</i>)	32.8 <i>ft</i> (10.0 <i>m</i>)
2006 Ford F250	16.9 <i>ft</i> (5.15 <i>m</i>)	32.8 <i>ft</i> (10.0 <i>m</i>)

4.1 Case 1: Guardrails Placed at the Curb Face

In this case, the 27-, 29-, and 31-inch guardrails were evaluated when placed at the curb face and impacted by both the Dodge Neon and Ford F250. Two impact angles, 25° and 15°, were used in the evaluation. The impact speed used in all simulations was 44 mph (70 km/hour). Table 4.3 gives a summary of the simulation results that were used to evaluate guardrail performance in terms of vehicular responses.

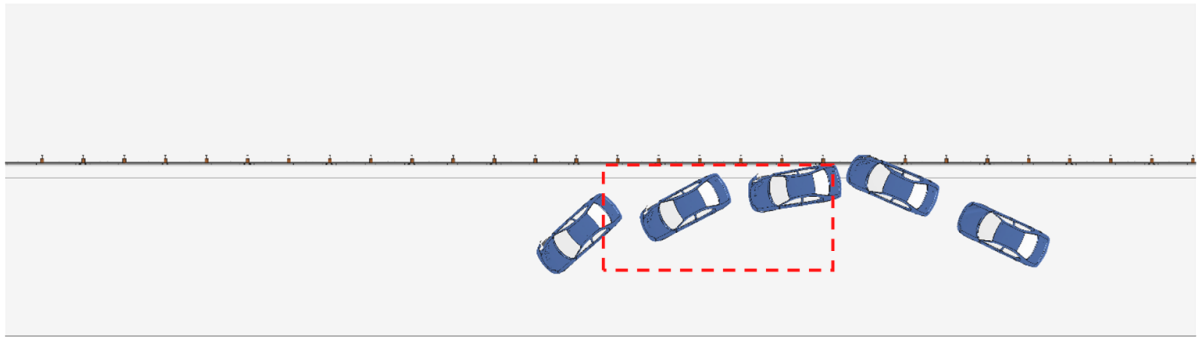
Table 4.3: Simulation results of Case 1 (guardrails placed at the curb face)

Guardrail Height	Test Vehicle	Impact Angle	Simulation Results
27 inch	Dodge Neon	25°	The vehicle passed the exit box criterion but had a large exit angle
		15°	The vehicle passed the exit box criterion and was safely redirected
	Ford F250	25°	The vehicle passed the exit box criterion and was safely redirected
		15°	The vehicle passed the exit box criterion and was safely redirected
29 inch	Dodge Neon	25°	The vehicle snagged on the guardrail with a large rotation
		15°	The vehicle passed the exit box criterion and was safely redirected
	Ford F250	25°	The vehicle failed the exit box criterion by a small amount
		15°	The vehicle passed the exit box criterion and was safely redirected
31 inch	Dodge Neon	25°	The vehicle snagged on the guardrail with a large rotation
		15°	The vehicle passed the exit box criterion and was safely redirected
	Ford F250	25°	The vehicle snagged on the guardrail with a large rotation
		15°	The vehicle passed the exit box criterion and was safely redirected

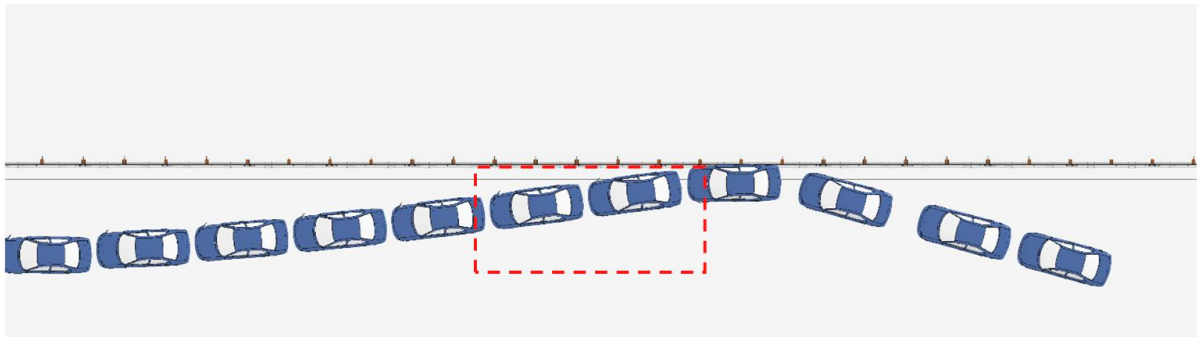
4.1.1 The 27-inch Guardrail at the Curb Face

Figure 4.2 shows the top view of vehicle trajectory of the Dodge Neon impacting at 25° and 15° into the 27-inch guardrail placed at the curb face. The W-beam guardrail is shown in its

original shape and the exit box is shown by the rectangle in dash lines. It can be seen that the vehicle was safely redirected for both impacts according to the MASH exit box criterion.

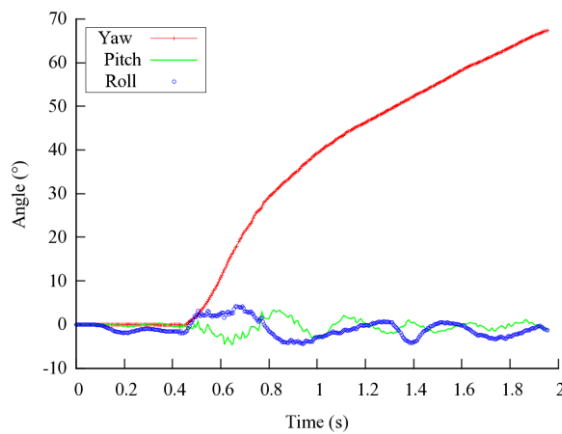


a. At 44 mph (70 km/hour) and 25°

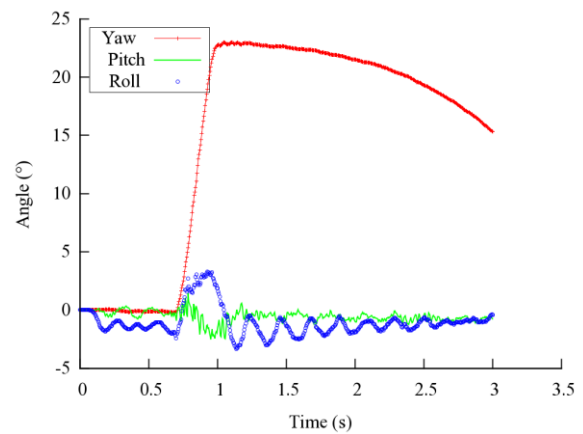


b. At 44 mph (70 km/hour) and 15°

Fig. 4.2: A Dodge Neon impacting the 27-inch guardrail at the curb face.



a. At 44 mph (70 km/hour) and 25°



b. At 44 mph (70 km/hour) and 15°

Fig. 4.3: Yaw, pitch, and roll angles of Dodge Neon impacting the 27-inch guardrail at the curb face.

The yaw, pitch, and roll angles of the Dodge Neon in both the 25° and 15° impacts are shown in Fig. 4.3. The exit angles of these two impacts were determined to be 15° and 8°, respectively, by subtracting the impact angles from the respective yaw angles at exit (i.e., 40° and 23°). It should be noted that although the exit box criterion was met in the 25° impact, the vehicle was not safely redirected due to the continuous spin after leaving the exit box as indicated by the increasing yaw angle. The roll and pitch angles of both cases were less than five degrees in either positive or negative direction; they passed the MASH evaluation criterion F, which specified a maximum 75° roll or pitch angle.

Figure 4.4 shows the permanent deformations of the guardrail under the impacts by the Dodge Neon at 25° and 15°. It can be seen that the damaged guardrail sections are small and localized; this serves as an indication of relatively low-severity impact from the small car.

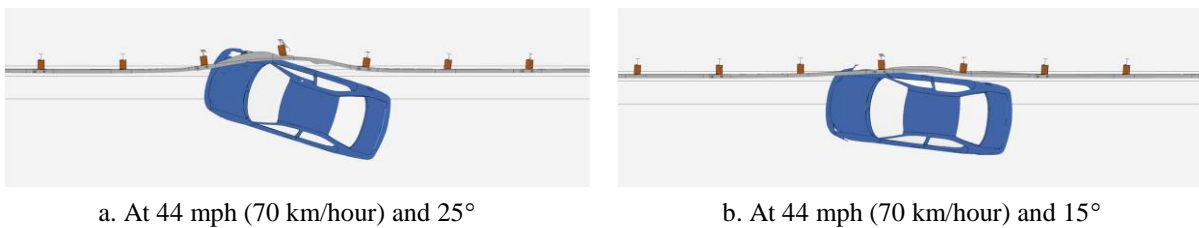


Fig. 4.4: Permanent deformation of the 27-inch guardrail at the curb face and impacted by a Dodge Neon.

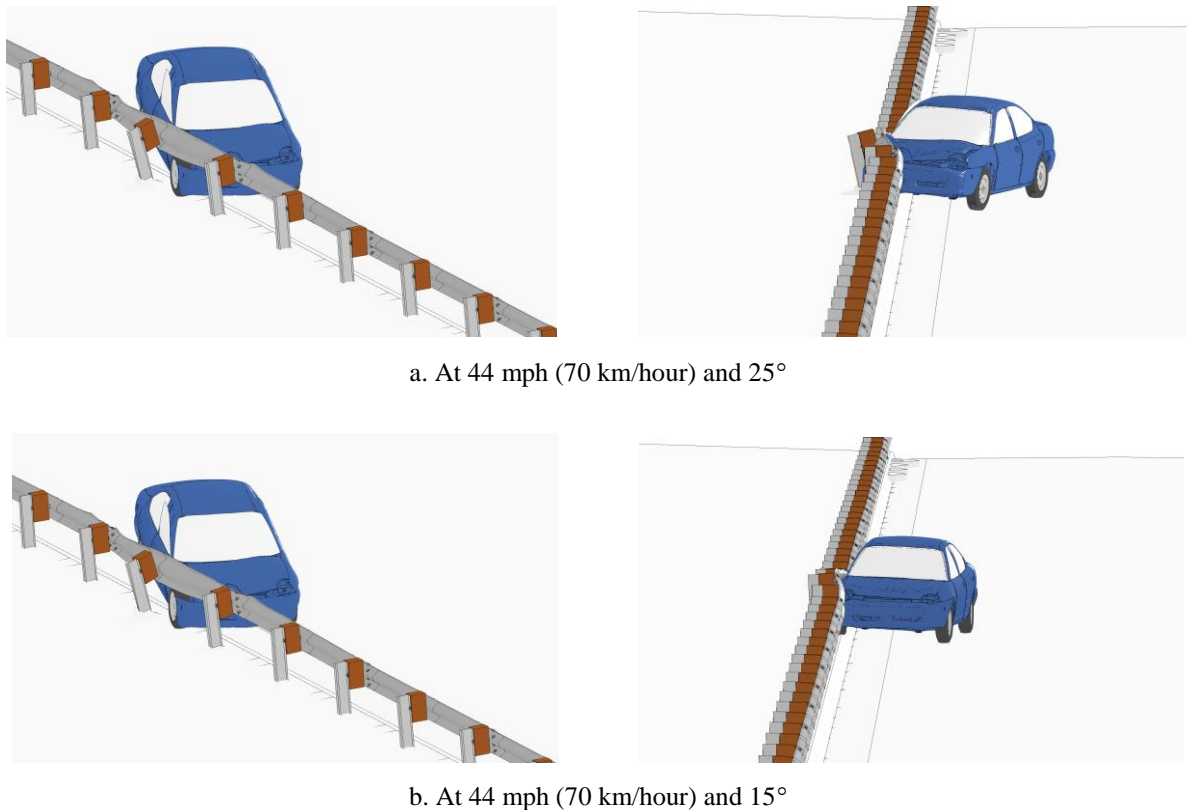


Fig. 4.5: Simulations of Dodge Neon impacting the 27-inch guardrail at the curb face.

Figure 4.5 shows the detailed views of vehicle-barrier interactions while the vehicle running up the curb and impacting the guardrail. Figures 4.6 and 4.7 show the time histories of transverse displacements and velocities measured at the center of gravity (CG) point of the vehicle in the 25° and 15° impacts, respectively. The transverse velocities, along with the exit angle, could be used to determine if a redirection was safe or temporary. For example, if the transverse velocity of a redirected vehicle remained large, the redirection could be followed by a secondary collision if the exit angle was also large. For the case of the Dodge Neon, the transverse velocities were 5 and 1 mph for the 25° and 15° impacts, respectively, towards the travel lane. The small transverse velocities confirmed the safe redirection of the Dodge Neon.

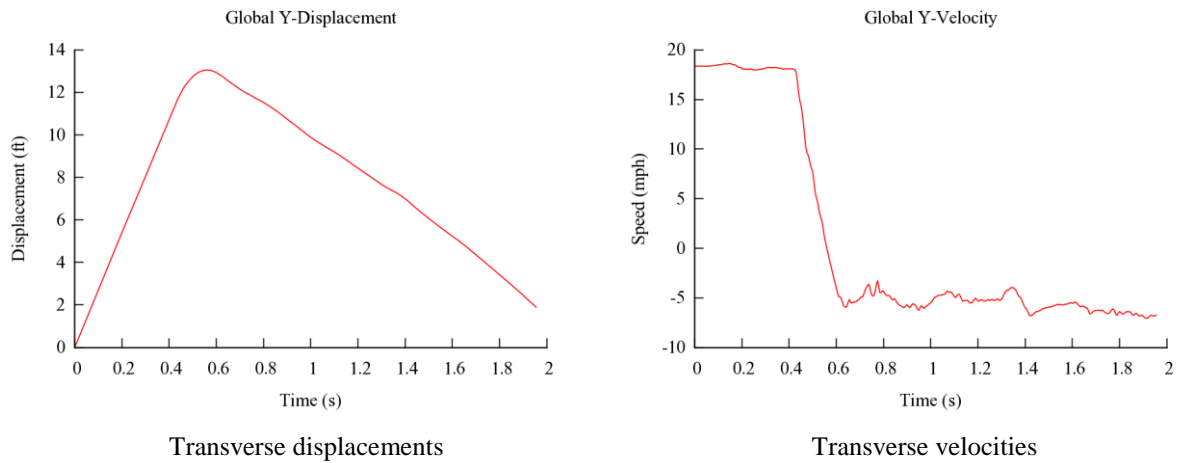


Fig. 4.6: Transverse displacements and velocities of the Dodge Neon impacting the 27-inch guardrail at the curb face at 44 mph (70 km/hour) and 25°.

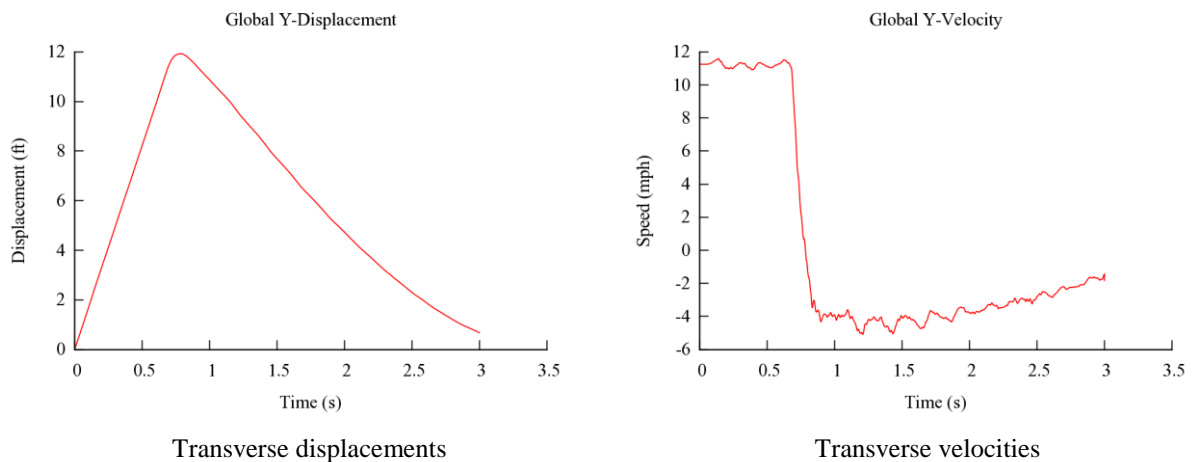
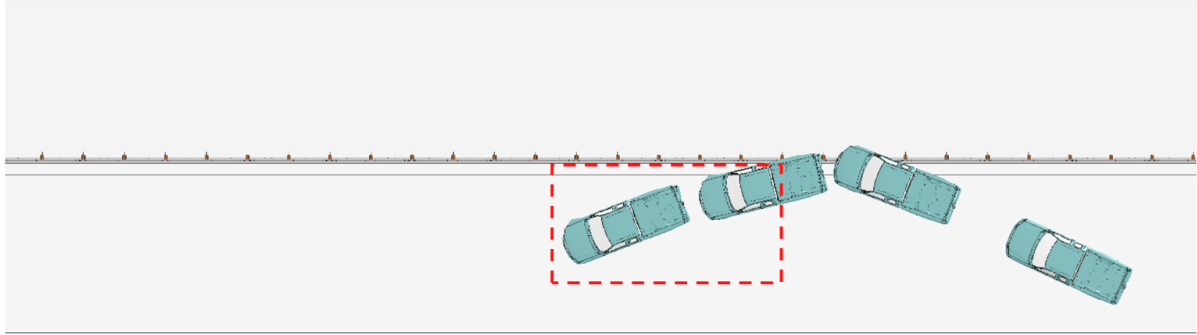


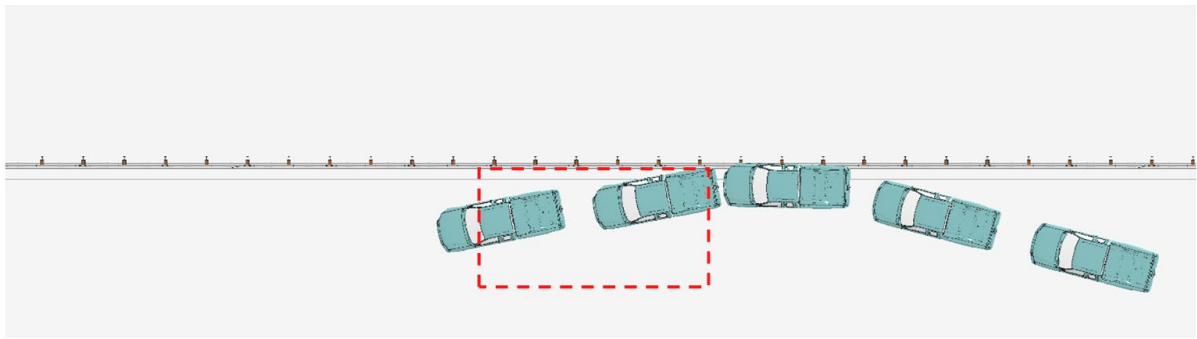
Fig. 4.7: Transverse displacements and velocities of the Dodge Neon impacting the 27-inch guardrail at the curb face at 44 mph (70 km/hour) and 15°.

Under impacts of the Ford F250 at both 25° and 15°, the 27-inch W-beam guardrail placed at the curb face was found to perform well. Figure 4.8 shows the top view of vehicle trajectory

of the Ford F250 in both cases along with the exit boxes. Similar to the cases of the Dodge Neon, the W-beam guardrail is shown in its original shape and the exit box is shown by the rectangle in dash lines. It can be seen that the vehicle was safely redirected for both impacts according to the MASH exit box criterion.

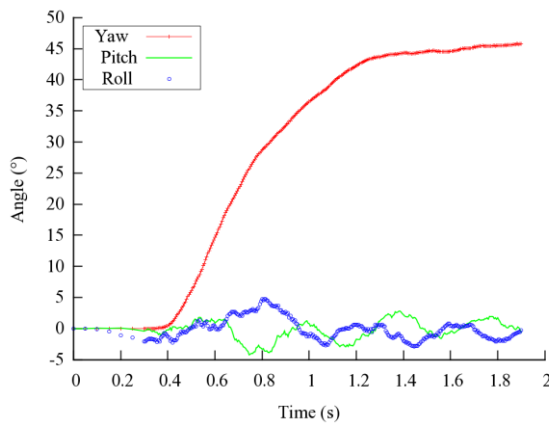


a. At 44 mph (70 km/hour) and 25°

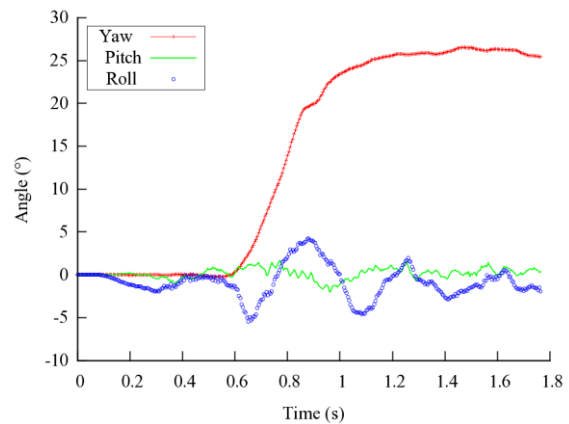


b. At 44 mph (70 km/hour) and 15°

Fig. 4.8: A Ford F250 impacting the 27-inch guardrail at the curb face.



a. At 44 mph (70 km/hour) and 25°



b. At 44 mph (70 km/hour) and 15°

Fig. 4.9: Yaw, pitch, and roll angles of Ford F250 impacting the 27-inch guardrail at the curb face.

The yaw, pitch, and roll angles of the Ford F250 in both the 25° and 15° impacts are shown in Figure 4.9. The exit angles of these two impacts were determined to be 19° and 10°, respectively, by subtracting the impact angles (i.e., 25° and 15°) from the respective yaw angles at exit (i.e., 44° and 25°). For the 25° impact, the exit angle of the Ford F250 was slightly larger than that of the Dodge Neon in the 25° impact; however, the Ford F250 did not exhibit any spin as seen on the Dodge Neon. In addition, the roll and pitch angles in both the 25° and 15° impacts by Ford F250 were less than five degrees in either positive or negative direction and thus passed the MASH evaluation criterion F, which specified a maximum 75° roll or pitch angle.

Figure 4.10 shows the permanent deformations of the 27-inch guardrail under impacts by the Ford F250 at 25° and 15°. It can be seen that the transverse deflection of the guardrail under the 25° impact was significantly larger than that in the 15° impact. The guardrail's transverse deflection under the 15° impact by Ford F250 was similar to that by the Dodge Neon, but the guardrail's transverse deflection under the 25° impact by the Ford F250 was significantly larger than that under the 25° impact by the Dodge Neon. This observation indicated that the guardrail was more susceptible to large-angle impacts by heavy vehicles (i.e., pickup trucks) than by small ones (i.e., passenger cars). Despite the large increase of vehicle mass, the 27-inch guardrail placed at the curb face was able to safely redirect the Ford F250 with an impact at 44 mph (70 km/hour) and 25°.

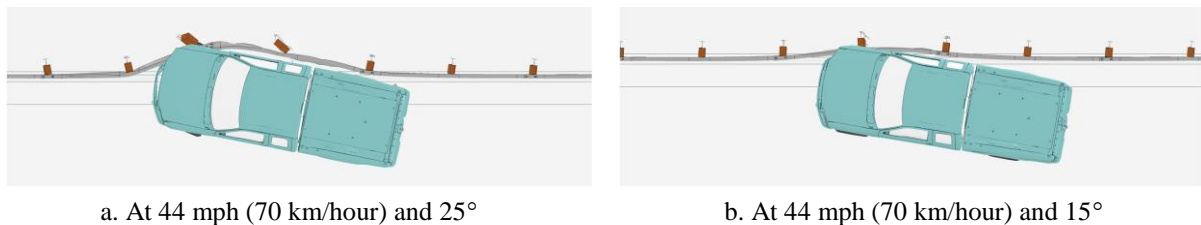
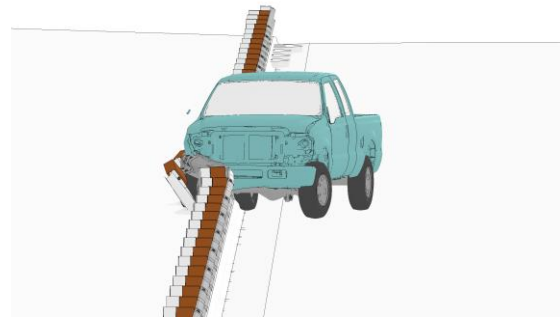
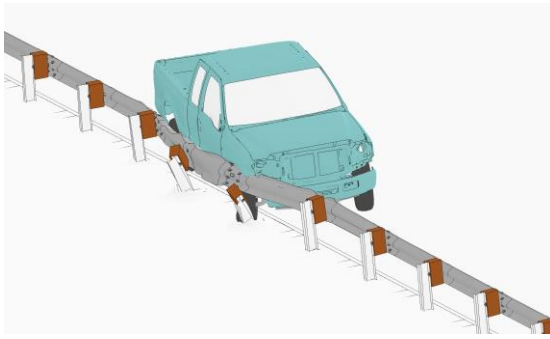


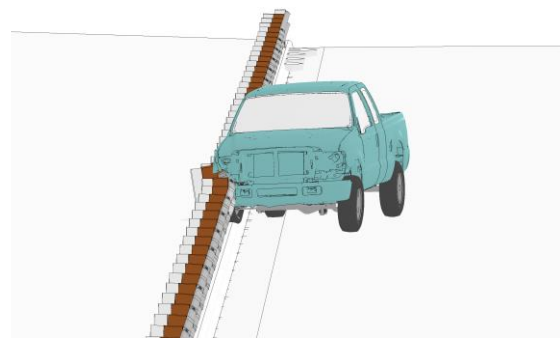
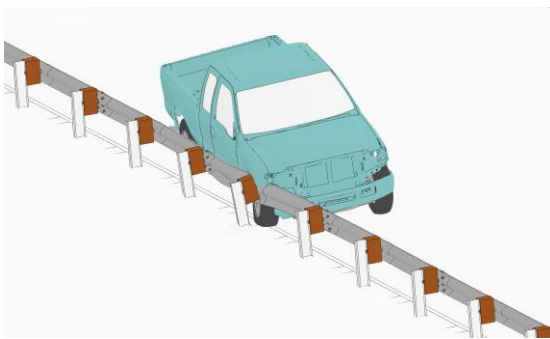
Fig. 4.10: Permanent deformation of 27-inch guardrail at the curb face and impacted by a Ford F250.

Figure 4.11 shows the detailed views of vehicle-barrier interactions while the Ford F250 running up the curb and impacting the guardrail. When installed at the face of curb, the 27-inch guardrail engaged well with the bumper cover and wheel fender of the Ford F250 and thus effectively redirected the vehicle. Due to its high profile, the Ford F250 had a better engagement with the guardrail than the Dodge Neon, which partially went under the W-beam rail in the 25° impact.

Figures 4.12 and 4.13 show the time histories of transverse displacements and velocities measured at the CG point of Ford F250 in the 25° and 15° impacts, respectively. For both cases, the transverse velocities were approximately 5 mph towards the travel lane, indicating a relatively small chance of getting involved in a secondary collision. The results in Figures 4.8 to 4.13, along with those of the Dodge Neon, indicated the effectiveness of the 27-inch guardrail placed at face of curb and impacted by a pickup truck and a passenger car at MASH TL-2 conditions.

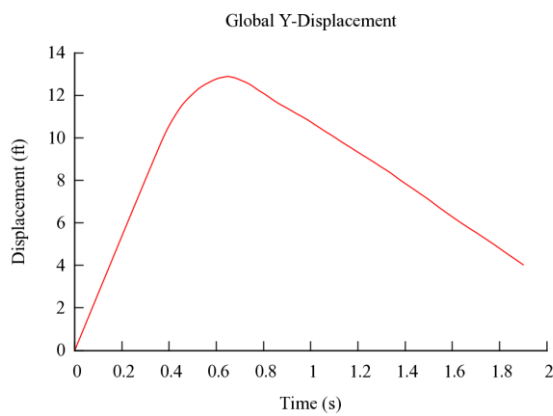


a. At 44 mph (70 km/hour) and 25°

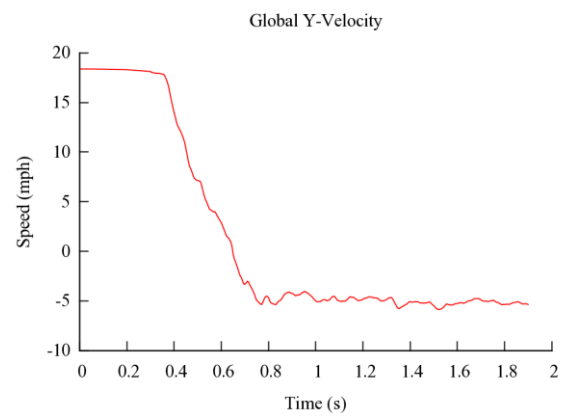


b. At 44 mph (70 km/hour) and 15°

Fig. 4.11: Simulations of Ford F250 impacting the 27-inch guardrail at the curb face.



Transverse displacements



Transverse velocities

Fig. 4.12: Transverse displacements and velocities of the Ford F250 impacting the 27-inch guardrail at the curb face at 44 mph (70 km/hour) and 25°.

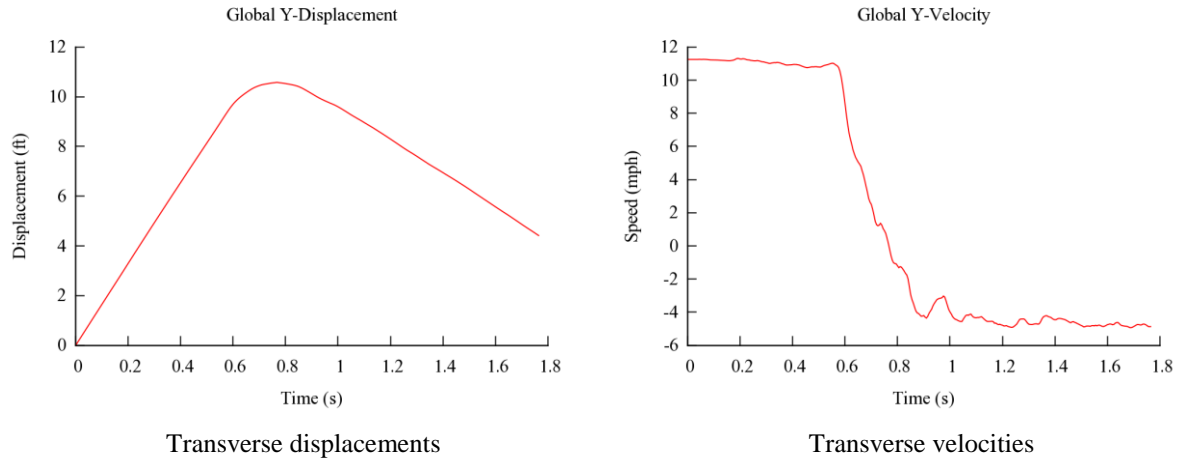
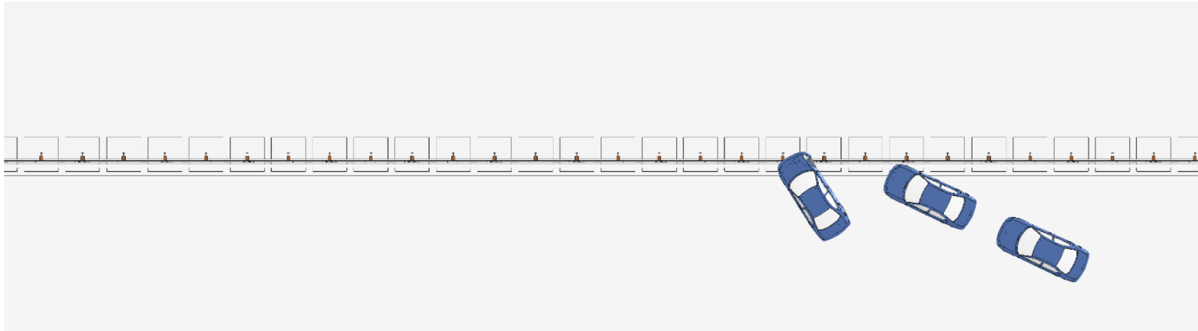


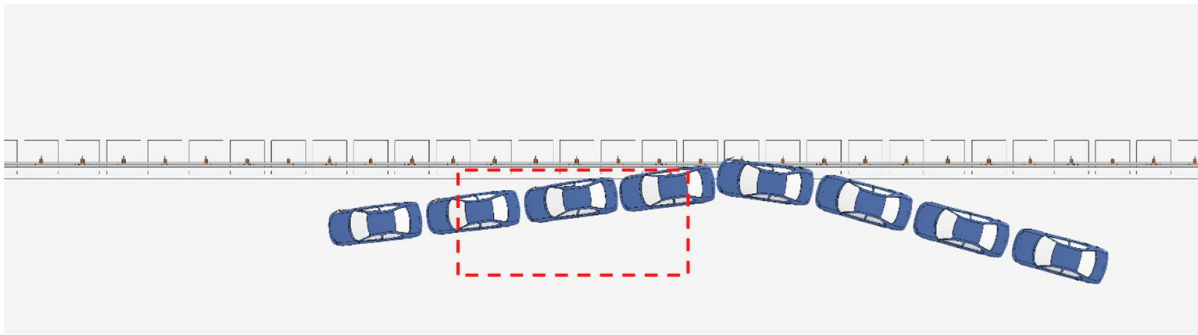
Fig. 4.13: Transverse displacements and velocities of the Ford F250 impacting the 27-inch guardrail at the curb face at 44 mph (70 km/hour) and 15°.

4.1.2 The 29-inch Guardrail at the Curb Face

Figure 4.14 shows the top view of vehicle trajectory of the Dodge Neon impacting the 29-inch guardrail placed at the curb face at 25° and 15°.



a. At 44 mph (70 km/hour) and 25°



b. At 44 mph (70 km/hour) and 15°

Fig. 4.14: A Dodge Neon impacting the 29-inch guardrail at the curb face.

Upon impacting at 25° on the 29-inch guardrail at the curb face, the Dodge Neon snagged on a guardrail post and spun about the post. This was due to the relatively low vehicle profile and the elevated rail height of the guardrail when placed at the face of curb. Since the vehicle did not lose contact with the guardrail (in its original position) during the entire course, the exit box was not needed for this case. Figure 4.14 shows the exit box for the 15° impact in which the MASH exit box criterion was satisfied and the vehicle was safely redirected.

The yaw, pitch, and roll angles of the Dodge Neon in both the 25° and 15° impacts are shown in Fig. 4.15. The exit angle of the 15° impact was determined to be 7° by subtracting the impact angle from the yaw angle at exit (i.e., 22°). For the 25° impact, the negative yaw angle indicated a clockwise rotation of the vehicle.

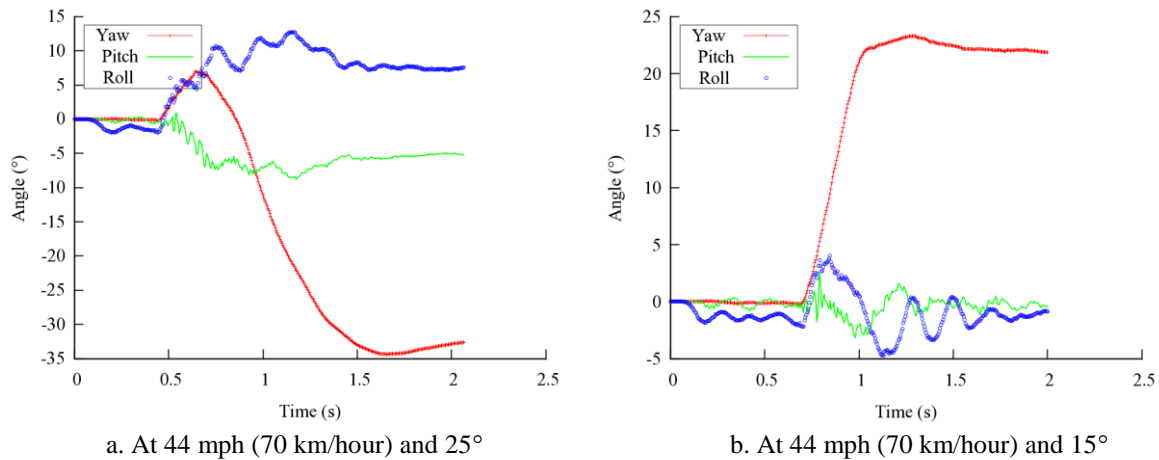


Fig. 4.15: Yaw, pitch, and roll angles of Dodge Neon impacting the 29-inch guardrail at the curb face.

The permanent deformations of the 29-inch guardrail under impacts by the Dodge Neon at 25° and 15° are shown in Fig. 4.16. It can be seen that the transverse deflection of the guardrail in the 25° impact was significantly larger than that in the 15° impact. Compared to the 27-inch guardrail under the 25° impact by the Dodge Neon (see Fig. 4.4a), the 29-inch guardrail had a significantly larger transverse deflection. At the 29-inch rail height, the guardrail had very small engagement with the vehicle's bumper cover and fender. The Dodge Neon intruded under the rail, engaged with the rail on the hood, and dragged the rail forward, resulting in a large transverse deflection of the guardrail.

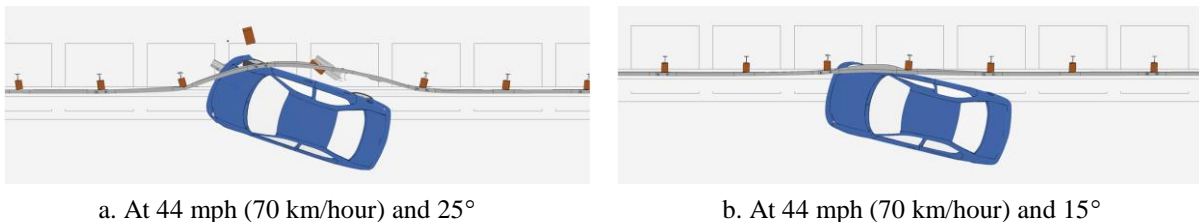
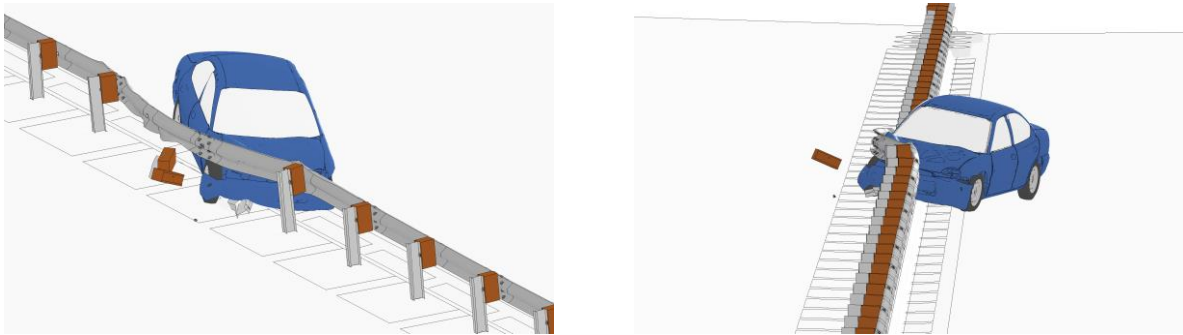
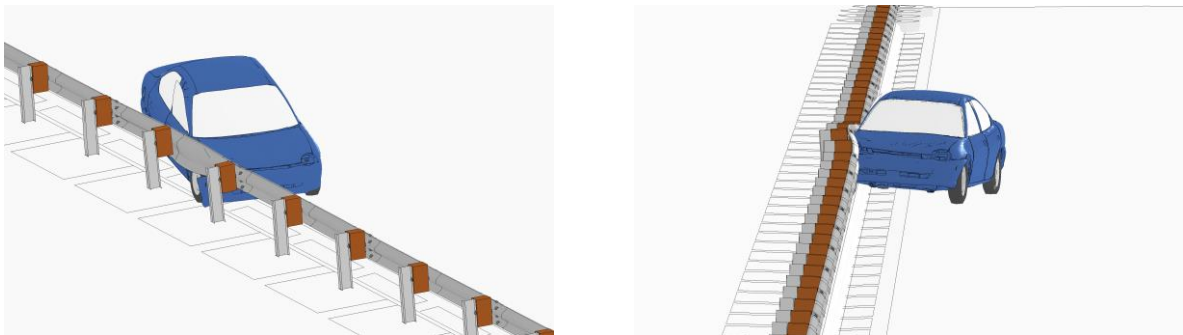


Fig. 4.16: Permanent deformation of the 29-inch guardrail at the curb face and impacted by a Dodge Neon.

Figure 4.17 shows the detailed views of vehicle-barrier interactions while the Dodge Neon running up the curb and impacting the 29-inch guardrail. In the 25° impact, due to the vehicle's low front profile and compressed suspension when climbing up the curb, the rail of the 29-inch guardrail did not have much engagement with the vehicle's bumper cover and wheel fender. Therefore, the vehicle intruded under the guardrail and snagged on a post. In the 15° impact, the vehicle's right side had more contact with the rail, which helped redirect the vehicle as seen in Fig.14b.



a. At 44 mph (70 km/hour) and 25°



b. At 44 mph (70 km/hour) and 15°

Fig. 4.17: Simulations of Dodge Neon impacting the 29-inch guardrail at the curb face.

Figures 4.18 and 4.19 show the time histories of transverse displacements and velocities measured at the CG point of the Dodge Neon in the 25° and 15° impacts, respectively. For the 25° impact, the transverse velocity of the vehicle was approximately zero, indicating no further displacement would occur towards either the travel lane or the guardrail. In this case, since the vehicle was snagged on the guardrail and spun around a post, it was unlikely to get involved in a secondary collision even though the MASH exit box criterion was not met. For the 15° impact, the transverse velocity was less than 5 mph towards the travel lane, indicating a relatively small chance of getting involved in a secondary collision. The results in Figs. 4.14 to 4.19 indicated that the 29-inch guardrail placed at face of curb could safely redirect a small car that impacted the guardrail at a small angle (e.g., 15°) and could cause snagging on a small vehicle impacting at a relatively large angle (e.g., 25°).

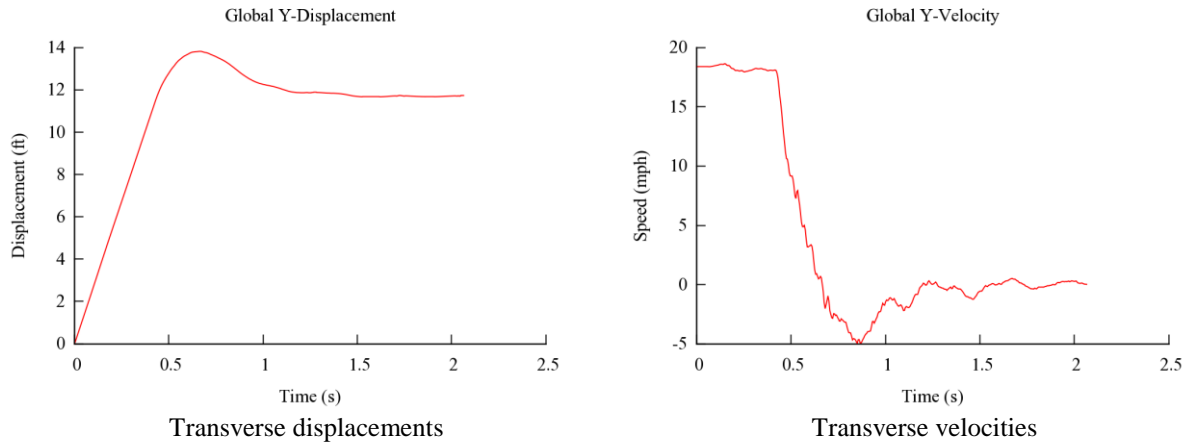


Fig. 4.18: Transverse displacements and velocities of the Dodge Neon impacting the 29-inch guardrail at the curb face at 44 mph (70 km/hour) and 25°.

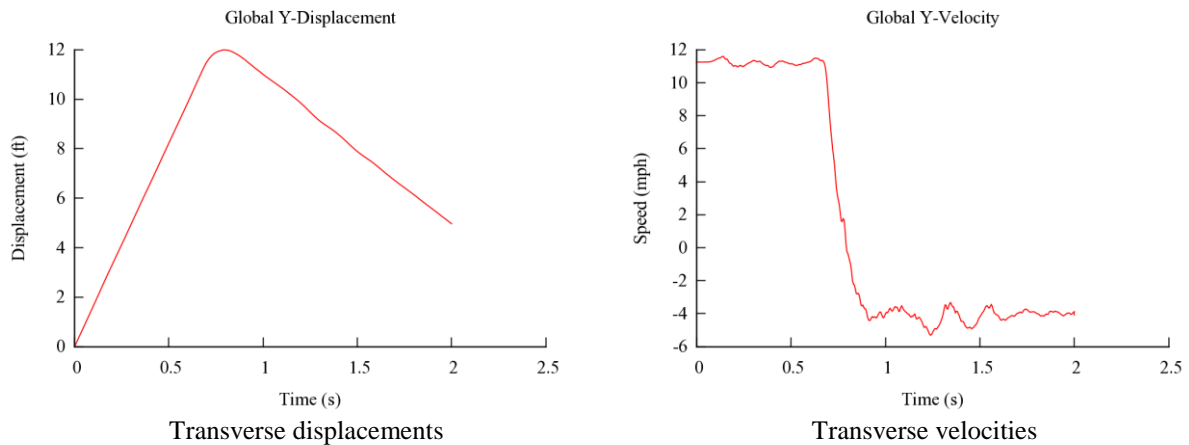
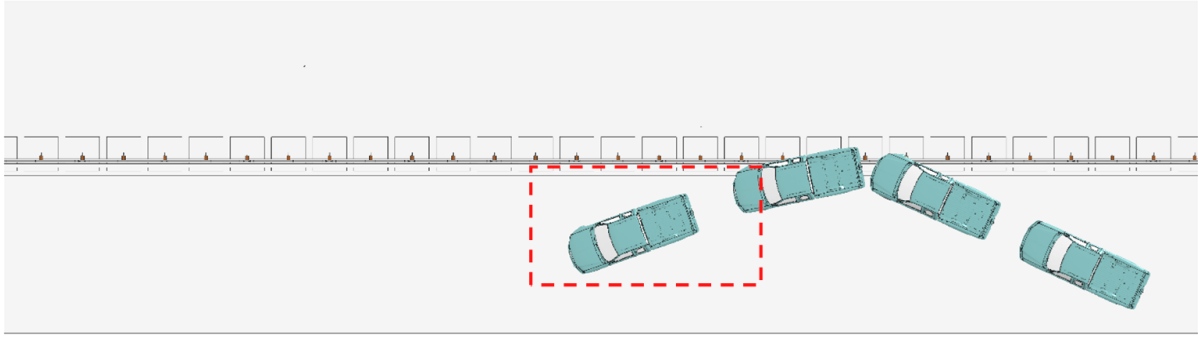
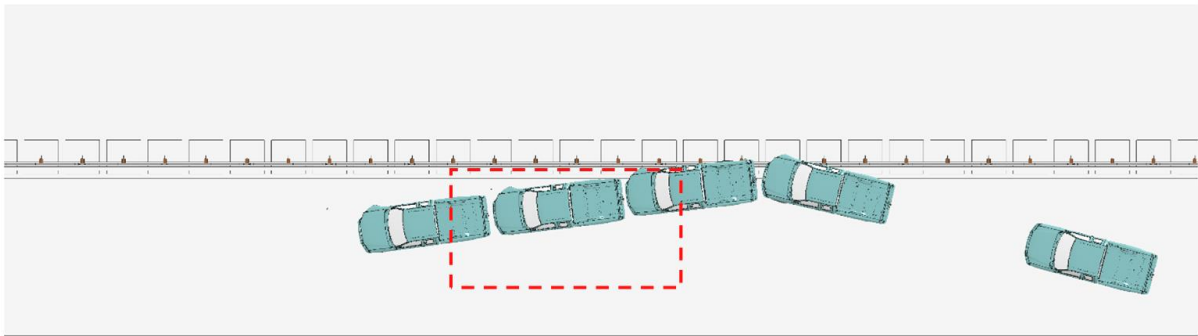


Fig. 4.19: Transverse displacements and velocities of the Dodge Neon impacting the 29-inch guardrail at the curb face at 44 mph (70 km/hour) and 15°.

Figure 4.20 shows the top view of vehicle trajectory of the Ford F250 in the 25° and 15° impacts on the 29-inch guardrail placed at the curb face, along with the exit boxes. In the 25° impact, the Ford F250 went out of the exit box from the bottom-left corner and thus did not meet the MASH exit box criterion. It should be noted that in the exit box criterion, the vehicle's wheel track rather than the vehicle's width is used to determine if the vehicle is within the exit box during a certain period (from the right-side to left-side of the exit box in Fig. 4.1). Therefore, the Ford F250 in Fig. 4.20a only touches the bottom side of the exit box by a small amount by wheel track marks. As pointed by Gowat and Gabauera (2013), the MASH exit box alone might not give a reliable indication of the possibility of a secondary collision; it worked better when the exit angle was also used. For the 15° impact, the 29-inch guardrail placed at the curb face met the MASH exit box criterion and safely redirected the Ford F250.

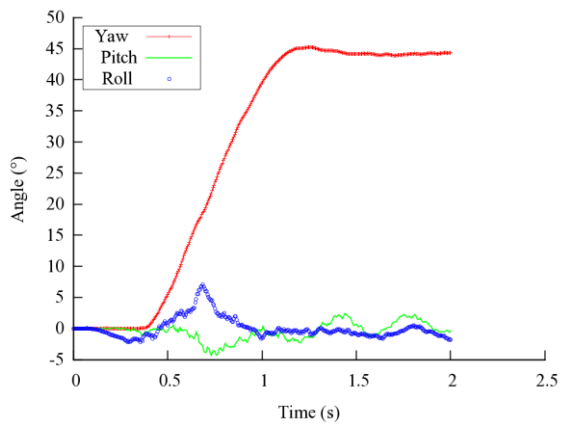


a. At 44 mph (70 km/hour) and 25°

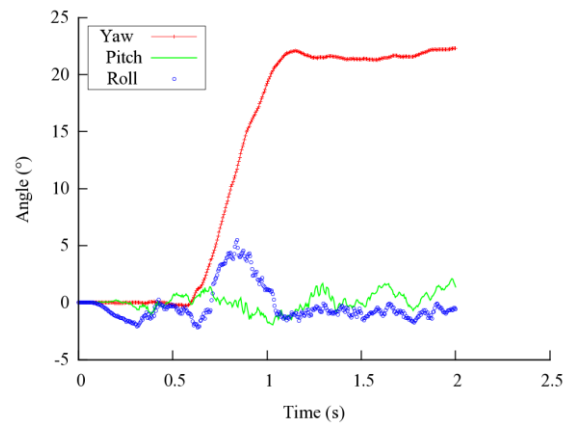


b. At 44 mph (70 km/hour) and 15°

Fig. 4.20: A Ford F250 impacting the 29-inch guardrail at face of curb.



a. At 44 mph (70 km/hour) and 25°



b. At 44 mph (70 km/hour) and 15°

Fig. 4.21: Yaw, pitch, and roll angles of Ford F250 impacting the 29-inch guardrail at face of curb.

The yaw, pitch, and roll angles of the Ford F250 in both the 25° and 15° impacts are shown in Fig. 4.21. The exit angles of these two impacts were determined to be 21° and 7°, respectively, by subtracting the impact angles from the respective yaw angles at exit (i.e., 46°

and 22°). The roll and pitch angles in both impacts were less than five degrees in either positive or negative direction and thus passed the MASH evaluation criterion F, which specified a maximum 75° roll or pitch angle.

The permanent deformations of the 29-inch guardrail impacted by the Ford F250 at 25° and 15° are shown in Fig. 4.22. The transverse deflections of the guardrail in both cases were relatively small and localized, though the guardrail deformation in the 25° impact was significantly larger than that in the 15° impact. In both cases, the vehicle had good interactions with the guardrail, as can be seen from Fig. 4.23.

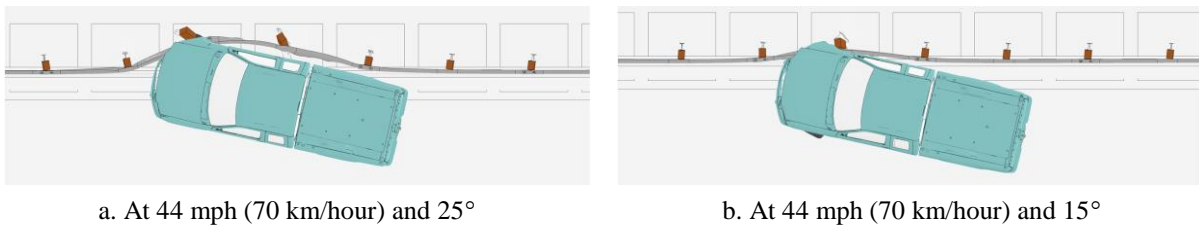


Fig. 4.22: Permanent deformation of the 29-inch guardrail at the curb face and impacted by a Ford F250.

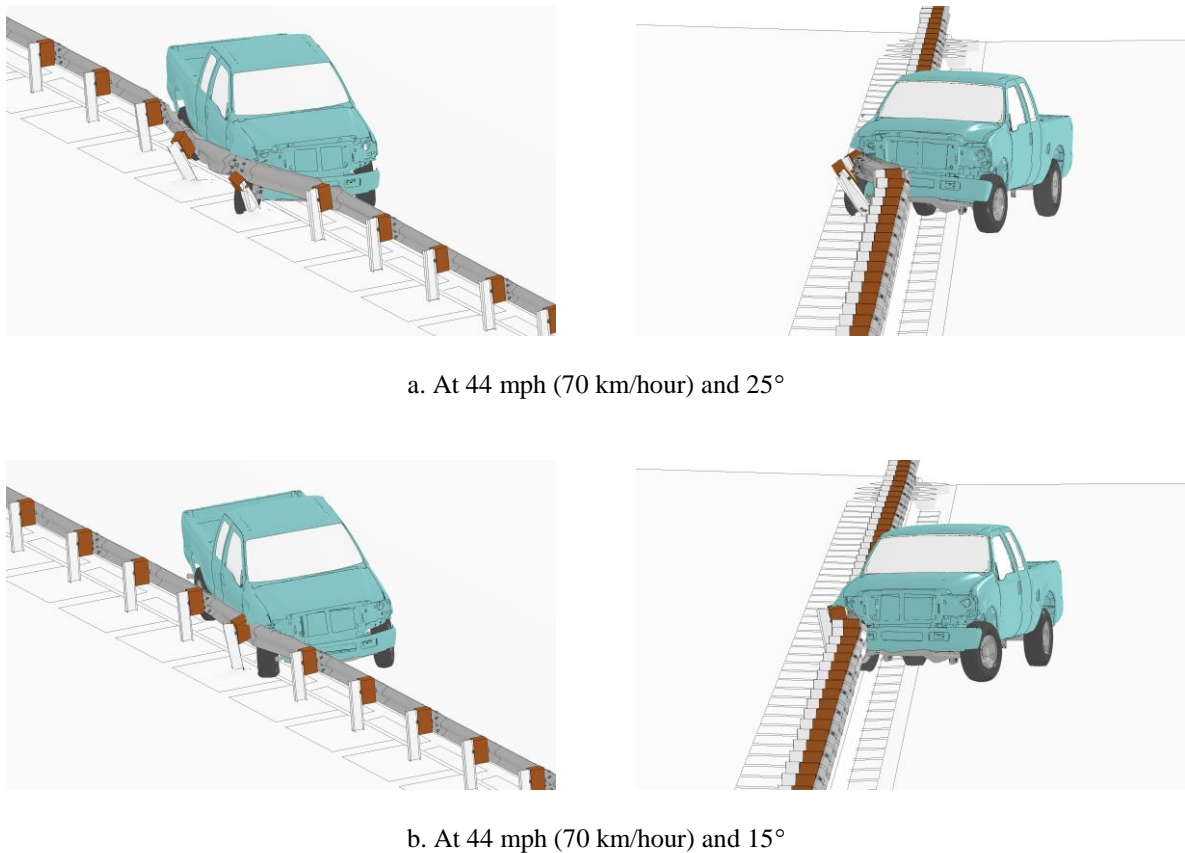


Fig. 4.23: Simulations of Ford F250 impacting the 29-inch guardrail at the curb face.

Figures 4.24 and 4.25 show the time histories of transverse displacements and velocities measured at the CG point of the Ford F250 in the 25° and 15° impacts, respectively. The transverse velocities of both cases were approximately 5 mph towards the travel lane. Considering the exit box criterion, exit angle, and transverse velocity, the Ford F250 had a relatively small chance of getting involved in a secondary collision in the 25° impact. For the 15° impact, the Ford F250 is unlikely to get involved in a secondary collision.

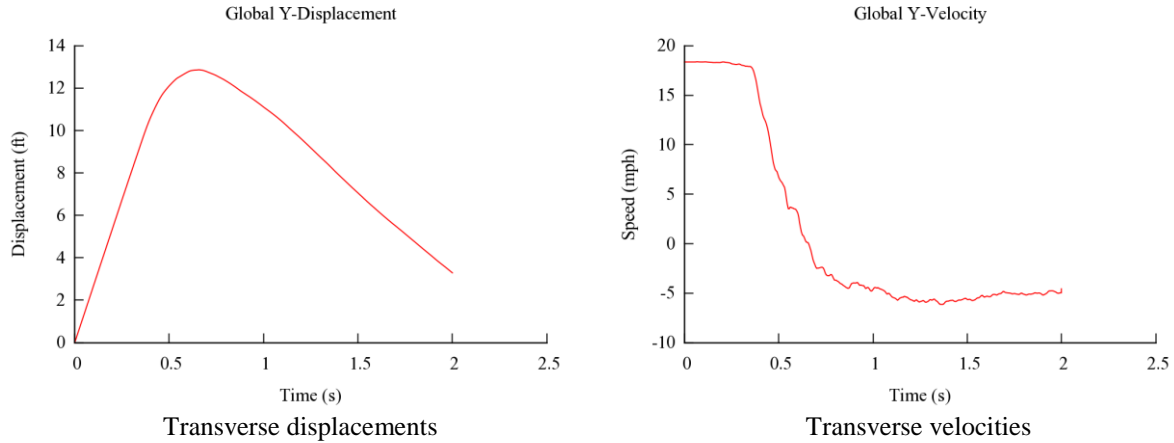


Fig. 4.24: Transverse displacements and velocities of the Ford F250 impacting the 29-inch guardrail at the curb face at 44 mph (70 km/hour) and 25°.

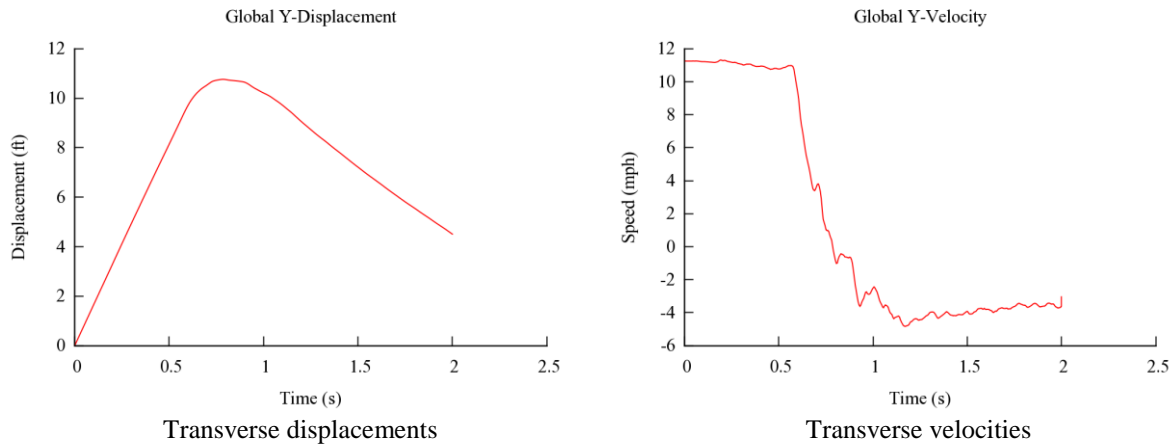
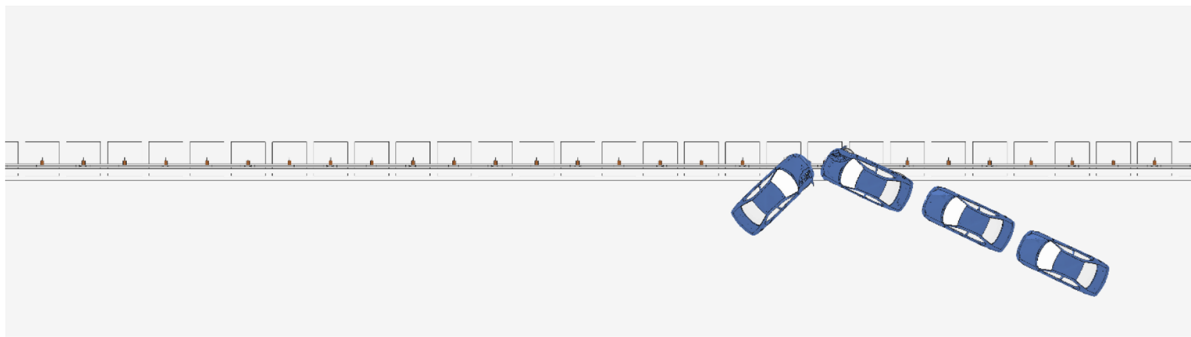


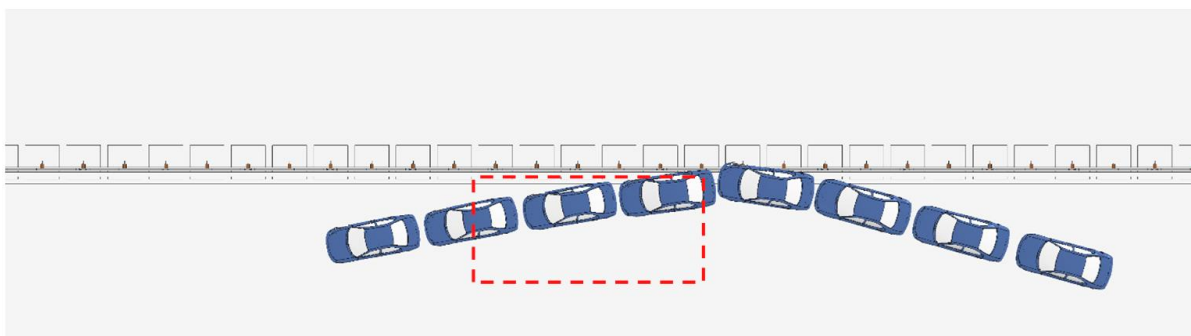
Fig. 4.25: Transverse displacements and velocities of the Ford F250 impacting the 29-inch guardrail at the curb face at 44 mph (70 km/hour) and 15°.

4.1.3 The 31-inch Guardrail at the Curb Face

The 31-inch guardrail had a similar performance to the 29-inch guardrail when placed at the curb face and impacted by a Dodge Neon at 25° and 15°. Figure 4.26 shows the vehicle trajectory of the Dodge Neon in both impacts. It can be seen that the vehicle snagged on the guardrail post in the 25° impact and was redirected in the 15° impact.



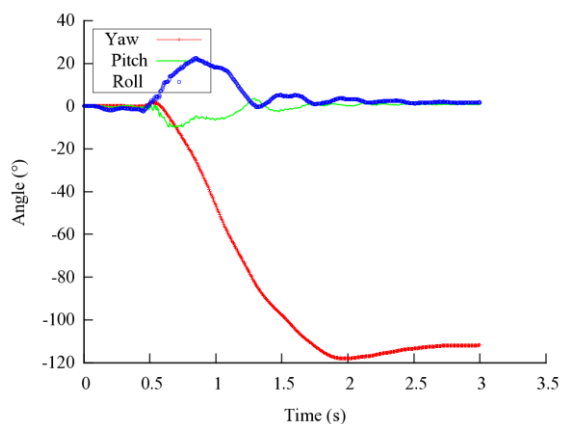
a. At 44 mph (70 km/hour) and 25°



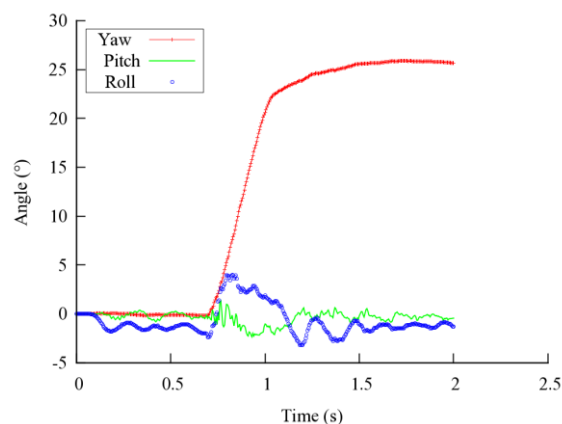
b. At 44 mph (70 km/hour) and 15°

Fig. 4.26: A Dodge Neon impacting the 31-inch guardrail at face of curb.

In Fig. 4.26, there is no exit box for the 25° impact, because the Dodge Neon snagged on a guardrail post and rotated about the post without leaving the guardrail. The yaw, pitch, and roll angles of the Dodge Neon are shown in Fig. 4.27. The exit angle of the 15° impact was determined to be 9° by subtracting the impact angle from the yaw angle at exit (24°). For the 25° impact, the negative yaw angle indicated a clockwise rotation of the vehicle. For the 15° impact, the small yaw angle and satisfaction to the exit box criterion indicated a safe redirect.



a. At 44 mph (70 km/hour) and 25°



b. At 44 mph (70 km/hour) and 15°

Fig. 4.27: Yaw, pitch, and roll angles of Dodge Neon impacting the 31-inch guardrail at the curb face.

The permanent deformations of the 31-inch guardrail under impacts of the Dodge Neon at 25° and 15° are shown in Fig. 4.16. It can be seen that the transverse deflections of the guardrail in both impacts were small and localized. Recall that in the case of the 29-inch guardrail impacted by the Dodge Neon at 25°, the increased rail height caused strong interaction between the rail and vehicle's hood, resulting in a significantly larger transverse deflection of the guardrail. In the case of the 31-inch guardrail, the further increased rail height caused the rail to have less interaction with the vehicle, resulting in a partial vehicle under-riding (see Fig. 4.28a) without developing a large transverse deflection of the rail.



Fig. 4.28: Permanent deformation of the 31-inch guardrail at the curb face and impacted by a Dodge Neon.

Figure 4.29 shows the detailed views of vehicle-barrier interactions while the Dodge Neon climbing up the curb and impacting the guardrail. In the 25° impact, the Dodge Neon went under the guardrail and snagged on a post. In the 15° impact, the vehicle had more contact with the rail on the right side, which helped redirect the vehicle.

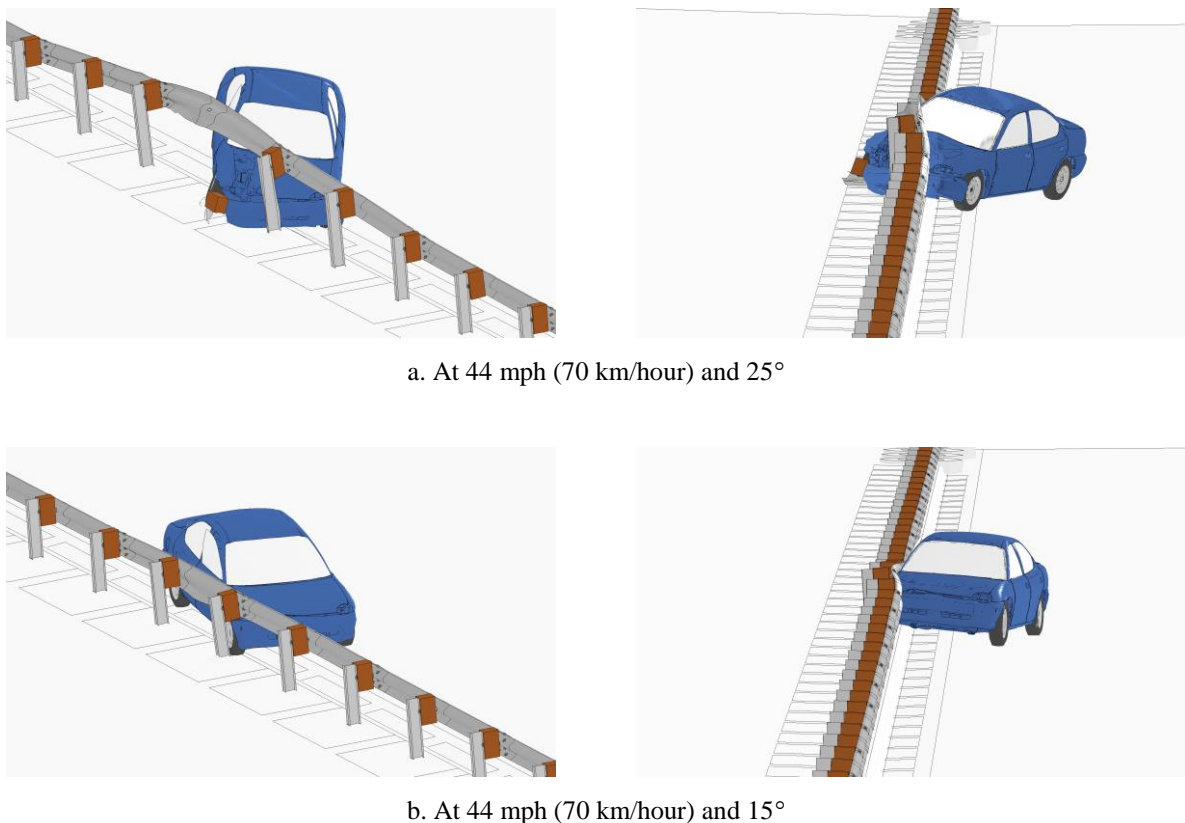


Fig. 4.29: Simulations of Dodge Neon impacting the 31-inch guardrail at the curb face.

Figures 4.30 and 4.31 show the time histories of transverse displacements and velocities measured at the CG point of the Dodge Neon in the 25° and 15° impacts, respectively. For the 25° impact, the transverse velocity of the vehicle was approximately zero, indicating no further displacement would occur towards either the travel lane or the guardrail. For the 15° impact, the transverse velocity was less than 5 mph towards the travel lane. For both cases, the probability of having a secondary collision was small even though the MASH exit box criterion was not met in the 25° impact.

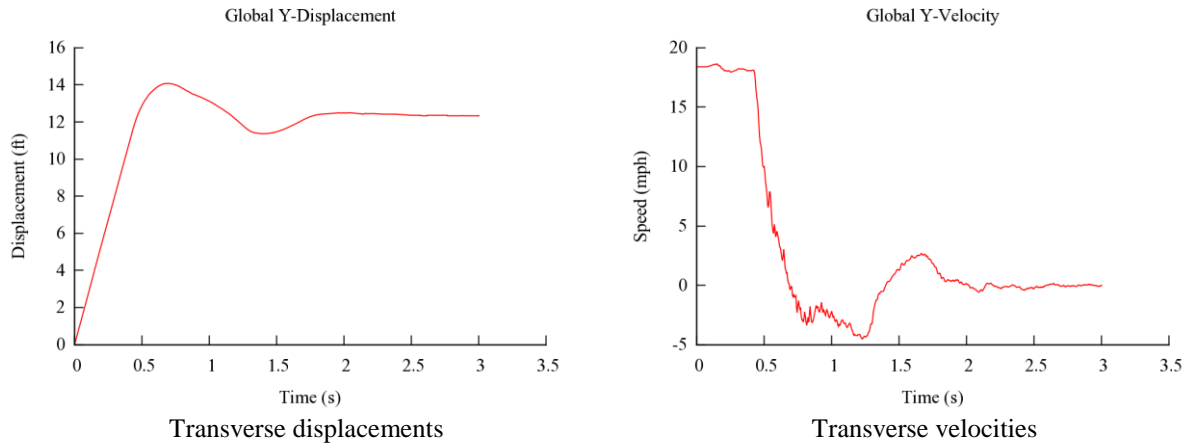


Fig. 4.30: Transverse displacements and velocities of the Dodge Neon impacting the 31-inch guardrail at the curb face at 44 mph (70 km/hour) and 25°.

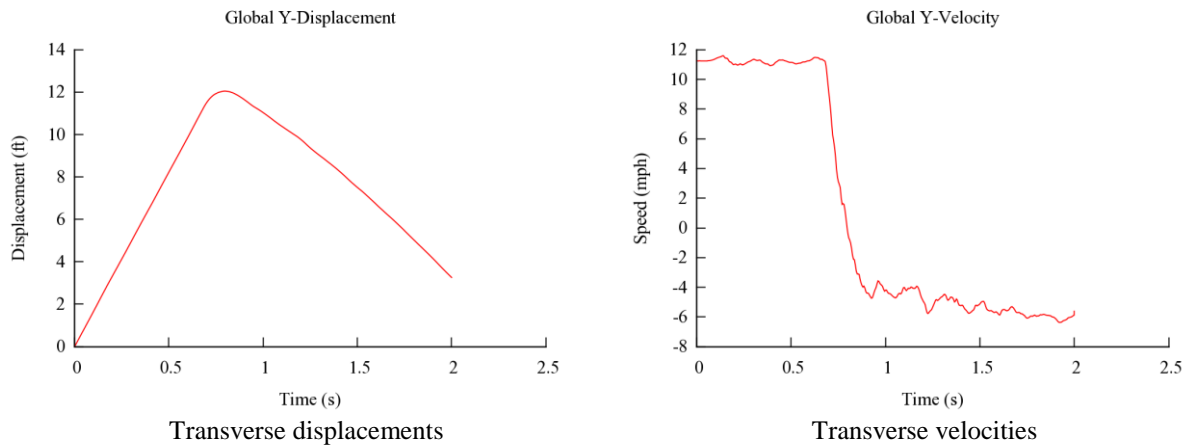
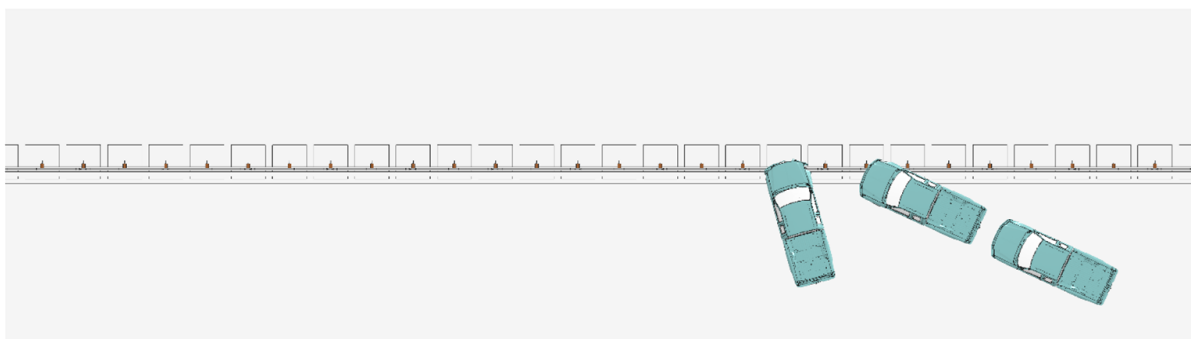
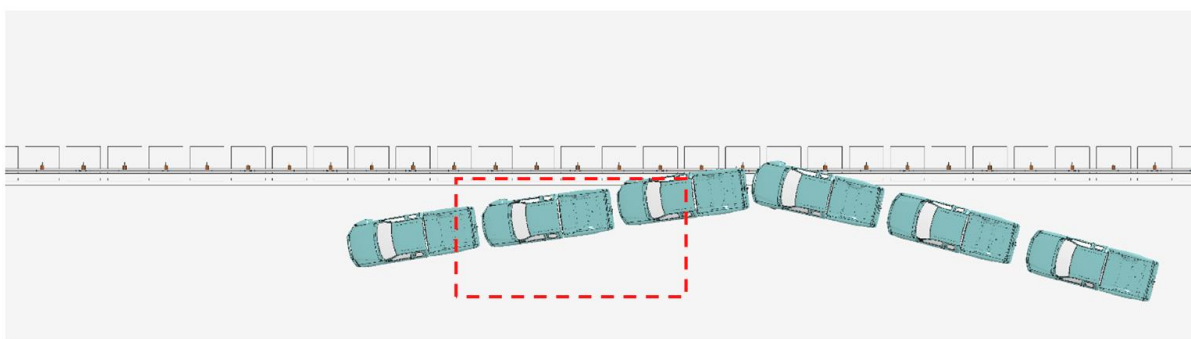


Fig. 4.31: Transverse displacements and velocities of the Dodge Neon impacting the 31-inch guardrail at the curb face at 44 mph (70 km/hour) and 15°.

Figure 4.32 shows the vehicle trajectory of the Ford F250 impacting the 31-inch guardrail placed at the curb face at 25° and 15°. In the 25° impact, the vehicle snagged on the guardrail post, similar to the case of the 31-inch guardrail impacted by a Dodge Neon at 25°. For the 15° impact, the MASH exit box criterion was met and the vehicle was redirected.



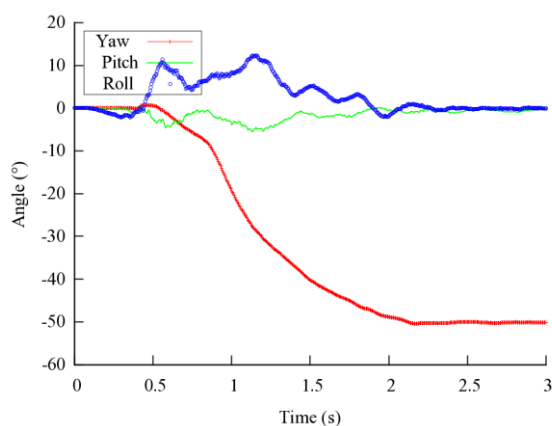
a. At 44 mph (70 km/hour) and 25°



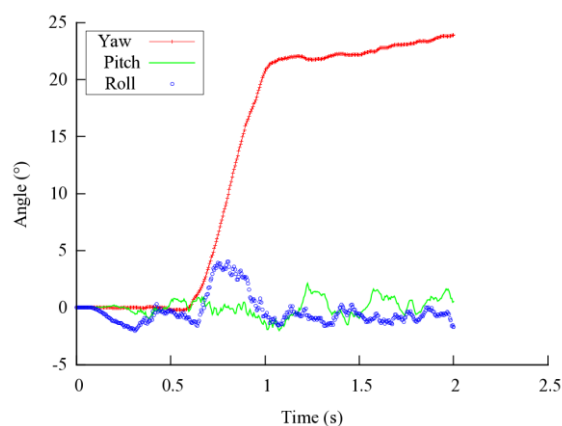
b. At 44 mph (70 km/hour) and 15°

Fig. 4.32: A Ford F250 impacting the 31-inch guardrail at the curb face.

The yaw, pitch, and roll angles of the Ford F250 are shown in Figure 4.33. The exit angle of the 15° impact was determined to be 7° by subtracting the impact angle from the yaw angle at exit (i.e., 22°). For the 25° impact, the negative yaw angle indicated a clockwise rotation of the vehicle. The roll and pitch angles in both impacts were less than three degrees in either positive or negative direction and thus passed the MASH evaluation criterion F.

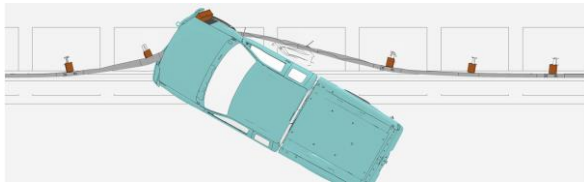


a. At 44 mph (70 km/hour) and 25°

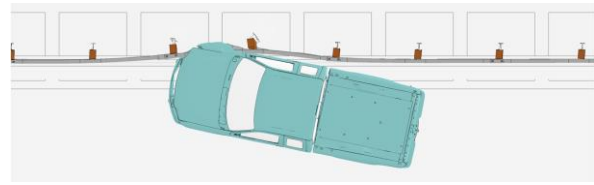


b. At 44 mph (70 km/hour) and 15°

Fig. 4.33: Yaw, pitch, and roll angles of Ford F250 impacting the 31-inch guardrail at the curb face.



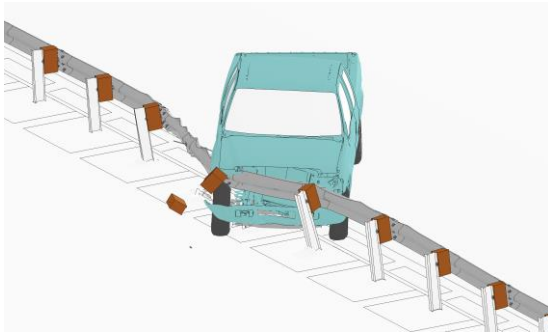
a. At 44 mph (70 km/hour) and 25°



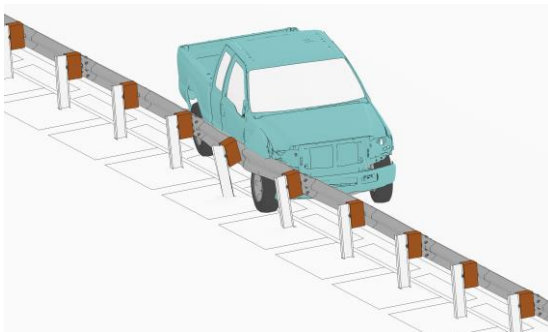
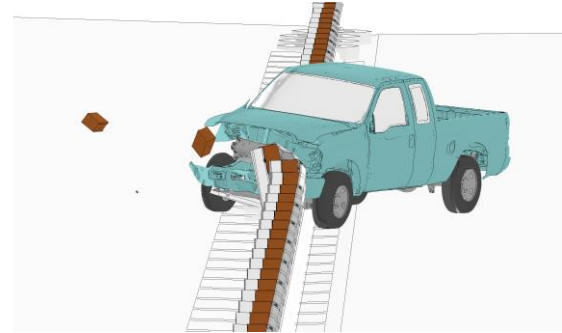
b. At 44 mph (70 km/hour) and 15°

Fig. 4.34: Permanent deformation of the 31-inch guardrail at the curb face and impacted by a Ford F250.

For the 25° impact, the transverse rail deflection of the 31-inch guardrail was similar to that of the 29-inch guardrail; however, the Ford F250 intruded more under the 31-inch guardrail than the 29-inch guardrail due to the increased rail height. Figure 4.35 shows the detailed views of vehicle-barrier interactions while the Ford F250 climbing up the curb and impacting the 31-inch guardrail. It can be seen from Fig. 4.35a that the rail of the 31-inch guardrail went under the hood of the Ford F250. This entanglement, though helped containing the vehicle, did not help redirecting the vehicle. Upon impacting the next post, the Ford F250 snagged on the guardrail and started to rotate clockwise when viewed from top.



a. At 44 mph (70 km/hour) and 25°



b. At 44 mph (70 km/hour) and 15°

Fig. 4.35: Simulations of Ford F250 impacting the 31-inch guardrail at the curb face.

Figures 4.36 and 4.37 show the time histories of transverse displacements and velocities measured at the CG point of the Ford F250 in the 25° and 15° impacts, respectively. For the 25° impact, the transverse velocity of the vehicle was approximately zero, indicating no further displacement would occur towards either the travel lane or the guardrail. The Ford F250 basically stuck on the guardrail (indicated by the zero transverse velocity in Fig. 4.33a) with no rotation (indicated by the constant yaw angle in Fig. 4.36a) after 2.2 seconds. For the 15° impact, the transverse velocity was approximately 4 mph towards the travel lane. For both cases, the probability of having a secondary collision was very small even though the MASH exit box criterion was not met in the 25° impact.

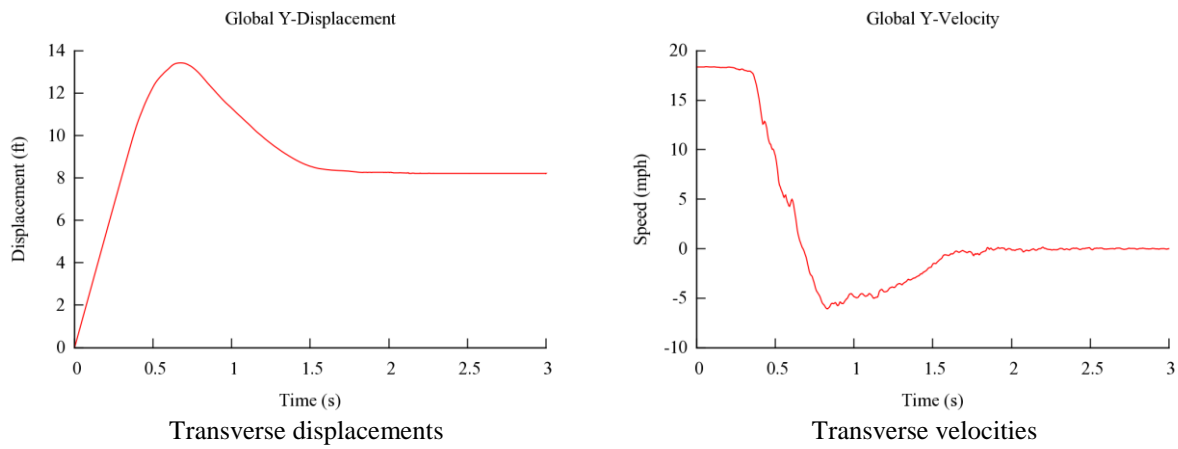


Fig. 4.36: Transverse displacements and velocities of the Ford F250 impacting the 31-inch guardrail at the curb face at 44 mph (70 km/hour) and 25°.

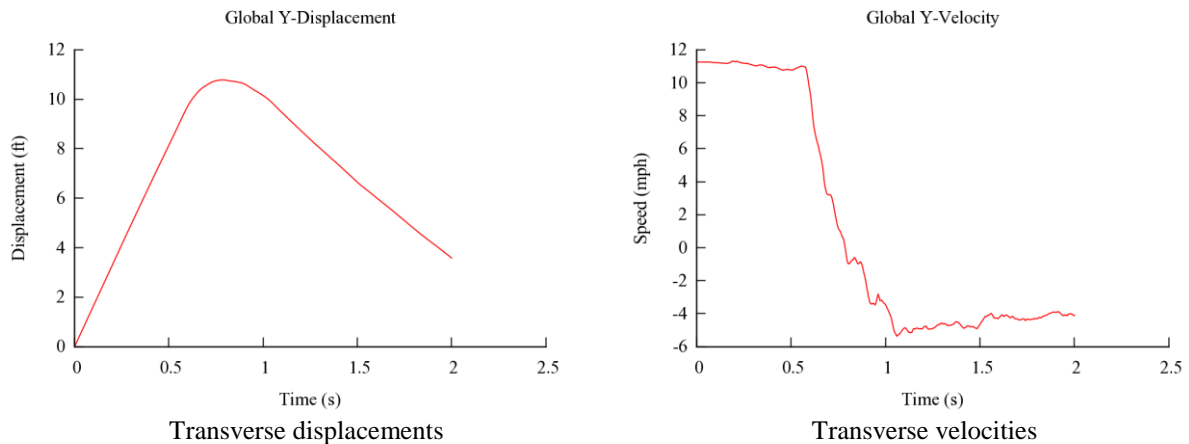


Fig. 4.37: Transverse displacements and velocities of the Ford F250 impacting the 31-inch guardrail at the curb face at 44 mph (70 km/hour) and 15°.

4.2 Case 2: Guardrails Placed at 12-ft from the Curb Face

In this case, guardrails at the placement heights of 27, 29 and 31 inches were placed at 12 feet from the curb face and evaluated under impacts of both the Dodge Neon and Ford F250. Two impact angles, 25° and 15°, were used in the evaluation. An impact speed of 44 mph (70 km/hour) was used in all simulations. Table 4.4 gives a summary of the guardrail performance in terms of vehicular responses.

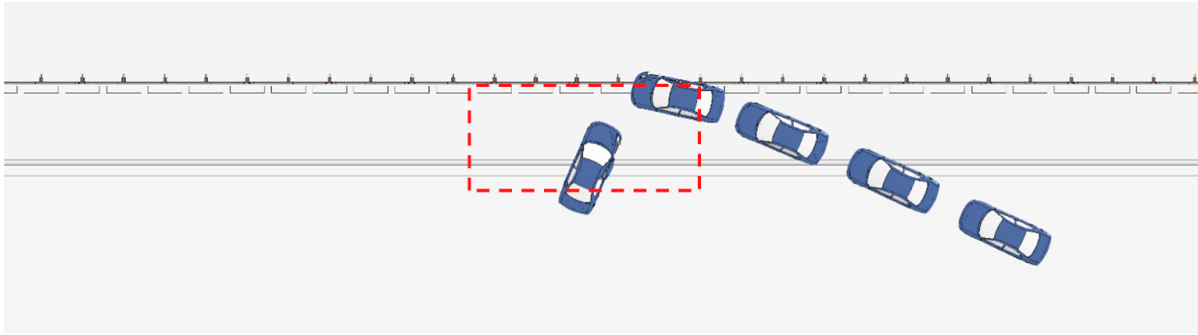
Table 4.4: Simulation results of Case 2 (guardrails placed at 12 feet from the curb face)

Guardrail Height	Test Vehicle	Impact Angle	Simulation Results
27 inch	Dodge Neon	25°	The vehicle failed the exit box criterion with a large spin
		15°	The vehicle passed the exit box criterion and was safely redirected
	Ford F250	25°	The vehicle passed the exit box criterion and was safely redirected
		15°	The vehicle passed the exit box criterion and was safely redirected
29 inch	Dodge Neon	25°	The vehicle passed the exit box criterion and was safely redirected
		15°	The vehicle passed the exit box criterion and was safely redirected
	Ford F250	25°	The vehicle passed the exit box criterion and was safely redirected
		15°	The vehicle passed the exit box criterion and was safely redirected
31 inch	Dodge Neon	25°	The vehicle passed the exit box criterion and was safely redirected
		15°	The vehicle passed the exit box criterion and was safely redirected
	Ford F250	25°	The vehicle passed the exit box criterion and was safely redirected
		15°	The vehicle passed the exit box criterion and was safely redirected

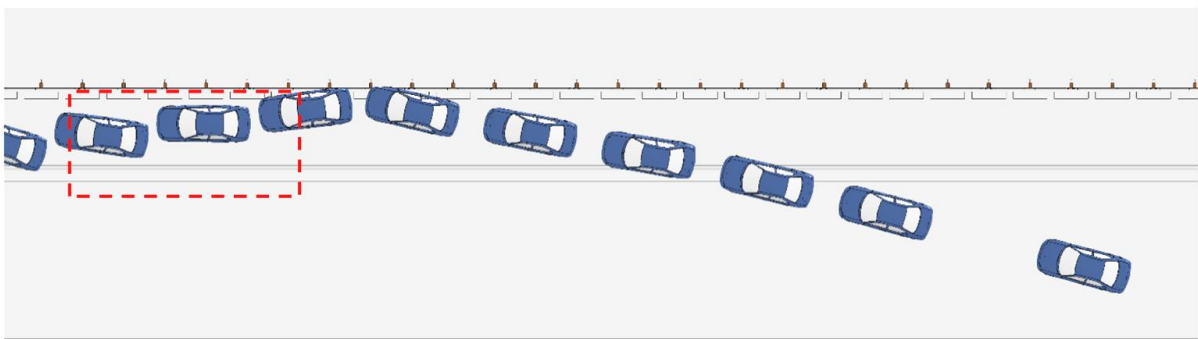
4.2.1 The 27-inch Guardrail Placed at 12 feet from the Curb Face

In this case, the impacting vehicle started off the travel lane, went over the curb, and hit the 27-inch guardrail. Figure 4.38 shows the top view of vehicle trajectory of the Dodge Neon impacting the guardrail at 25° and 15°. The W-beam guardrail is shown in its original shape and the exit box is shown by the rectangle in dash lines. It can be seen that the 27-inch guardrail at 12 feet from the curb face satisfied the MASH exit box criterion in the 15° impact, but failed to stay within the exit box in the case of 25° impact.

The yaw, pitch, and roll angles of the Dodge Neon in both the 25° and 15° impacts are shown in Fig. 4.39. The exit angles of these two impacts were determined to be 18° and 8°, respectively, by subtracting the impact angles from the respective yaw angles at exit (i.e., 43° and 23°). It should be noted that although the vehicle did not have a very large exit angle in the 25° impact, the vehicle continuously spun and consequently went outside the exit box, as seen from the continuously increasing yaw angle. The roll and pitch angles of both cases were less than three degrees in either positive or negative direction and thus passed the MASH evaluation criterion F, which specified a maximum 75° roll or pitch angle.

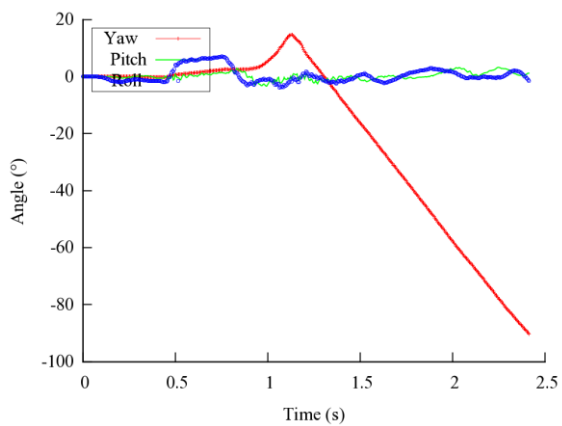


a. At 44 mph (70 km/hour) and 25°

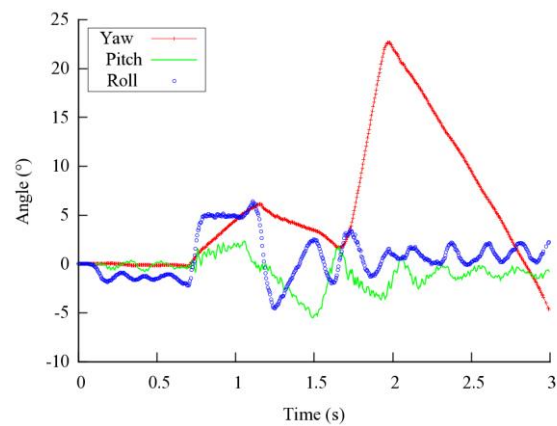


b. At 44 mph (70 km/hour) and 15°

Fig. 4.38: A Dodge Neon impacting the 27-inch guardrail at 12 feet from the curb face.



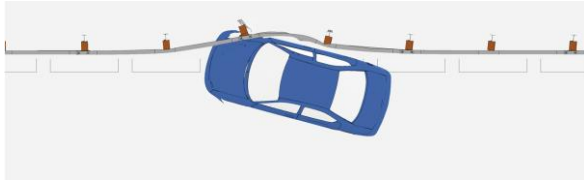
a. At 44 mph (70 km/hour) and 25°



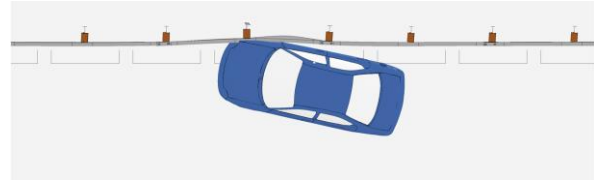
b. At 44 mph (70 km/hour) and 15°

Fig. 4.39: Yaw, pitch, and roll angles of Dodge Neon impacting 27-inch guardrail at 12 feet from the curb face.

Figure 4.40 shows the permanent deformations of the guardrail under impacts of the Dodge Neon at 25° and 15°. It can be seen that the damaged guardrail sections are small and localized; this serves as an indication of the relatively low impact severity of the small car.



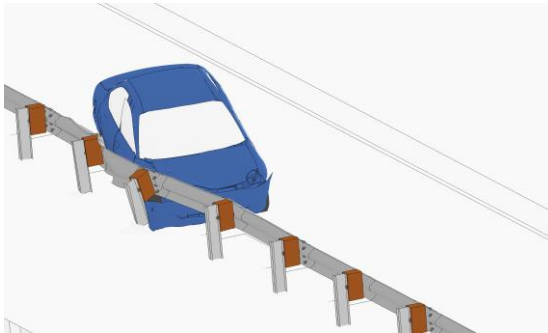
a. At 44 mph (70 km/hour) and 25°



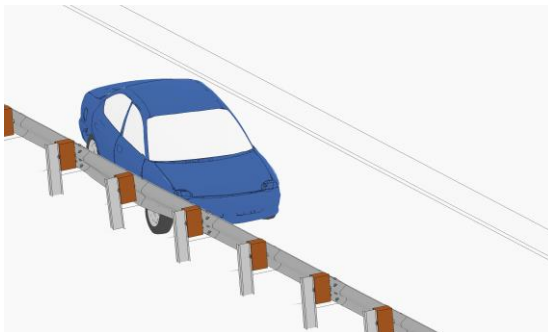
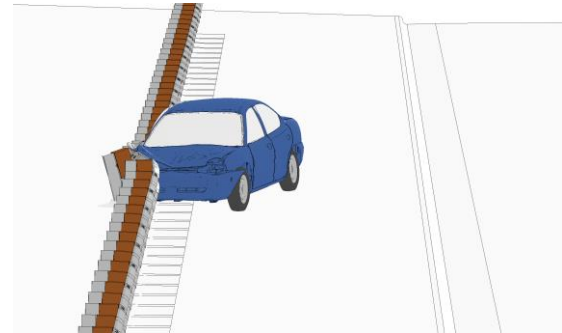
b. At 44 mph (70 km/hour) and 15°

Fig. 4.40: Permanent deformation of the 27-inch guardrail at 12 feet from the curb face and impacted by a Dodge Neon.

Figure 4.41 shows the detailed views of vehicle-barrier interactions after the vehicle climbed up the curb and impacted the guardrail. Figures 4.42 and 4.43 show the time histories of transverse displacements and velocities measured at the center of gravity (CG) point of the vehicle in the 25° and 15° impacts, respectively. For the case of the 25° impact, the transverse velocity remained at 5 mph towards the travel lane with spinning (i.e., loss of control of the vehicle). As seen in Fig. 4.38a, the vehicle has run down the curb at 2 seconds so the chance of getting involved in a secondary collision is relatively high. For the 15° impact, the transverse velocity was approximately 1 mph towards the travel lane, which indicated that the Dodge Neon was unlikely to get involved in a secondary collision.



a. At 44 mph (70 km/hour) and 25°



b. At 44 mph (70 km/hour) and 15°

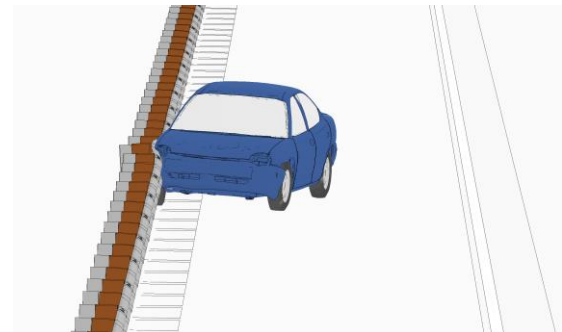


Fig. 4.41: Simulations of Dodge Neon impacting the 27-inch guardrail at 12 feet from the curb face.

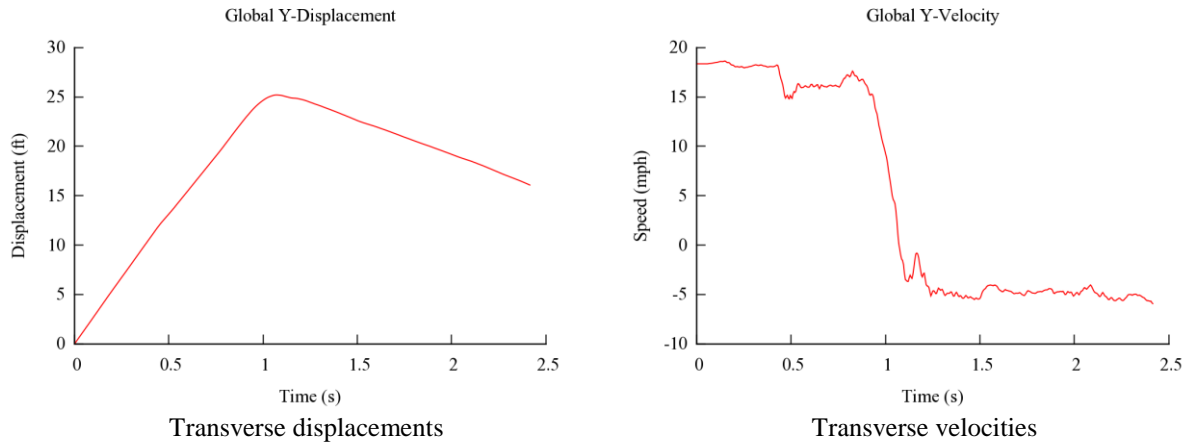


Fig. 4.42: Transverse displacements and velocities of the Dodge Neon impacting the 27-inch guardrail at 12 feet from the curb face at 44 mph (70 km/hour) and 25°.

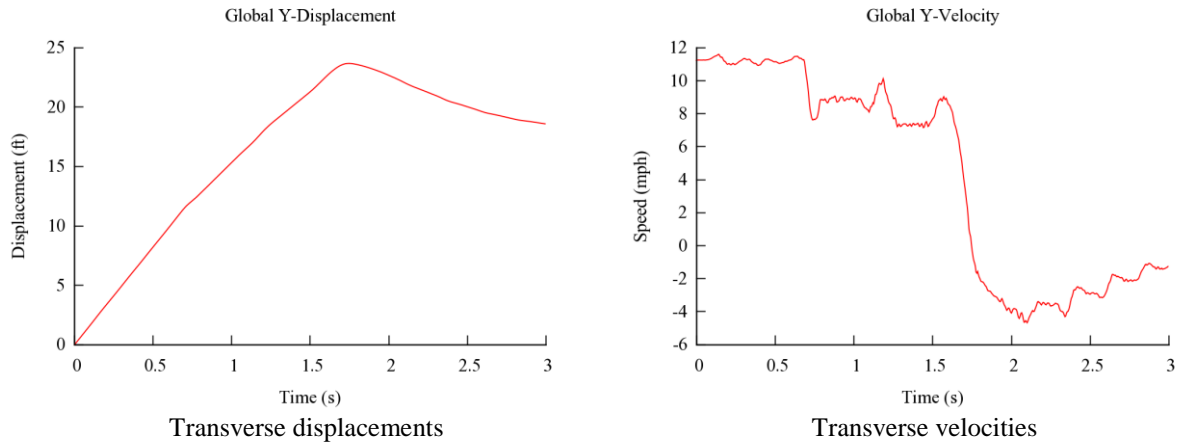
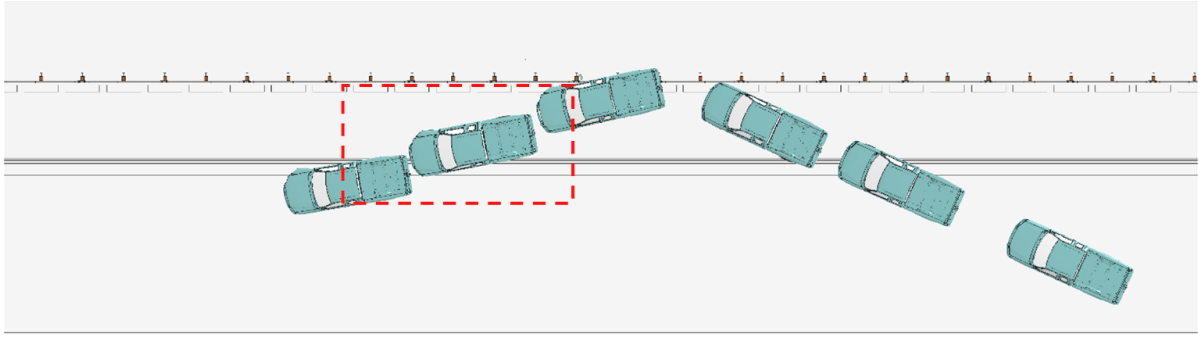


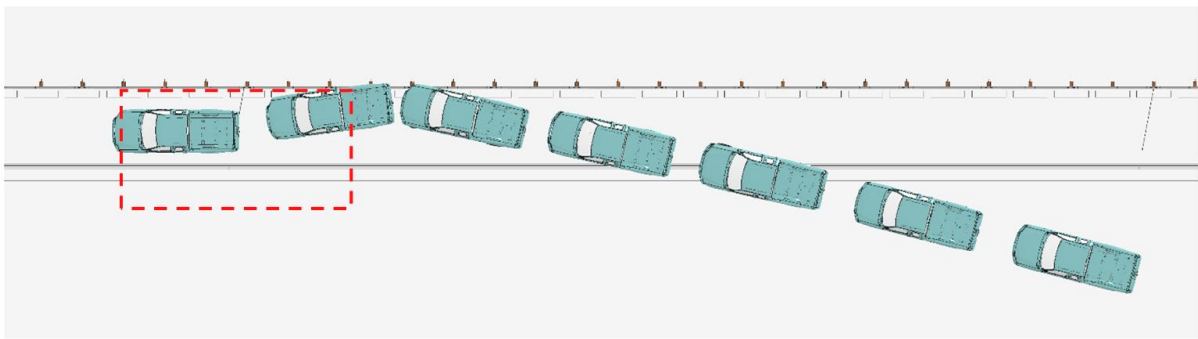
Fig. 4.43: Transverse displacements and velocities of the Dodge Neon impacting the 27-inch guardrail at 12 feet from the curb face at 44 mph (70 km/hour) and 15°.

In both the 25° and 15° impacts by the Ford F250 on the 27-inch W-beam guardrail placed at 12 feet from the curb face, the MASH exit box criterion was satisfied and the vehicle was redirected. Figure 4.44 shows the top view of vehicle trajectory of the Ford F250 in both cases along with the exit boxes. It should be noted that in the 25 impact, the wheel track of the Ford F250 are strictly within the exit box so the vehicle did not run out of the exit box.

The yaw, pitch, and roll angles of the Ford F250 in the 25° and 15° impacts are shown in Fig. 4.45. The exit angles of these two impacts were determined to be 20° and 8°, respectively, by subtracting the impact angles from the respective yaw angles at exit. For the 25° impact, the yaw angle of the Ford F250 was approximately 35°, indicating a 10° angle between the vehicle and the guardrail. The vehicle's yaw angle in the 15° impact was approximately 15°, indicating the vehicle being parallel with the guardrail. The roll and pitch angles in both impacts were less than 7.5 degrees in either positive or negative direction and thus passed the MASH evaluation criterion F, which specified a maximum 75° roll or pitch angle.

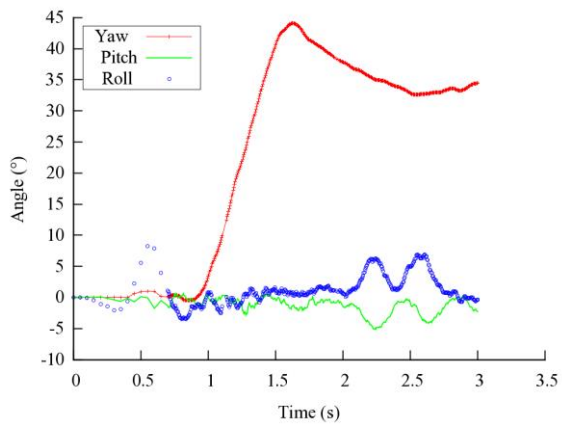


a. At 44 mph (70 km/hour) and 25°

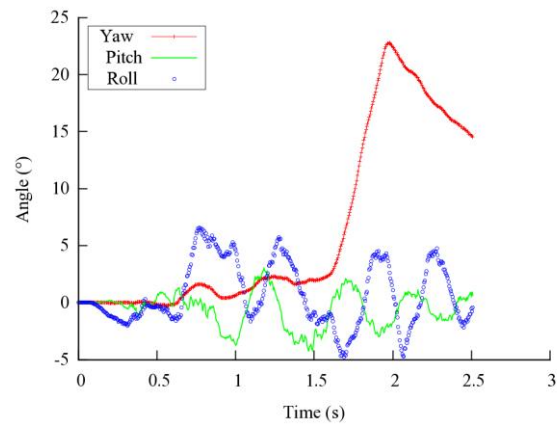


b. At 44 mph (70 km/hour) and 15°

Fig. 4.44: A Ford F250 impacting the 27-inch guardrail at 12 feet from the curb face.



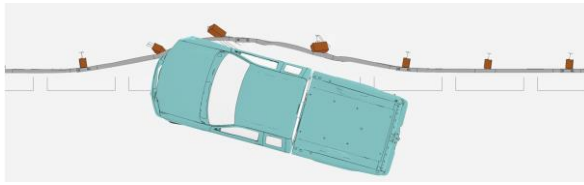
a. At 44 mph (70 km/hour) and 25°



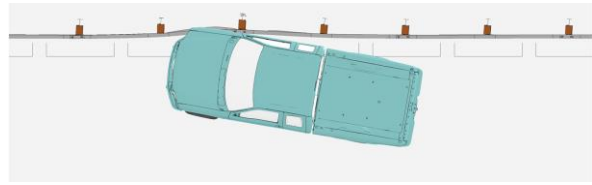
b. At 44 mph (70 km/hour) and 15°

Fig. 4.45: Yaw, pitch, and roll angles of Ford F250 impacting 27-inch guardrail at 12 feet from the curb face.

The permanent deformations of the 27-inch guardrail under impacts of the Ford F250 at 25° and 15° are shown in Fig. 4.46. Figure 4.47 shows the detailed vehicle-guardrail interactions in both impacts.

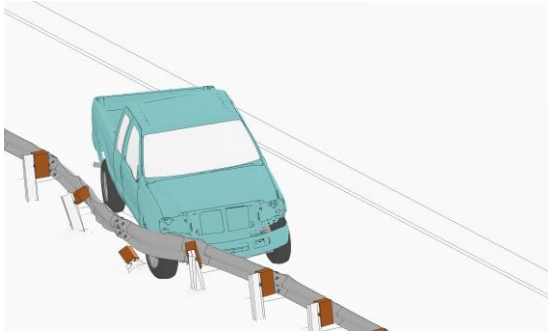


a. At 44 mph (70 km/hour) and 25°

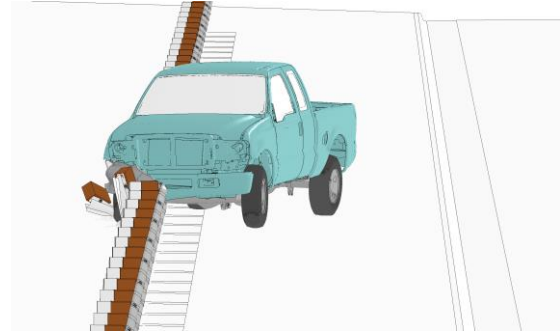


b. At 44 mph (70 km/hour) and 15°

Fig. 4.46: Permanent deformation of the 27-inch guardrail at 12 feet from the curb face and impacted by a Ford F250.



a. At 44 mph (70 km/hour) and 25°



b. At 44 mph (70 km/hour) and 15°

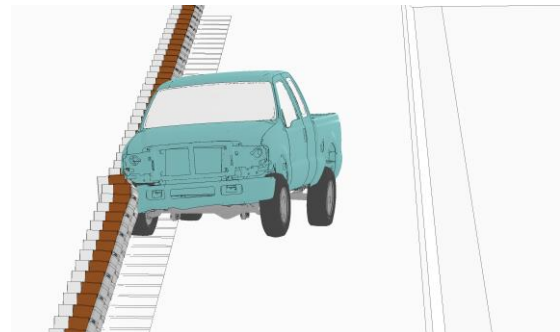
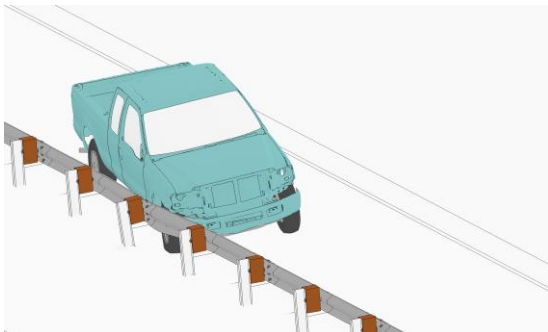


Fig. 4.47: Simulations of Ford F250 impacting the 27-inch guardrail at 12 feet from the curb face.

Figures 4.48 and 4.49 show the time histories of transverse displacements and velocities measured at the CG point of the Ford F250 in the 25° and 15° impacts, respectively. The transverse velocities of both cases were approximately 4 mph towards the travel lane. Considering the results on the exit box criterion, exit angle, and transverse velocity, the Ford F250 had a relatively small chance of getting involved in a secondary collision in the 25° impact. For the 15° impact, the Ford F250 is unlikely to get involved in a secondary collision.

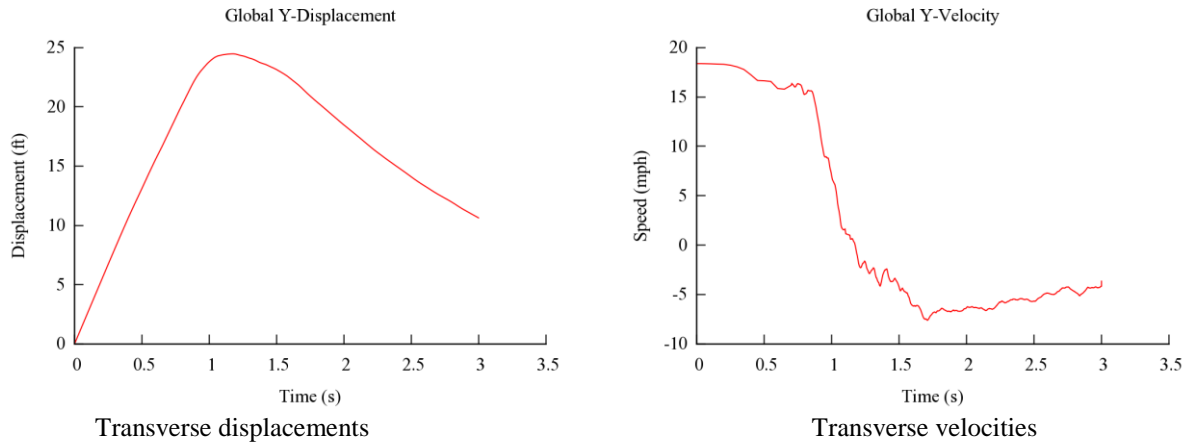


Fig. 4.48: Transverse displacements and velocities of the Ford F250 impacting the 27-inch guardrail at 12 feet from the curb face at 44 mph (70 km/hour) and 25°.

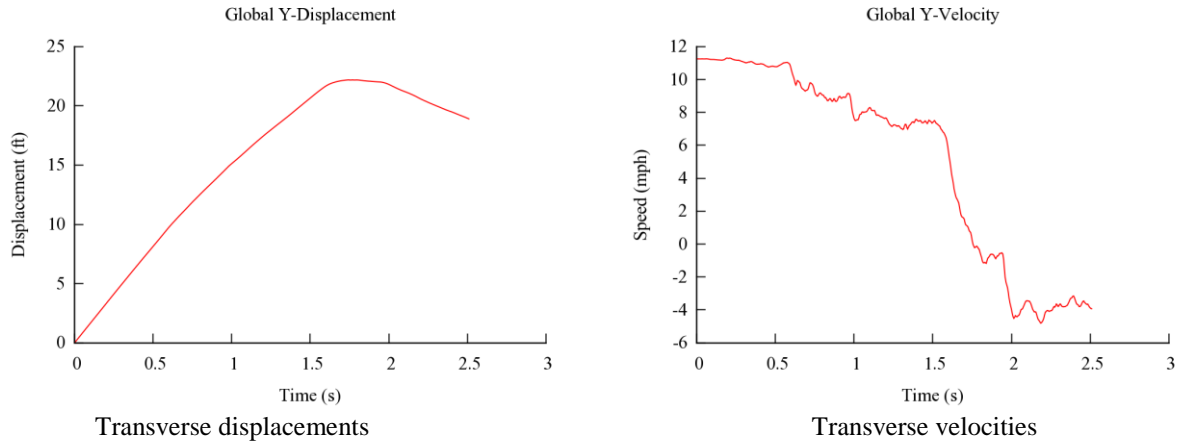
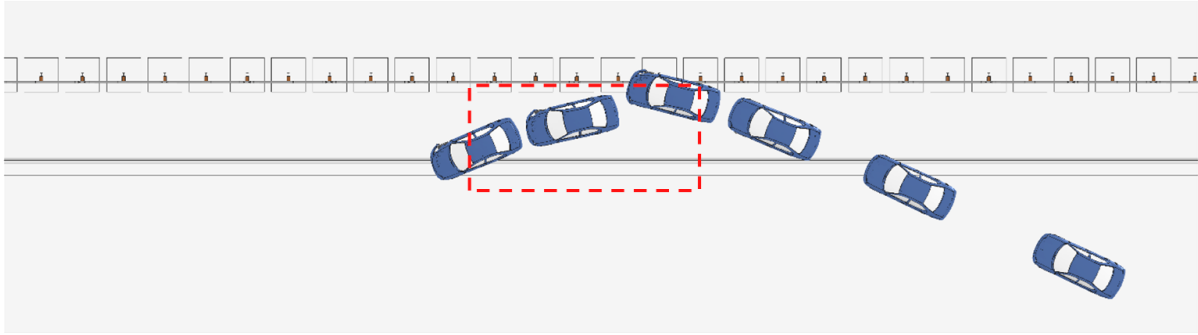


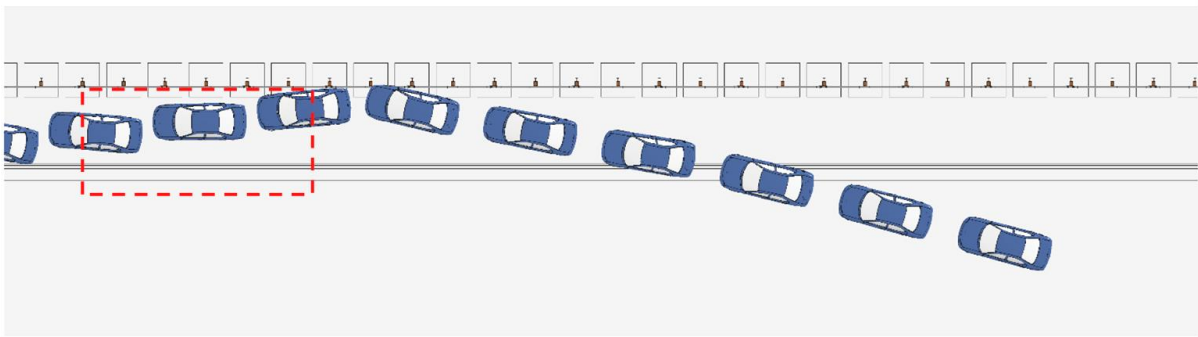
Fig. 4.49: Transverse displacements and velocities of the Ford F250 impacting the 27-inch guardrail at 12 feet from the curb face at 44 mph (70 km/hour) and 15°.

4.2.2 The 29-inch Guardrail Placed at 12 feet from the Curb Face

Figure 4.50 shows the top view of vehicle trajectory of the Dodge Neon impacting the 29-inch guardrail placed at 12 feet from the curb face at 25° and 15°. It can be seen that the exit box criterion was satisfied for both cases. The yaw, pitch, and roll angles of the Dodge Neon in both the 25° and 15° impacts are shown in Fig. 4.51. The exit angles were determined to be 20° and 9° for the 25° and 15° impacts, respectively, by subtracting the impact angles from the respective yaw angles at exit (i.e., 45° and 24°). The roll and pitch angles in both the 25° and 15° impacts were less than five degrees in either positive or negative direction and thus passed the MASH evaluation criterion F, which specified a maximum 75° roll or pitch angle.

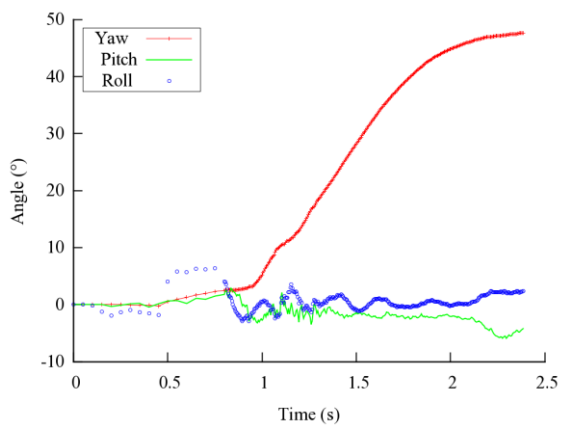


a. At 44 mph (70 km/hour) and 25°

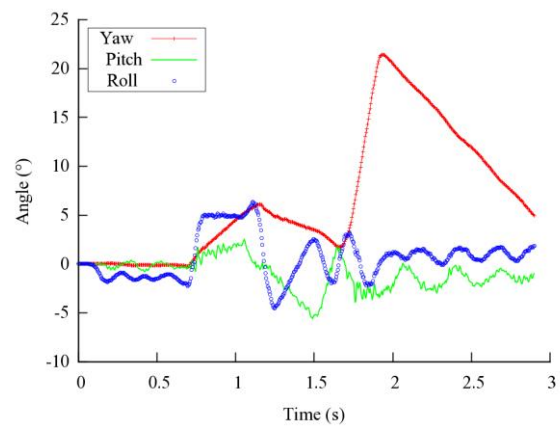


b. At 44 mph (70 km/hour) and 15°

Fig. 4.50: A Dodge Neon impacting the 29-inch guardrail at 12 feet from the curb face.



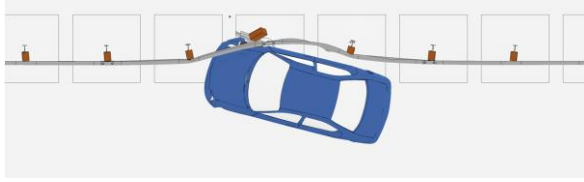
a. At 44 mph (70 km/hour) and 25°



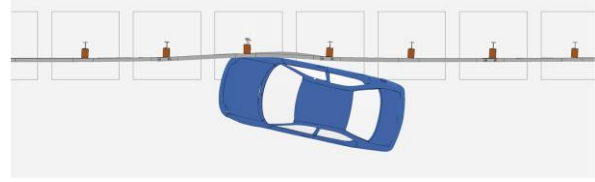
b. At 44 mph (70 km/hour) and 15°

Fig. 4.51: Yaw, pitch, and roll angles of Dodge Neon impacting 29-inch guardrail at 12 feet from the curb face.

Figure 4.52 shows the permanent deformations of the guardrail under impacts of the Dodge Neon. It can be seen that the damaged guardrail sections are small and localized.



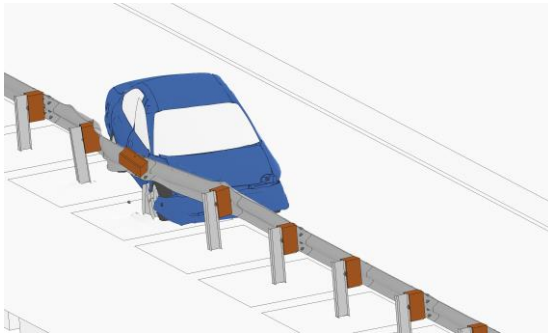
a. At 44 mph (70 km/hour) and 25°



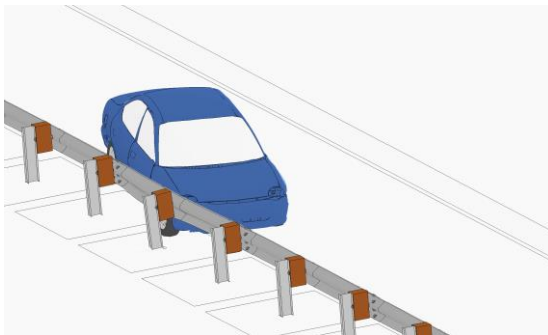
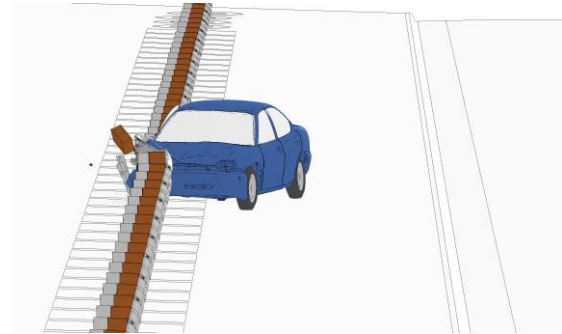
b. At 44 mph (70 km/hour) and 15°

Fig. 4.52: Permanent deformation of the 29-inch guardrail at 12 feet from the curb face and impacted by a Dodge Neon.

Figure 4.53 shows the detailed views of vehicle-barrier interactions for the 25° and 15° impacts by the Dodge Neon. Figures 4.54 and 4.55 show the time histories of transverse displacements and velocities at the CG point of the vehicle in these two impacts. The transverse velocities were 5 and 1 mph for the 25° and 15° impacts, respectively, towards the travel lane. The small transverse velocities, along with the relatively small exit angles and satisfaction to the exit box criterion, confirmed the safe redirection of the Dodge Neon in both cases.



a. At 44 mph (70 km/hour) and 25°



b. At 44 mph (70 km/hour) and 15°

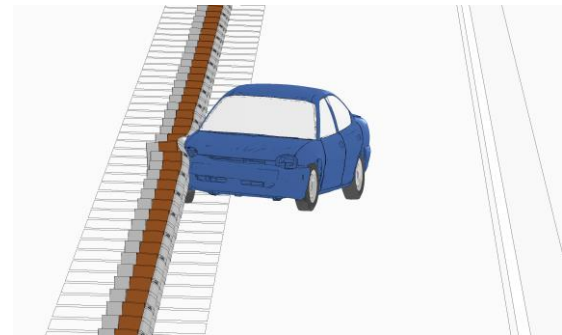


Fig. 4.53: Simulations of Dodge Neon impacting the 29-inch guardrail at 12 feet from the curb face.

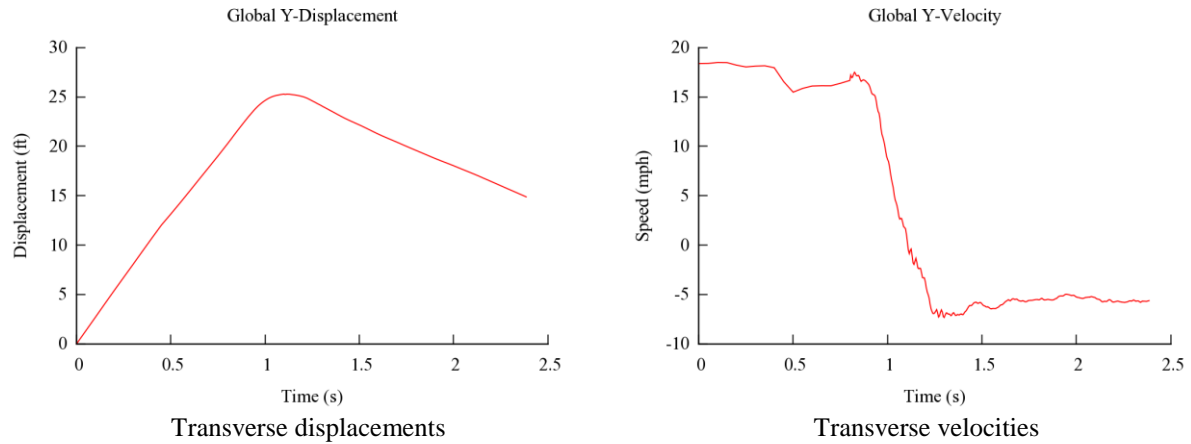


Fig. 4.54: Transverse displacements and velocities of the Dodge Neon impacting the 29-inch guardrail at 12 feet from the curb face at 44 mph (70 km/hour) and 25°.

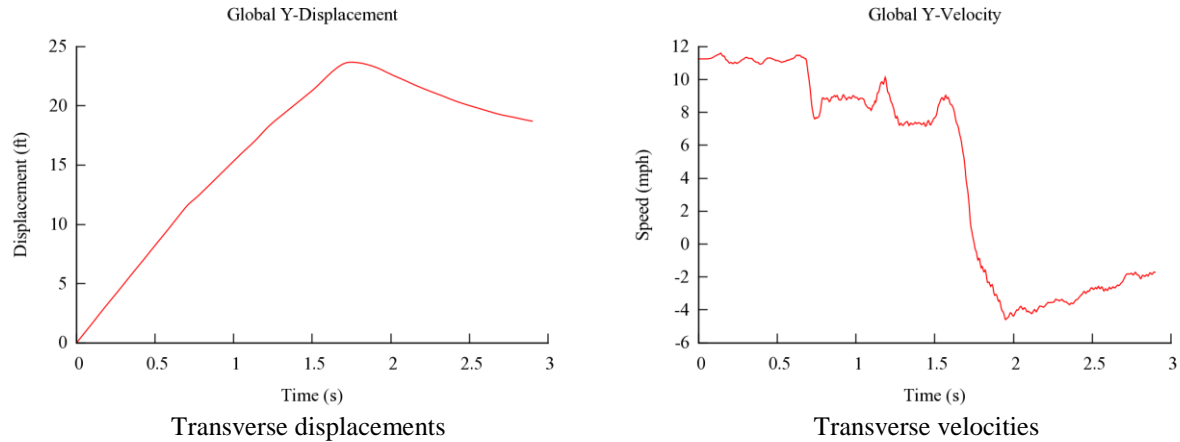
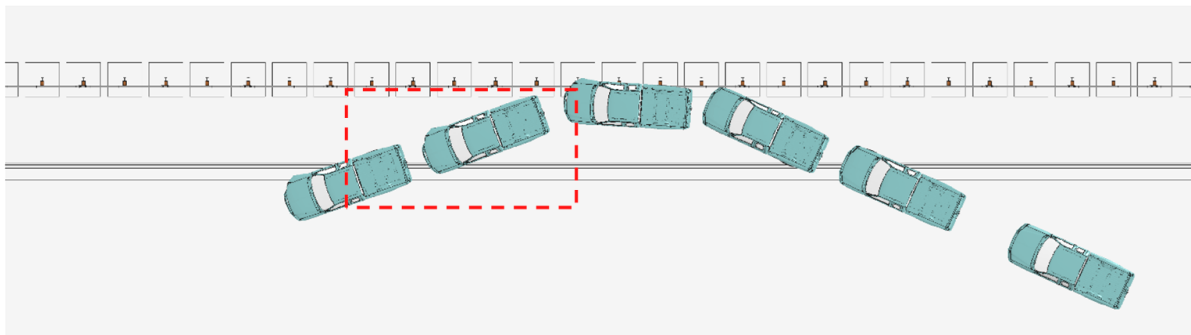
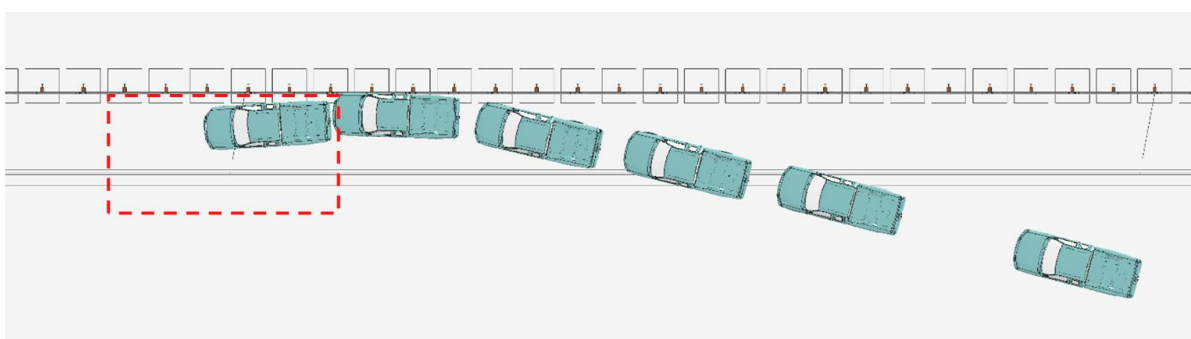


Fig. 4.55: Transverse displacements and velocities of the Dodge Neon impacting the 29-inch guardrail at 12 feet from the curb face at 44 mph (70 km/hour) and 15°.

Under impacts of the Ford F250 at 25° and 15°, the 29-inch W-beam guardrail placed at 12 feet from the curb face was found to perform well. Figure 4.56 shows the top view of vehicle trajectory of the Ford F250 in both cases along with the exit boxes. The yaw, pitch, and roll angles of both cases are shown in Fig. 4.57. The exit angles of these two impacts were determined to be 12° and 8°, respectively, by subtracting the impact angles from the respective yaw angles at exit (i.e., 37° and 23°). For the 15° impact, the last measure of yaw angle was approximately 17°, indicating a 2° angle between the Ford F250 and the guardrail. Although the Ford F250 had not gone through the entire box, the small yaw angle and the small transverse velocity would ensure the vehicle staying within the exit box while being redirected. The roll and pitch angles in both the 25° and 15° impacts by Ford F250 were less than 7.5 degrees in either positive or negative direction and thus passed the MASH evaluation criterion F, which specified a maximum 75° roll or pitch angle.

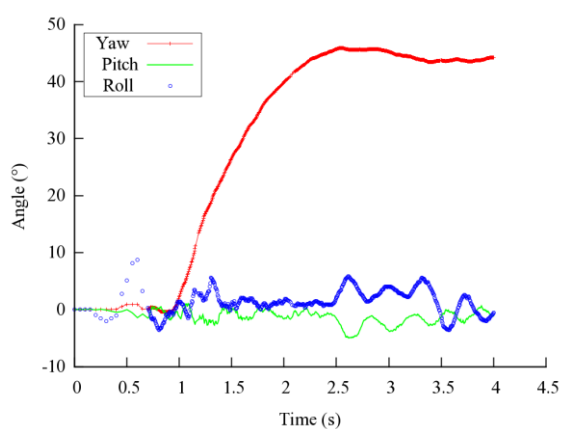


a. At 44 mph (70 km/hour) and 25°

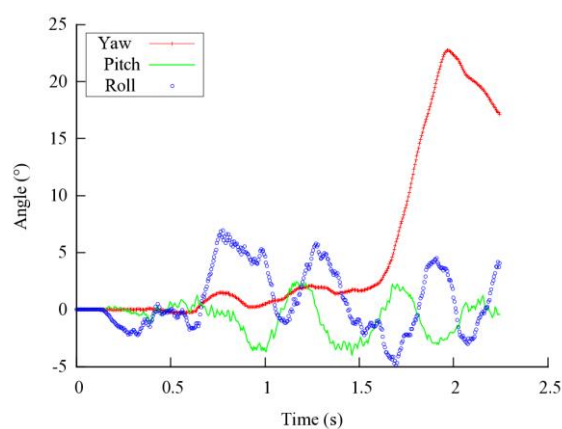


b. At 44 mph (70 km/hour) and 15°

Fig. 4.56: A Ford F250 impacting the 29-inch guardrail at 12 feet from the curb face.



a. At 44 mph (70 km/hour) and 25°



b. At 44 mph (70 km/hour) and 15°

Fig. 4.57: Yaw, pitch, and roll angles of Ford F250 impacting 29-inch guardrail at 12 feet from the curb face.

Figure 4.58 shows the permanent deformations of the guardrail under impacts of the Ford F250 at 25° and 15°. It can be seen that the transverse deflection of the guardrail in the 25°

impact was significantly larger than that in the 15° impact. However, the guardrail deformations in both cases were relatively small and localized.

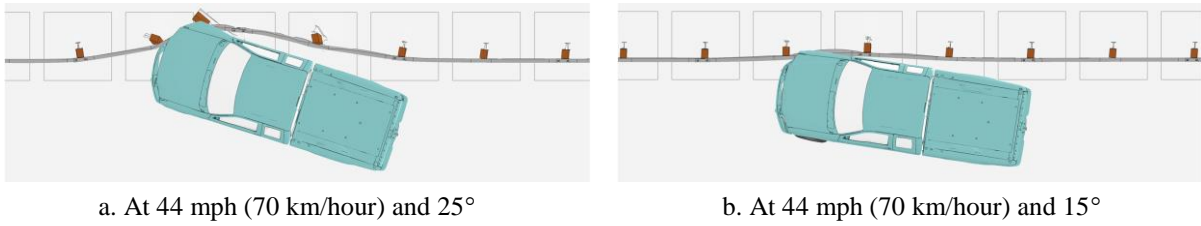


Fig. 4.58: Permanent deformation of the 29-inch guardrail at 12 feet from the curb face and impacted by a Ford F250.

Figure 4.59 shows the detailed views of vehicle-barrier interactions while the Ford F250 impacting the 29-inch guardrail. When installed at 12 feet from the curb face, the guardrail engaged well with the bumper cover and wheel fender of the Ford F250 and thus effectively redirected the vehicle in both impact cases.

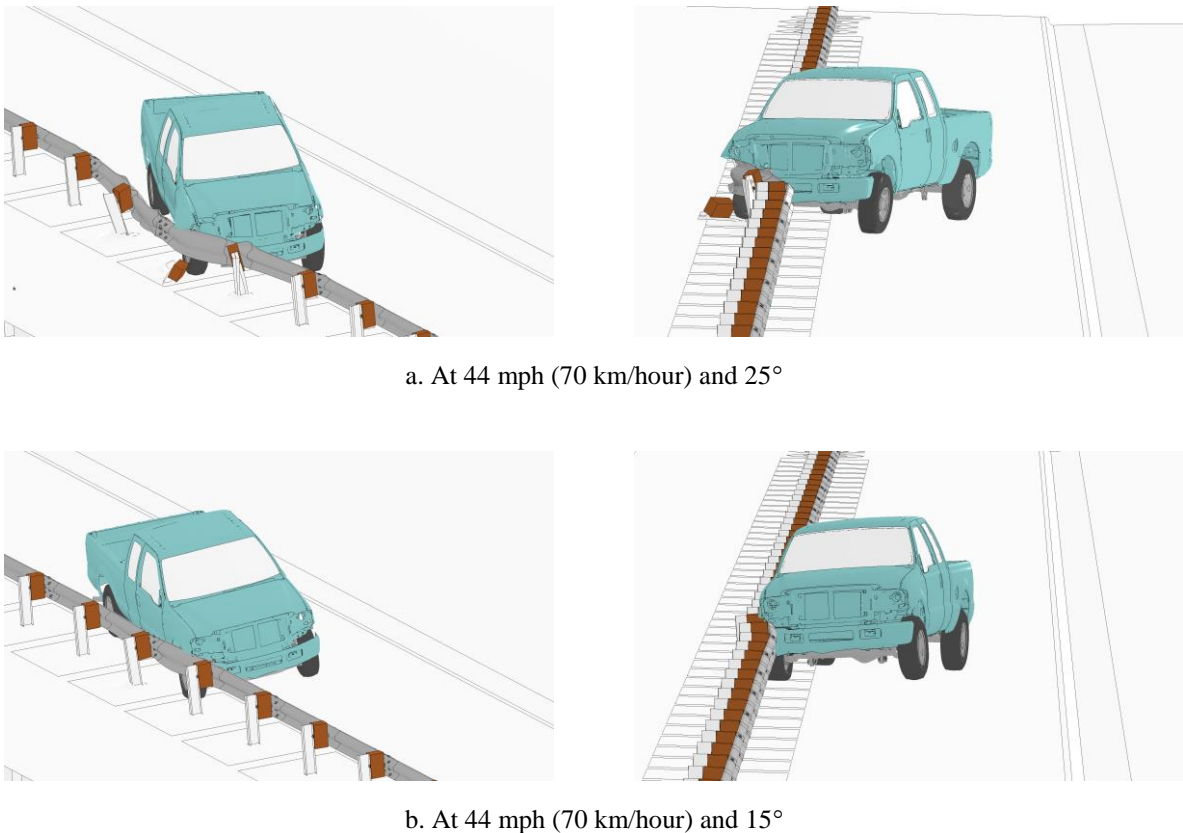


Fig. 4.59: Simulations of Ford F250 impacting the 29-inch guardrail at 12 feet from the curb face.

Figures 4.60 and 4.61 show the time histories of transverse displacements and velocities at the CG point of Ford F250 in the 25° and 15° impacts, respectively. For both cases, the

transverse velocities were approximately 4 mph towards the travel lane, indicating a relatively small chance of getting involved in a secondary collision. The results in Figs. 4.50 to 4.61 indicated that the 29-inch guardrail placed at 12 feet from the curb face was effective under impacts of both a pickup truck and a passenger car at 44 mph (70 km/hour).

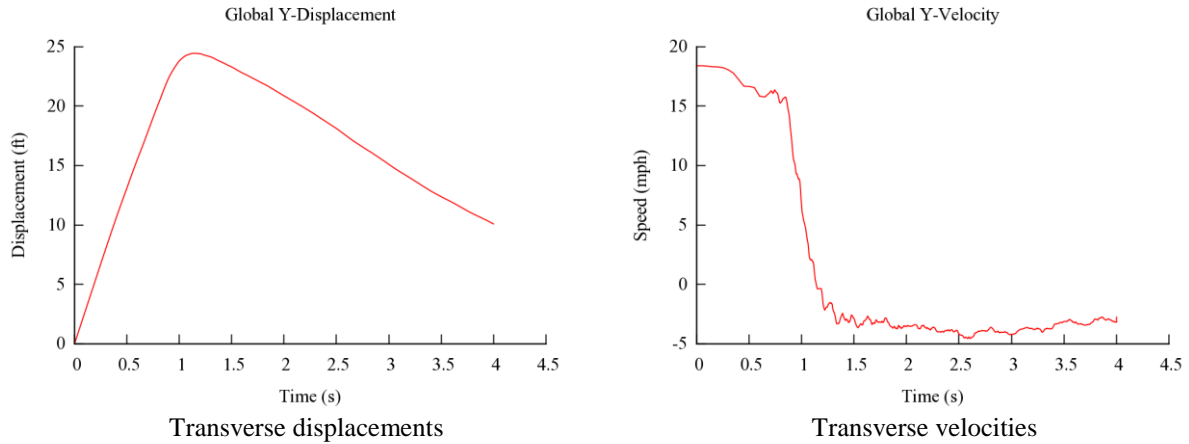


Fig. 4.60: Transverse displacements and velocities of the Ford F250 impacting the 29-inch guardrail at 12 feet from the curb face at 44 mph (70 km/hour) and 25°.

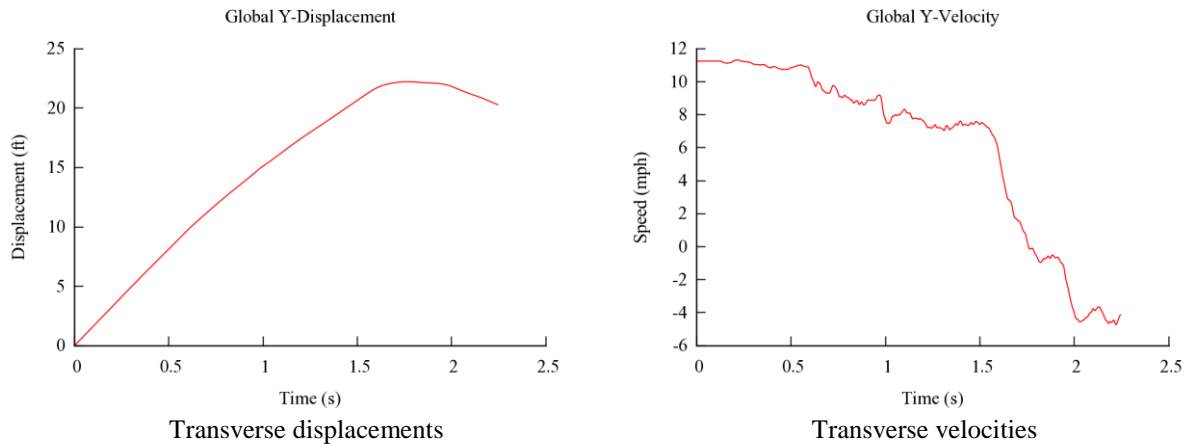
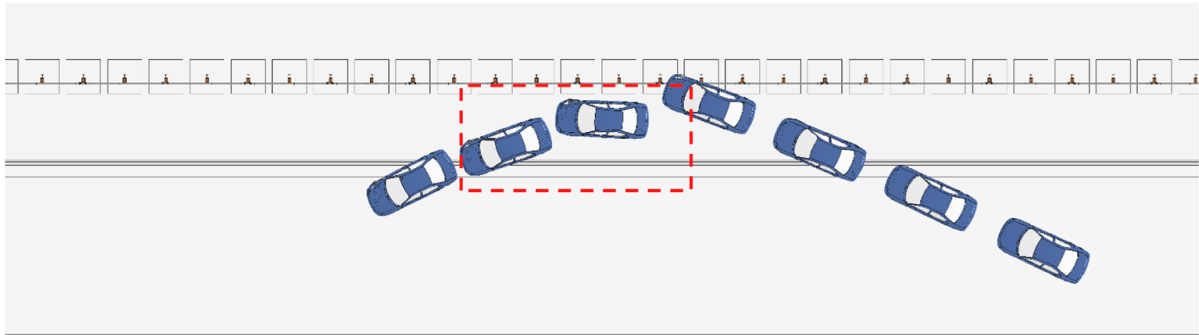


Fig. 4.61: Transverse displacements and velocities of the Ford F250 impacting the 29-inch guardrail at 12 feet from the curb face at 44 mph (70 km/hour) and 15°.

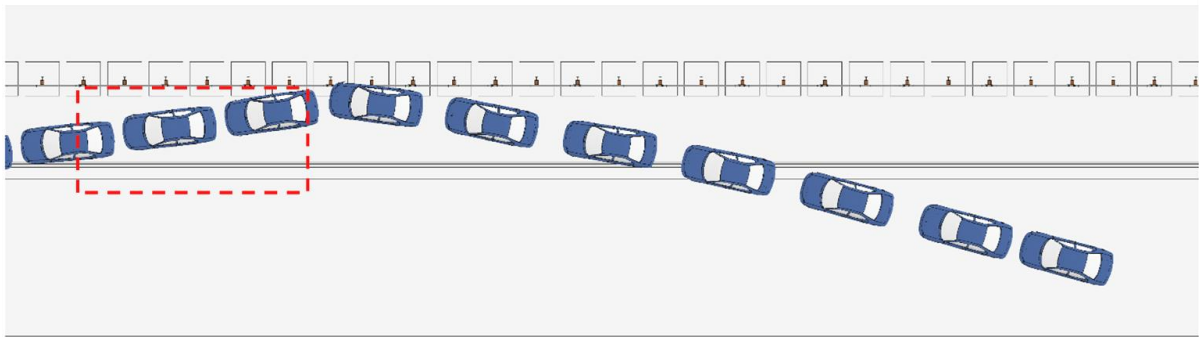
4.2.3 The 31-inch Guardrail Placed at 12 feet from the Curb Face

Under impacts of the Dodge Neon at 25° and 15°, the performance of the 31-inch guardrail was found to be similar to that of the 29-inch guardrail, both placed at 12 feet from the curb face. Figure 4.62 shows the top view of vehicle trajectory of the Dodge Neon impacting the 31-inch guardrail at 25° and 15°. It can be seen that the exit boxes criterion was satisfied for both cases. Figure 4.63 shows the yaw, pitch, and roll angles of the Dodge Neon in both the 25° and 15° impacts, with the exit angles of 20° and 9°, respectively. The roll and pitch

angles in both impacts were less than 7.5 degrees in either positive or negative direction and thus passed the MASH evaluation criterion F, which specified a maximum 75° roll or pitch angle.

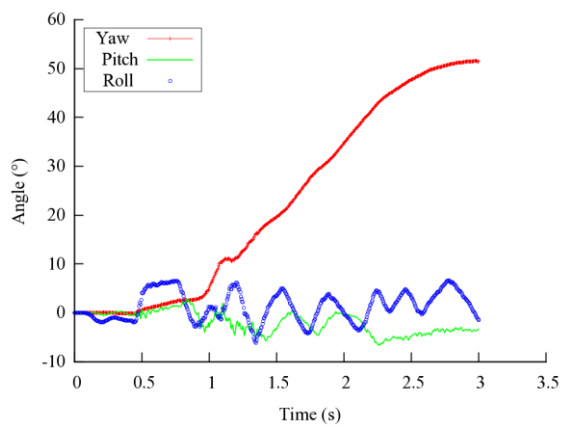


a. At 44 mph (70 km/hour) and 25°

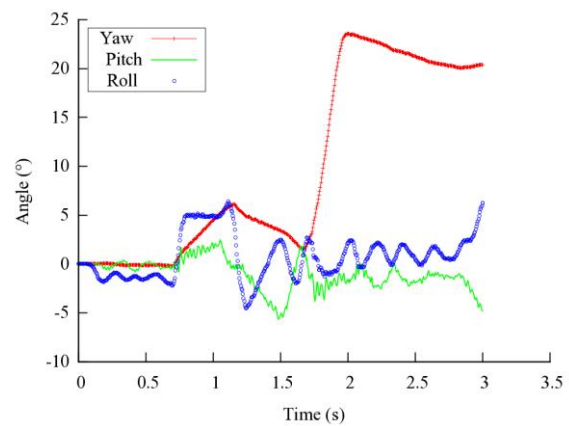


b. At 44 mph (70 km/hour) and 15°

Fig. 4.62: A Dodge Neon impacting the 31-inch guardrail at 12 feet from the curb face.



a. At 44 mph (70 km/hour) and 25°



b. At 44 mph (70 km/hour) and 15°

Fig. 4.63: Yaw, pitch, and roll angles of Dodge Neon impacting 31-inch guardrail at 12 feet from the curb face.

The permanent deformations of the 31-inch guardrail under impacts of the Dodge Neon were relatively small and localized, as seen in Fig. 4.64. The damaged guardrail sections were similar to those of the 29-inch guardrail shown in Fig. 4.52.

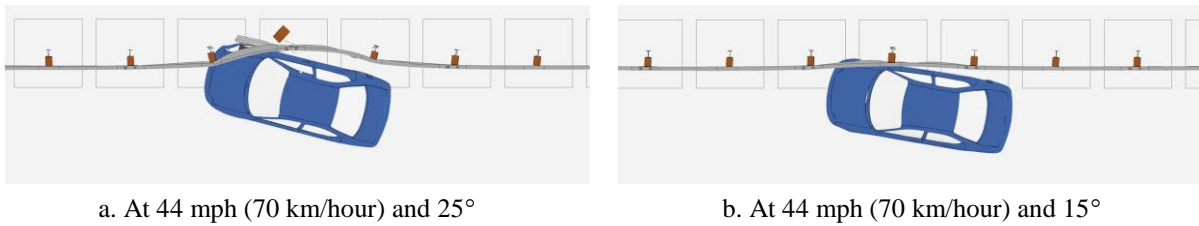
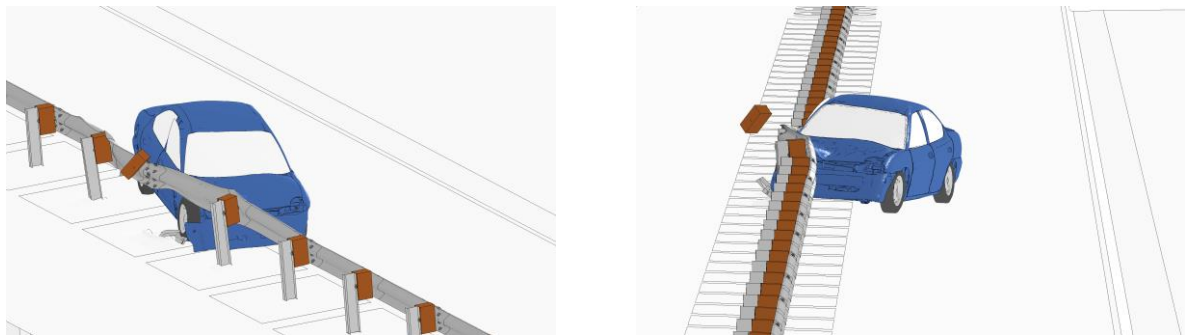
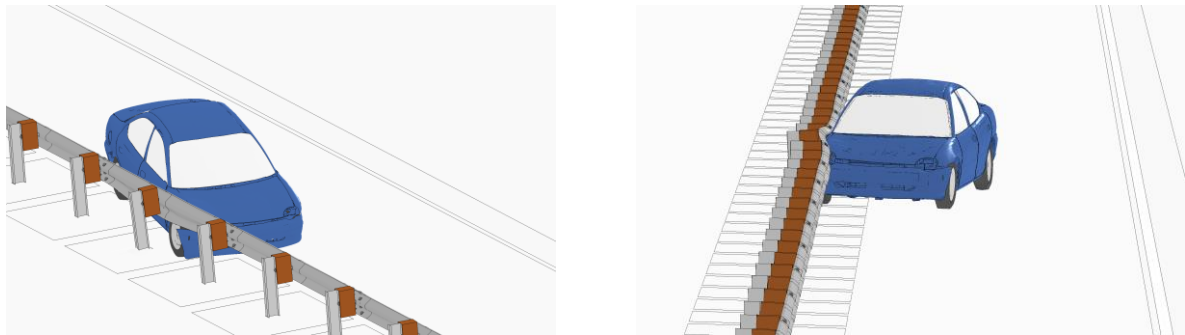


Fig. 4.64: Permanent deformation of the 31-inch guardrail at 12 feet from the curb face and impacted by a Dodge Neon.

Figure 4.65 shows the detailed views of vehicle-barrier interactions for the 25° and 15° impacts by the Dodge Neon. Figures 4.54 and 4.55 show the time histories of transverse displacements and velocities at the CG point of the vehicle in these two impacts. The transverse velocities were approximately 5 mph towards the travel lane for both cases. The results in Figs. 4.62 to 4.67 indicated that the Dodge Neon was safely redirected by the 31-inch guardrail placed at 12 feet from the curb face.



a. At 44 mph (70 km/hour) and 25°



b. At 44 mph (70 km/hour) and 15°

Fig. 4.65: Simulations of Dodge Neon impacting the 31-inch guardrail at 12 feet from the curb face.

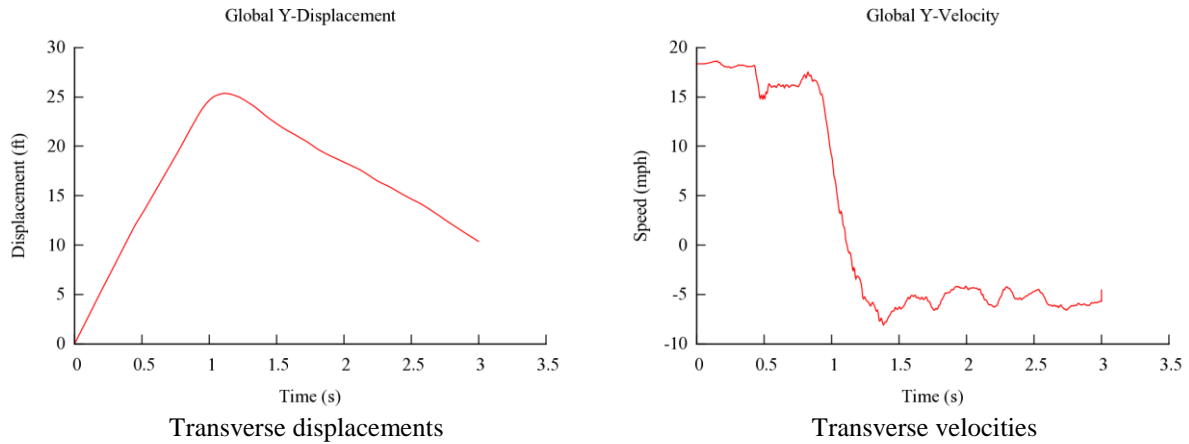


Fig. 4.66: Transverse displacements and velocities of the Dodge Neon impacting the 31-inch guardrail at 12 feet from the curb face at 44 mph (70 km/hour) and 25°.

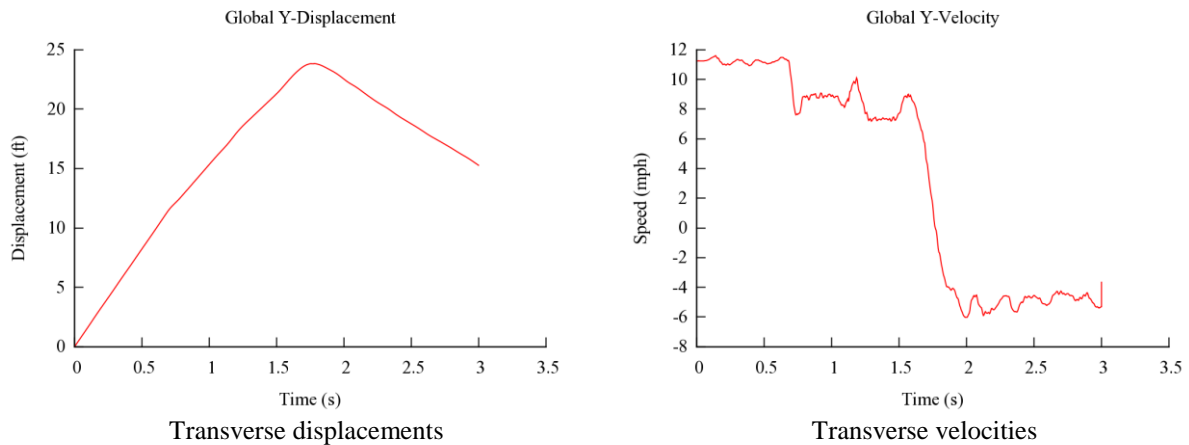
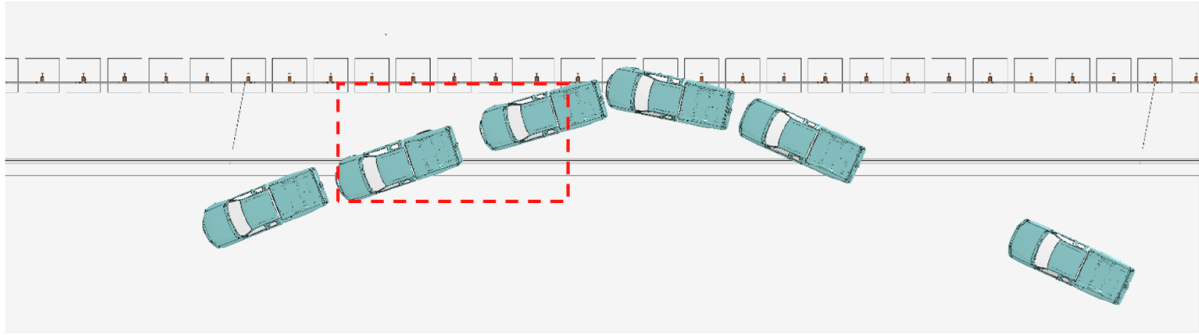


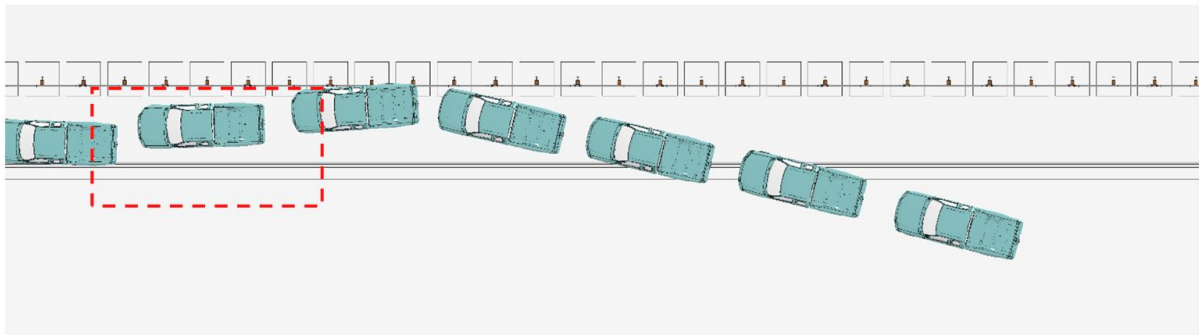
Fig. 4.67: Transverse displacements and velocities of the Dodge Neon impacting the 31-inch guardrail at 12 feet from the curb face at 44 mph (70 km/hour) and 15°.

Figure 4.68 shows the vehicle trajectory of the Ford F250 impacting the 31-inch guardrail at 25° and 15°. In the 25° impact, the 31-inch guardrail barely met the MASH exit box criterion, i.e., the wheel track went through the bottom left corner of the exit box. In the 15° impact, the exit box criterion was satisfied and the vehicle was smoothly redirected.

Figure 4.69 shows the yaw, pitch, and roll angles of the Ford F250 in both the 25° and 15° impacts, with exit angles of 15° and 8°, respectively. The roll and pitch angles in both impacts were less than 10 degrees in either positive or negative direction and thus passed the MASH evaluation criterion F, which specified a maximum 75° roll or pitch angle.

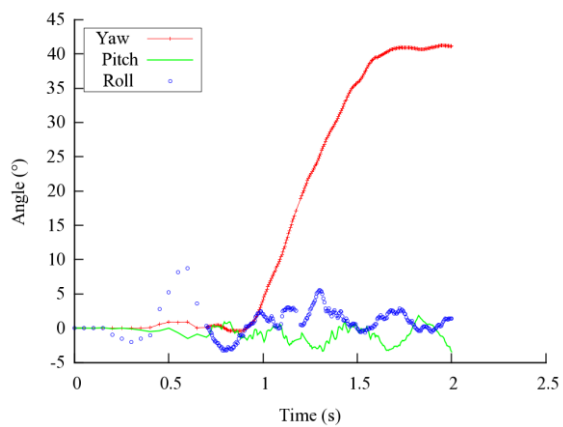


a. At 44 mph (70 km/hour) and 25°

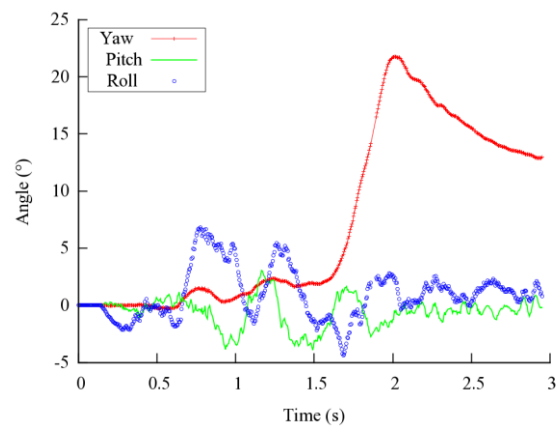


b. At 44 mph (70 km/hour) and 15°

Fig. 4.68: A Ford F250 impacting the 31-inch guardrail at 12 feet from the curb face.



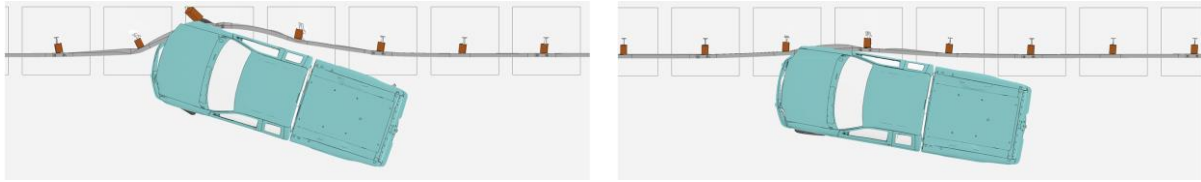
a. At 44 mph (70 km/hour) and 25°



b. At 44 mph (70 km/hour) and 15°

Fig. 4.69: Yaw, pitch, and roll angles of Ford F250 impacting 31-inch guardrail at 12 feet from the curb face.

Figure 4.70 shows the permanent deformations of the 31-inch guardrail under impacts of the Ford F250. The damaged guardrail sections are small and localized in both cases, though the guardrail deflection in the 25° impact was much larger than that in the 15° impact.

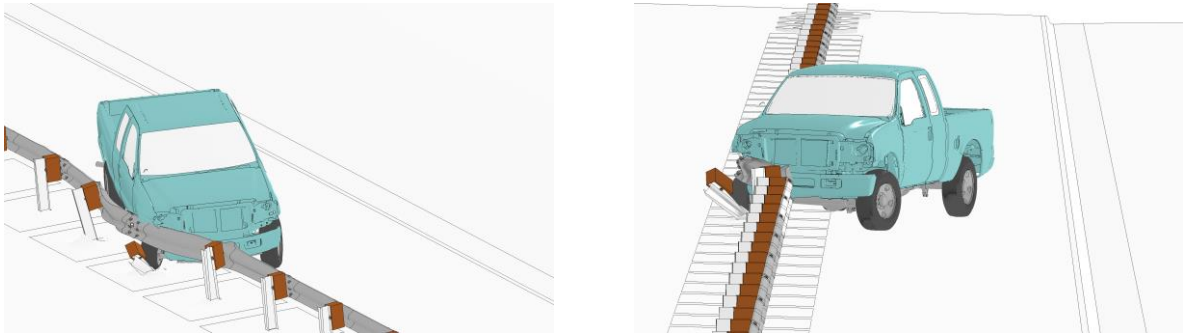


a. At 44 mph (70 km/hour) and 25°

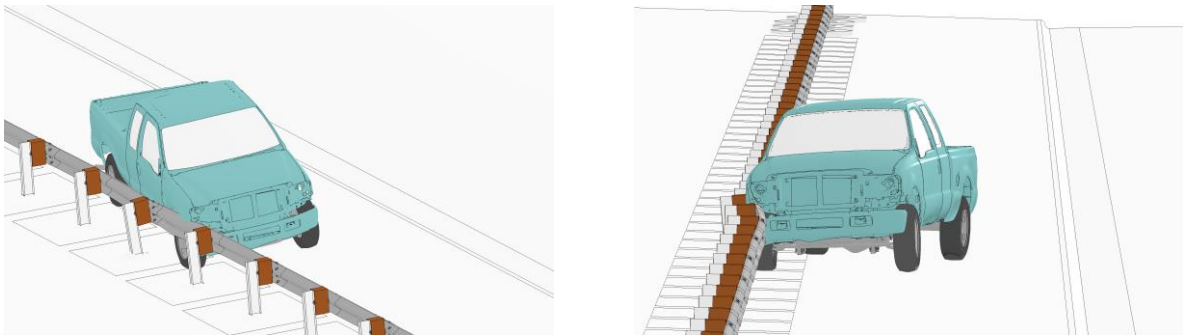
b. At 44 mph (70 km/hour) and 15°

Fig. 4.70: Permanent deformation of the 31-inch guardrail at 12 feet from the curb face and impacted by a Ford F250.

Figure 4.71 shows the detailed views of vehicle-barrier interactions for the 25° and 15° impacts by the Ford F250. Figures 4.72 and 4.73 show the time histories of transverse displacements and velocities at the CG point of the vehicle in these two impacts. It can be seen that the transverse velocities were approximately 4 mph towards the travel lane in both cases. The small transverse velocities, along with the relative small exit angles and satisfaction to the exit box criterion, confirmed the safe redirection of the Ford F250 in both cases.



a. At 44 mph (70 km/hour) and 25°



b. At 44 mph (70 km/hour) and 15°

Fig. 4.71: Simulations of Ford F250 impacting the 31-inch guardrail at 12 feet from the curb face.

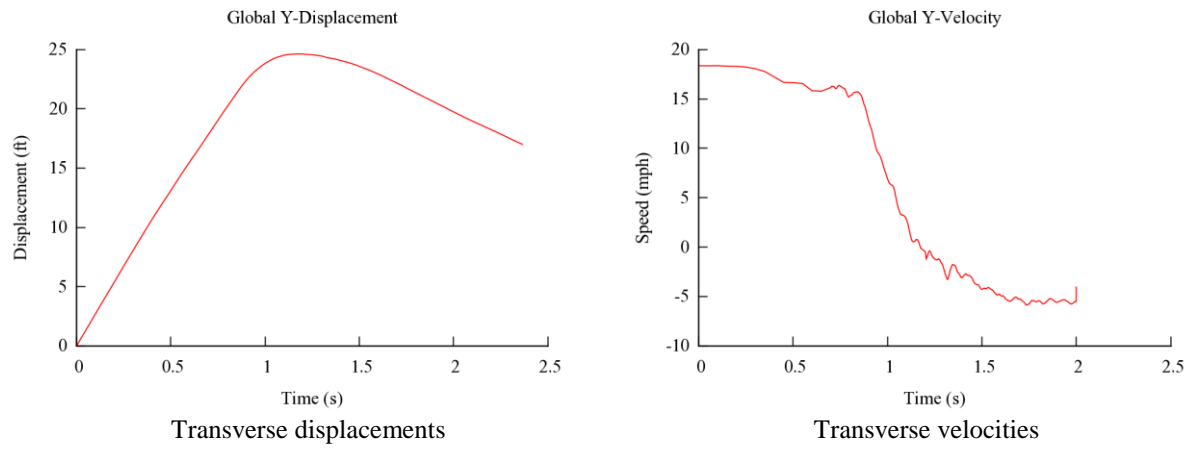


Fig. 4.72: Transverse displacements and velocities of the Ford F250 impacting the 31-inch guardrail at 12 feet from the curb face at 44 mph (70 km/hour) and 25°.

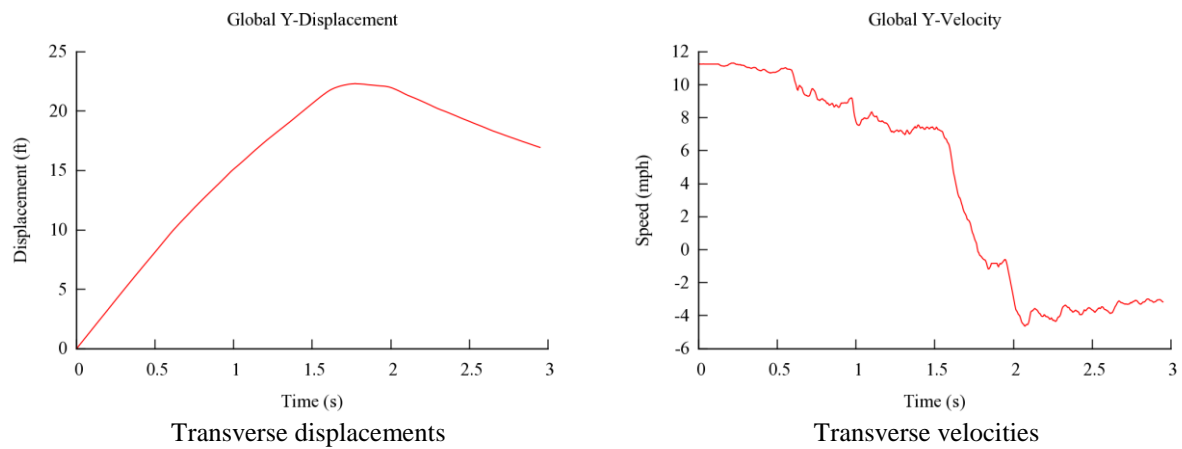


Fig. 4.73: Transverse displacements and velocities of the Ford F250 impacting the 31-inch guardrail at 12 feet from the curb face at 44 mph (70 km/hour) and 15°.

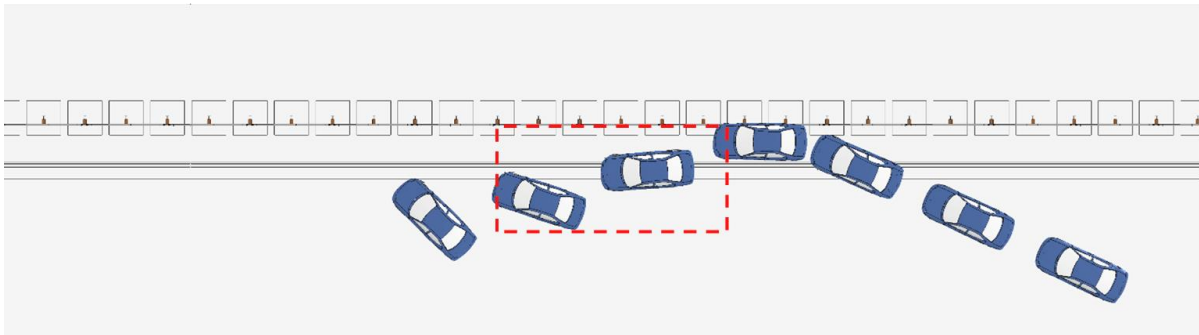
4.3 Case 3: Guardrails Placed at 6-ft from the Curb Face

In Case 3, only the 29-inch guardrail was evaluated when placed at 6 feet from the curb face and impacted by the Dodge Neon and Ford F250 at 25° and 15°. The results of the four simulations are summarized in Table 4.5.

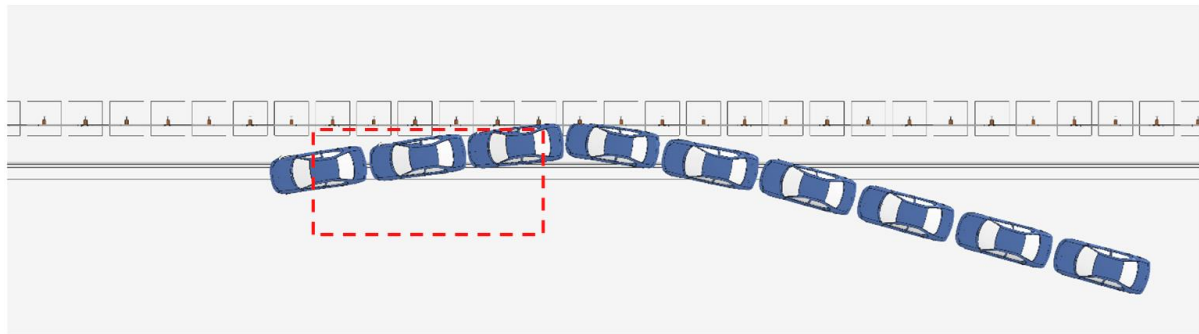
Table 4.5: Simulation results of Case 3 (guardrails placed at 6 feet from the curb face)

Guardrail Height	Test Vehicle	Impact Angle	Simulation Results
29 inch	Dodge Neon	25°	The vehicle failed the exit box criterion with a large spin
		15°	The vehicle passed the exit box criterion and was safely redirected
	Ford F250	25°	The vehicle overrode the guardrail
		15°	The vehicle passed the exit box criterion and was safely redirected

In this case, the impacting vehicle started from the edge of travel lane, went over the curb, and hit the 29-inch guardrail at 6 feet behind the curb. Figure 4.74 shows the vehicle trajectory of the Dodge Neon impacting the guardrail at 25° and 15° along with the exit boxes. It can be seen that the vehicle was contained in the exit box and safely redirected in the 15° impact, but failed to stay within the exit box in the case of the 25° impact.



a. At 44 mph (70 km/hour) and 25°



b. At 44 mph (70 km/hour) and 15°

Fig. 4.74: A Dodge Neon impacting the 29-inch guardrail at 6 feet from the curb face.

It can be seen from Fig. 4.74 that the Dodge Neon was initially redirected in the 25° impact, but started to spin when running down the curb. The yaw, pitch, and roll angles of the Dodge Neon in both the 25° and 15° impacts are shown in Fig. 4.75. The exit angles of these two impacts were determined to be 18° and 6°, respectively, by subtracting the impact angles from the respective yaw angles at exit (i.e., 43° and 21°). The MASH exit box criterion was not met in the 25° impact due to the vehicle spinning, which can be seen from the continuously increasing yaw angle. The roll and pitch angles of the 25° impact were higher than all the other impact cases by the Dodge Neon but still within ten degrees in either positive or negative direction and thus passed the MASH evaluation criterion F, which specified a maximum 75° roll or pitch angle. The MASH exit box criterion and the evaluation criterion F were both met in the 15° impact by the Dodge Neon.

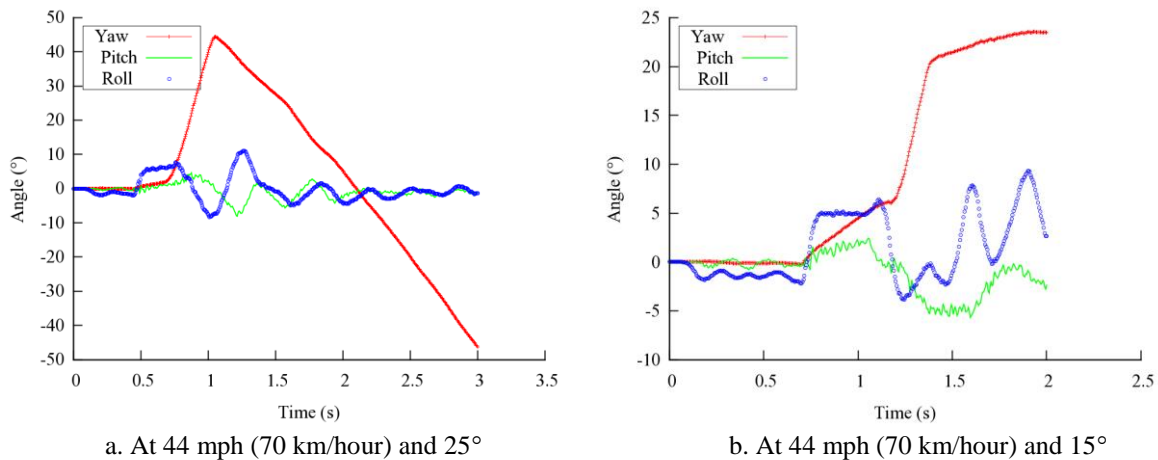


Fig. 4.75: Yaw, pitch, and roll angles of Dodge Neon impacting 29-inch guardrail at 6 feet from the curb face.

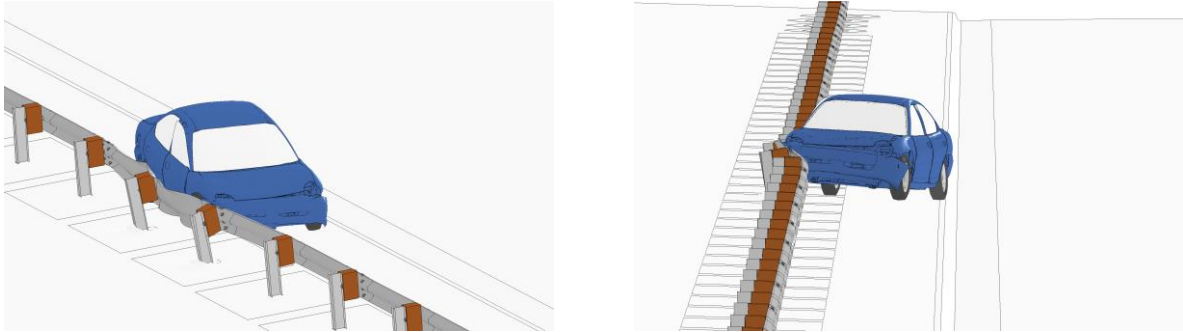
The permanent deformations of the 29-inch guardrail at 6 feet from the curb face were relatively small and localized under impacts of the Dodge Neon, as seen in Figure 4.76.



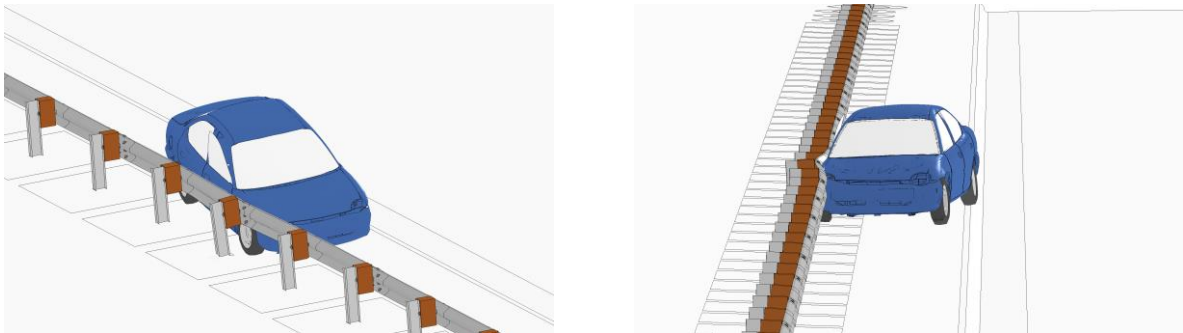
Fig. 4.76: Permanent deformation of the 29-inch guardrail at 6 feet from the curb face and impacted by a Dodge Neon.

Figure 4.77 shows the detailed views of vehicle-barrier interactions for the 25° and 15° impacts by the Dodge Neon. Figures 4.78 and 4.79 show the time histories of transverse displacements and velocities at the CG point of the vehicle in these two impacts. For the 25° impact, the transverse velocity was approximately zero, indicating that the vehicle would not move further towards the travel lane despite its spin. For the 15° impact, the transverse

velocity was approximately 5 mph towards the travel lane. Given the small exit angle, satisfaction to the MASH exit box criterion, and the small transverse velocity in the 15° impact, the Dodge Neon was unlikely to get involved in a secondary collision.



a. At 44 mph (70 km/hour) and 25°



b. At 44 mph (70 km/hour) and 15°

Fig. 4.77: Simulations of Dodge Neon impacting the 29-inch guardrail at 6 feet from the curb face.

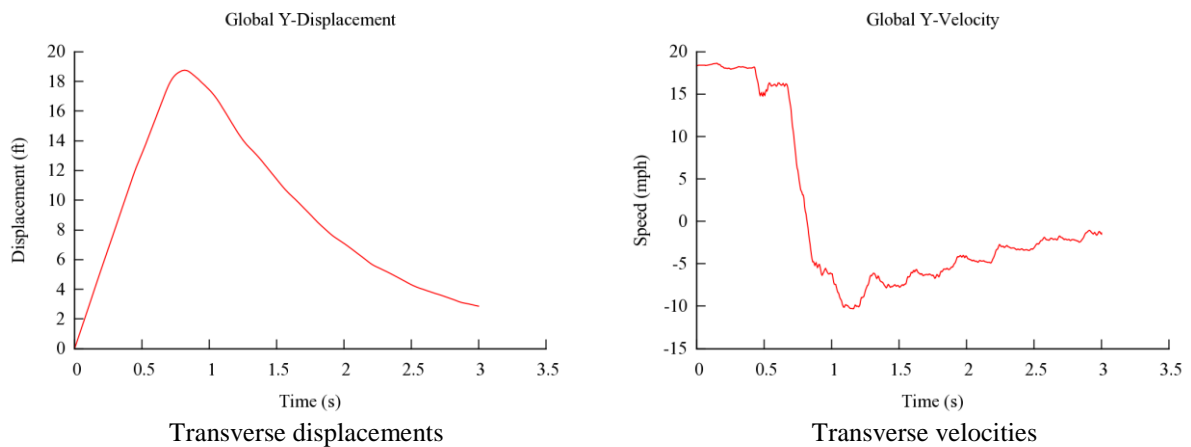


Fig. 4.78: Transverse displacements and velocities of the Dodge Neon impacting the 29-inch guardrail at 6 feet from the curb face at 44 mph (70 km/hour) and 25°.

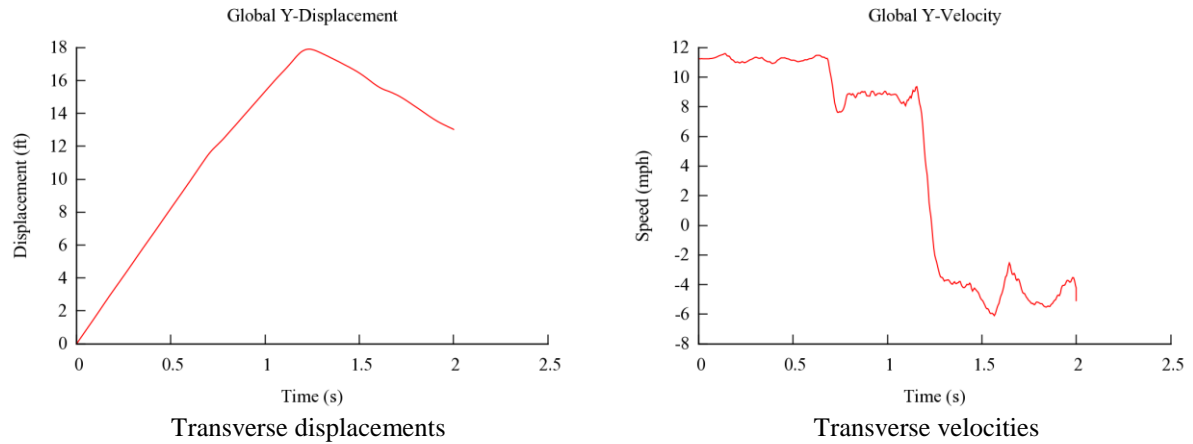
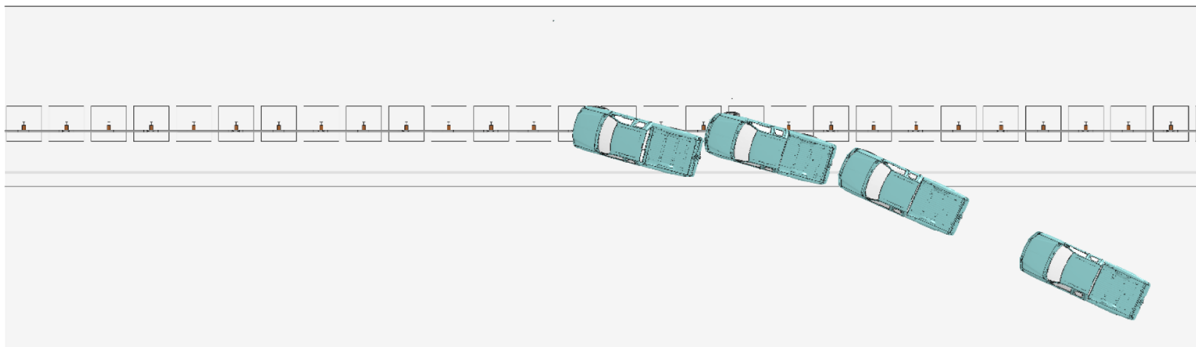
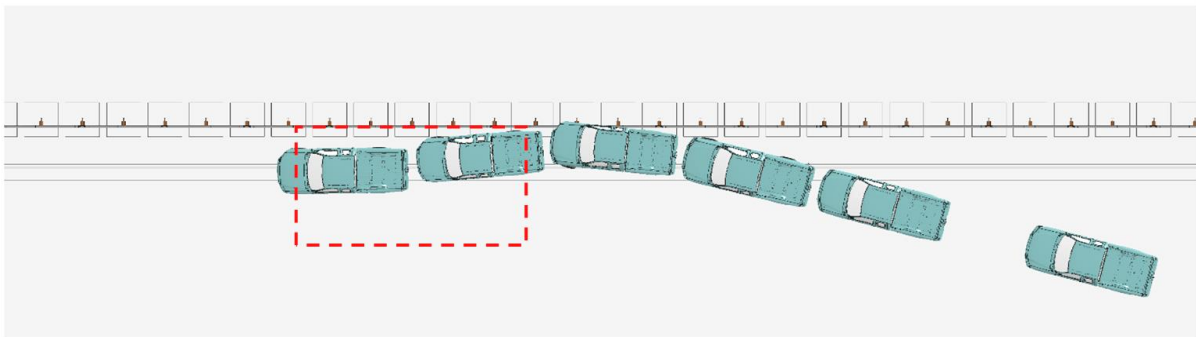


Fig. 4.79: Transverse displacements and velocities of the Dodge Neon impacting the 29-inch guardrail at 6 feet from the curb face at 44 mph (70 km/hour) and 15°.

Figure 4.80 shows the top view of vehicle trajectory of the Ford F250 impacting at 25° and 15° on the 29-inch guardrail at 6 feet from the curb face. The yaw, pitch, and roll angles of both cases are shown in Fig. 4.81.



a. At 44 mph (70 km/hour) and 25°



b. At 44 mph (70 km/hour) and 15°

Fig. 4.80: A Ford F250 impacting the 29-inch guardrail at 12 feet from the curb face.

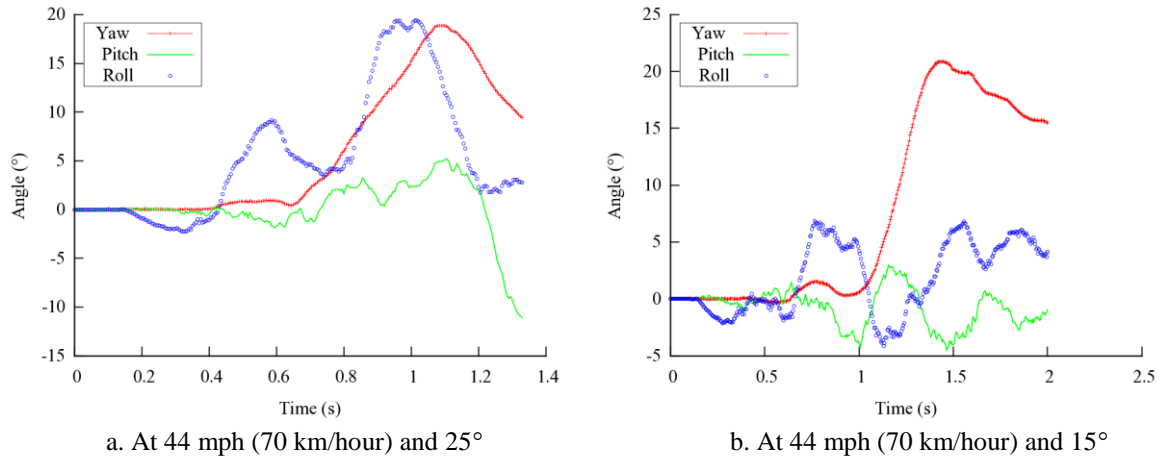


Fig. 4.81: Yaw, pitch, and roll angles of Ford F250 impacting 29-inch guardrail at 6 feet from the curb face.

In the 25° impact by the Ford F250, the 29-inch guardrail at 6 feet from the curb face failed to redirect the vehicle due to vaulting of the vehicle. After running up the curb, the Ford F250 vaulted and overrode the guardrail. Recall in the case of the 29-inch guardrail placed at 12 feet from the curb face, the Ford F250 was safely redirected in the 25° impact. This indicates that the Ford F250 has not fully landed before impacting the 29-inch guardrail at 6 feet from the curb face and thus overrides the guardrail.

In the 15° impact, the MASH exit box criterion was satisfied. The exit angle was determined to be 7° by subtracting the impact angle from the yaw angle at exit (22°). For this case, the last measure of yaw angle was approximately 17°, indicating a 2° angle between the Ford F250 and the guardrail. The roll and pitch angles of the Ford F250 in the 15° impact was less than 7.5 degrees in either positive or negative direction and thus passed the MASH evaluation criterion F, which specified a maximum 75° roll or pitch angle.

The deflections of the 29-inch guardrail under impacts by the Ford F250 were small in both the 25° and 15° impacts, as shown in Fig. 4.82. However, the permanent deformation of the guardrail in the 25° impact was large due to vehicle overriding.

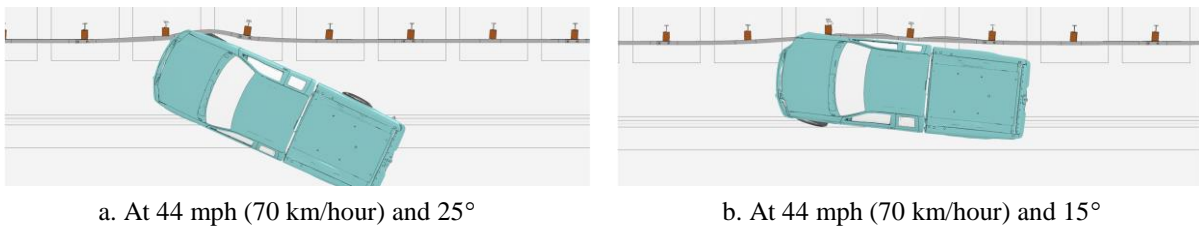
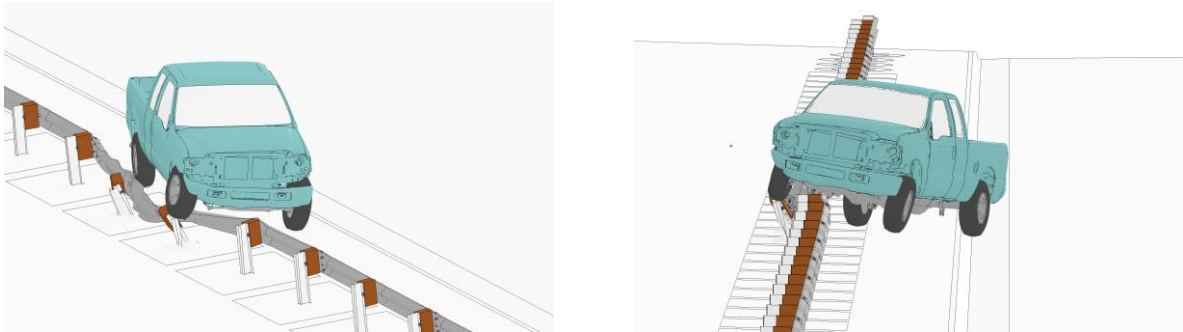


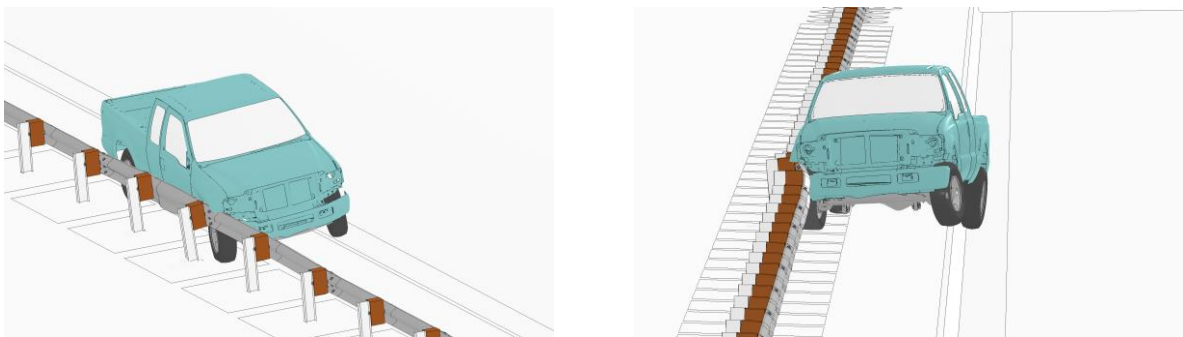
Fig. 4.82: Permanent deformation of the 29-inch guardrail at 6 feet from the curb face and impacted by a Ford F250.

Figure 4.83 shows the detailed views of vehicle-barrier interactions for the 25° and 15° impacts by the Ford F250. Figures 4.84 and 4.85 show the time histories of transverse displacements and velocities at the CG point of the vehicle. For the 25° impact, the

transverse velocity was approximately zero, indicating that the vehicle would remain on top of the guardrail. For the 15° impact, the transverse velocity was approximately 2 mph towards the travel lane. The results in Figs. 4.80 to 4.85 indicated that the Ford F250 was safely redirected in the 15° impact and was unlikely to get involved in a secondary collision.



a. At 44 mph (70 km/hour) and 25°



b. At 44 mph (70 km/hour) and 15°

Fig. 4.83: Simulations of Ford F250 impacting the 29-inch guardrail at 6 feet from the curb face.

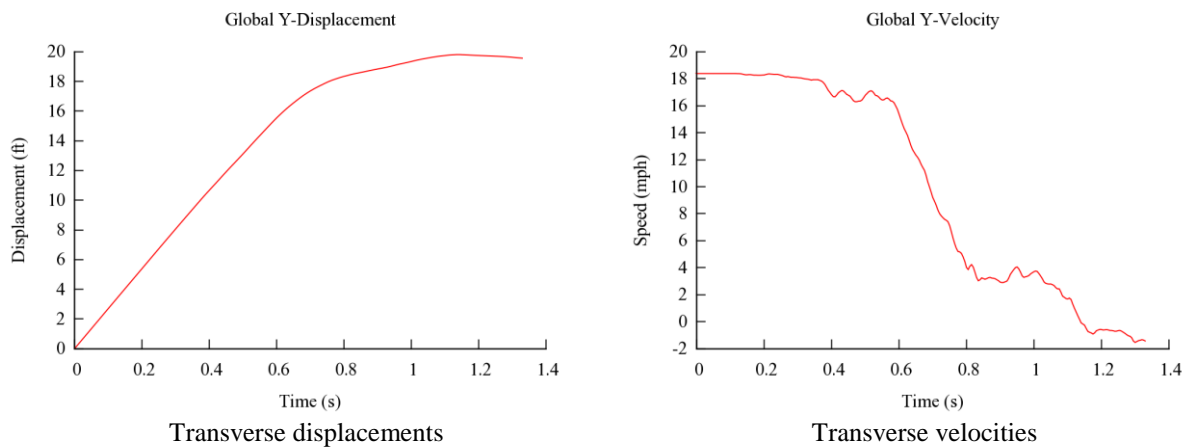


Fig. 4.84: Transverse displacements and velocities of the Ford F250 impacting the 29-inch guardrail at 6 feet from the curb face at 44 mph (70 km/hour) and 25°.

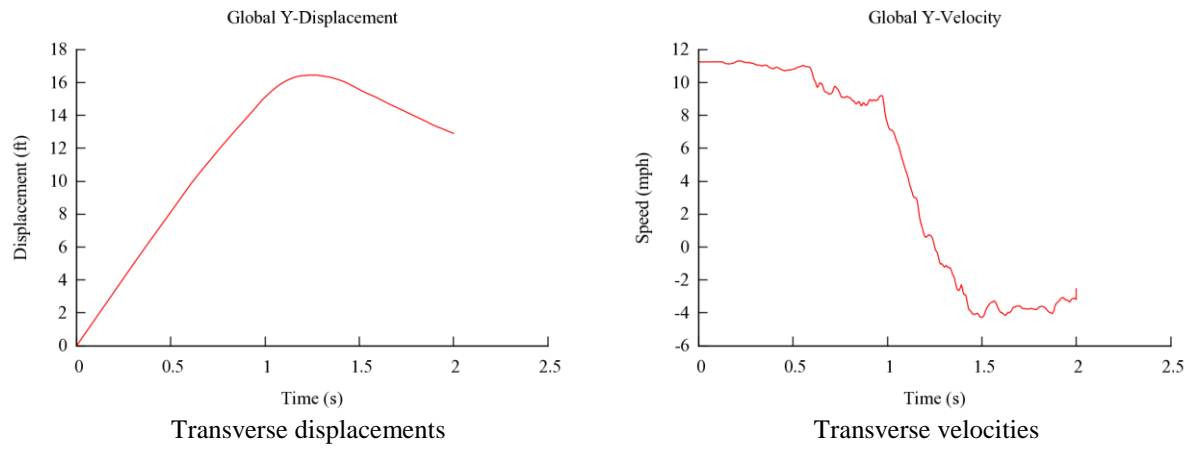
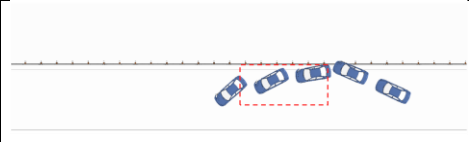
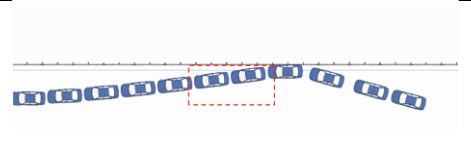
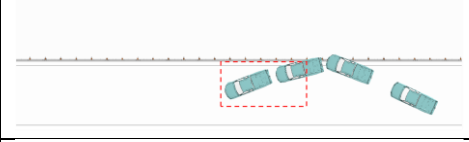
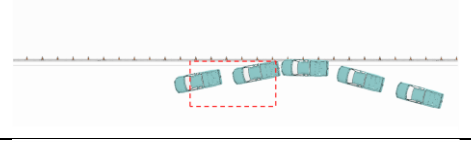
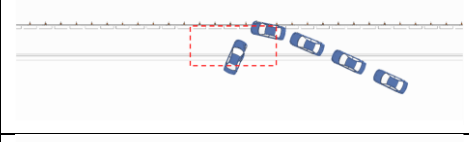
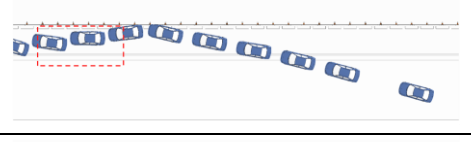
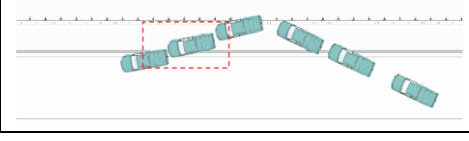
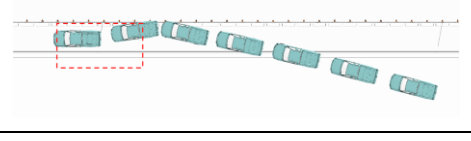


Fig. 4.85: Transverse displacements and velocities of the Ford F250 impacting the 29-inch guardrail at 6 feet from the curb face at 44 mph (70 km/hour) and 15°.

4.4 Comparison of Guardrail Performance at Different Locations

In Sections 4.1 to 4.3, the performance of guardrails at 27-, 29-, and 31-inch placement heights were evaluated and compared when installed at the same locations behind the curb. In this section, the performance of each guardrail is compared when placed at different locations. Tables 4.6, 4.7, and 4.8 give a summary of the vehicle redirection characteristics of the 27-, 29-, and 31-inch guardrails, respectively.

Table 4.6: Vehicle redirection characteristics of the 27-inch guardrail




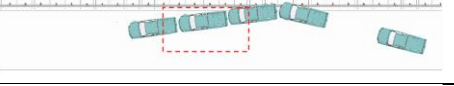




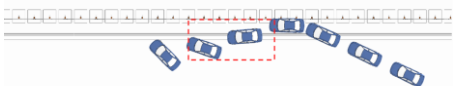


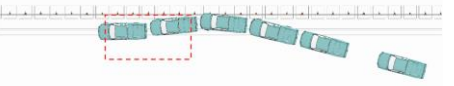
Guardrail Location	Test Vehicle	Impact Angle	
		25°	15°
At the curb face	Dodge Neon		
	Ford F250		
At 12 feet from the curb face	Dodge Neon		
	Ford F250		

The 27-inch guardrail was evaluated at two locations: at the curb face and at 12 feet from the curb face. Under the 15° impacts by both the Dodge Neon and Ford F250, the 27-inch guardrail at both locations met the MASH exit box criterion and safely redirected the vehicles. It was also observed that the 27-inch guardrail redirected both vehicles with smaller exit angles at 12 feet from the curb face than at the curb face. In all of the four 15° impacts, the vehicles were safely redirected.

In the 25° impacts, the 27-inch guardrail satisfied the MASH exit box criterion when placed at the curb face and impacted by both the Dodge Neon and Ford F250, though the Dodge Neon experienced a large spin after leaving the exit box. When placed at 12 feet from the curb face, the 27-inch guardrail satisfied the MASH exit box criterion when impacted by the Ford F250, but failed when impacted by the Dodge Neon due to a large vehicle spin.

Considering the vehicles' exit angle, distance from the travel lane after being redirected, and post-impact vehicular spin, the 27-inch guardrail is considered to perform better at 12 feet from the curb face than at the curb face.

Table 4.7: Vehicle redirection characteristics of the 29-inch guardrail









Guardrail Location	Test Vehicle	Impact Angle	
		25°	15°
At the curb face	Dodge Neon		
	Ford F250		
At 12 feet from the curb face	Dodge Neon		
	Ford F250		
At 6 feet from the curb face	Dodge Neon		
	Ford F250		

The 29-inch guardrail was evaluated at three locations: at the curb face, at 12 feet from the curb face, and at 6 feet from the curb face. Under the 15° impacts by both vehicles, the 29-inch guardrail met the MASH exit box criterion and was able to safely redirect the vehicles at all three locations. Among the three locations, the 29-inch guardrail at 12 feet from the curb face had the best vehicle redirection characteristics and the largest distance from the travel lane after redirection, followed by the location at 6 feet from the curb face.

In the 25° impacts, the 29-inch guardrail at 12 feet from the curb face satisfied the MASH exit box criterion when impacted by both vehicles. At 6 feet from the curb face, the 29-inch guardrail failed the MASH exit box criterion for both vehicles: the Dodge Neon was first redirected followed by a large spin, and the Ford F250 overrode the guardrail due to vaulting. When placed at the curb face, the 29-inch guardrail met the MASH exit box criterion for the Ford F250 impact but caused the Dodge Neon to snag on the guardrail.

Considering the vehicles' exit angle, distance from the travel lane after being redirected, and post-impact vehicular spin, the 29-inch guardrail is considered to perform the best at 12 feet from the curb face than at the curb face and at 6 feet from the curb face.

Table 4.8: Vehicle redirection characteristics of the 31-inch guardrail

Guardrail Location	Test Vehicle	Impact Angle	
		25°	15°
At the curb face	Dodge Neon		
	Ford F250		
At 12 feet from the curb face	Dodge Neon		
	Ford F250		

The 31-inch guardrail was evaluated at two locations: at the curb face and at 12 feet from the curb face. It can be seen that the 31-inch guardrail at both locations met the MASH exit box criterion in the 15° impacts by both the Dodge Neon and Ford F250. The 31-inch guardrail was able to redirect both vehicles with smaller exit angles when placed at 12 feet from the curb face than at the curb face. In all of the four 15° impacts, the vehicles were safely redirected.

In the 25° impacts, the 31-inch guardrail satisfied the MASH exit box criterion when placed at 12 feet from the curb face for both vehicles, though it barely met the criterion under impact of the Ford F250. When placed at the curb face, the 31-inch guardrail caused both vehicles to snag on the guardrail.

Considering the vehicles' exit angle, distance from the travel lane after being redirected, and post-impact vehicular spin, the 31-inch guardrail is considered to perform better at 12 feet from the curb face than at the curb face.

5. Findings and Conclusions

In this project, finite element simulations were performed to study the performance of W-beam guardrails at placement heights of 27, 29 and 31 inches when placed at the face of or behind the curb. The impact simulations were performed using a 1996 Dodge Neon passenger car and a 2006 Ford F250 pickup truck at an impact speed of 44 mph (70 km/hour) and at two impact angles, 25° and 15°, for all three guardrail placement heights. The simulation results provided insight into the vehicle redirection characteristics as well as guardrail performance in relation to guardrail heights and locations when placed at the face of or behind the curb. Some of the major research findings are summarized as follows.

- The 27-inch W-beam guardrail performed effectively under impacts of the passenger car and pickup truck at an impact speed of 44 mph (70 km/hour) and a 15° impact angle, both at the curb face and at 12 feet from the curb face.

In the 25° impacts by the Dodge Neon, the 27-inch guardrail at both locations caused temporary vehicle snagging followed by vehicle spins. In the 25° impact by the Ford F250, the 27-inch guardrail at both locations met the MASH exit-box criterion and the vehicle was redirected with no spins.

In all of the cases in which the vehicles were redirected, it was also observed that the 27-inch guardrail redirected both vehicles with smaller exit angles at 12 feet from the curb face than at the curb face. Considering the vehicles' exit angle, distance from the travel lane after being redirected, and post-impact vehicular spin, the 27-inch guardrail was considered to perform better at 12 feet from the curb face than at the curb face.

- The 29-inch W-beam guardrail was evaluated at three locations: at the curb face, at 12 feet from the curb face, and at 6 feet from the curb face. The 29-inch guardrail met the MASH exit box criterion and safely redirected the vehicles at all three locations under impacts of the passenger car and pickup truck at an impact speed of 44 mph (70 km/hour) and a 15° impact angle. Among all the 15° impacts, the 29-inch guardrail performed the best 12 feet from the curb face, followed by 6 feet from the curb face, and at the curb face.

The 29-inch guardrail at 12 feet from the curb face also satisfied the MASH exit box criterion when impacted by both vehicles at 25°. At 6 feet from the curb face, the 29-inch guardrail failed the MASH exit box criterion for both vehicles: the Dodge Neon was first redirected followed by a large spin, and the Ford F250 overrode the guardrail due to vaulting. When placed at the curb face, the 29-inch guardrail met the MASH exit box criterion for the Ford F250 impact but caused the Dodge Neon to snag on the guardrail.

Considering the vehicles' exit angle, distance from the travel lane after being redirected, and post-impact vehicular spin, the 29-inch guardrail is considered to perform the best at 12 feet from the curb face than at the curb face and at 6 feet from the curb face.

- The 31-inch guardrail, both at 12 feet from the curb face and at the curb face, met the MASH exit box criterion in the 15° impacts by both the Dodge Neon and Ford F250. The 31-inch guardrail was able to redirect both vehicles in the 15° impacts, with the exit angles smaller for guardrail at 12 feet from the curb face than at the curb face.

In the 25° impacts, the 31-inch guardrail satisfied the MASH exit box criterion when placed at 12 feet from the curb face for both vehicles, though it barely met the criterion under the impact of the Ford F250. When placed at the curb face, the 31-inch guardrail caused both vehicles to snag on the guardrail in the 25° impact.

Considering the vehicles' exit angle, distance from the travel lane after being redirected, and post-impact vehicular spin, the 31-inch guardrail is considered to perform better at 12 feet from the curb face than at the curb face.

- It was observed that the transverse guardrail deflections were relatively small and localized in all the impacts. However, the guardrail deflections were generally much larger in the 25° impact than those in the 15° impact for the same vehicle. Under impacts of the same vehicle at the same angle, there was no noticeable difference in guardrail deflections among all guardrail heights (i.e., 27, 29, and 31 inches).
- The MASH evaluation criterion F, which specified a maximum roll or pitch angle of 75°, was satisfied in all of the simulations. All three W-beam guardrail placement heights did not cause vehicle rollovers at all locations behind the curb.

The simulation results suggested that the W-beam guardrails at 29- and 31-inch placement heights and at 12 feet from the curb face could safely redirect the Dodge Neon and Ford F250 impacting the guardrail at 25° and 15°. At this location, the 29-inch guardrail resulted in slightly better vehicle redirection characteristics than the 31-inch guardrail under the same impact conditions.

The 27-inch guardrail satisfied the MASH exit box criterion under the 15° impacts by the Dodge Neon and Ford F250 at both locations (i.e., at 12 feet from the curb face and at the curb face). The vehicles were safely redirected with very small exit angles in the 15° impacts. In the 25° impacts, the 27-inch guardrail placed at both locations could safely redirect the Ford F250, with a smaller exit angle at 12 feet from curb face than at the curb face. Under impacts of the Dodge Neon at 25°, the 27-inch guardrail at both locations caused vehicle snagging followed by spinning.

It should be noted that the simulation results of this project can be used to interpret the performance trends of W-beam guardrails. They should not be used to draw definitive conclusions about their performance for a specific crash event because some factors that could affect the performance were not considered in the simulations for this project. These factors included, but were not limited to, impact locations along the longitudinal axes of the barriers, soil conditions, and driver behaviors. Nevertheless, finite element analysis was demonstrated to be a useful tool in crash analysis and could be used in future investigations of other research issues.

6. Recommendations

Based on the simulation results of this project, it was determined that the 29- and 31-inch W-beam guardrails met the MASH TL-2 requirements when placed at 12 feet from the curb face. The 27-inch guardrails at the curb face and at 12 feet from the curb face are effective under vehicular impacts at a small angle (i.e., 15°), but may cause small vehicles (e.g., Dodge Neon) to snag and spin under impacts at a large angle (i.e., 25°). The placement of 29- and 31-inch guardrails at 12 feet from the face of curb should be considered for new installations and/or resurfacing projects where practicable.

7. Implementation and Technology Transfer Plan

The simulation results of this project will be submitted to NCDOT for consideration in future projects to install or retrofit W-beam guardrails when allowed by site conditions and deemed necessary by NCDOT personnel. Detailed simulation results will be provided to NCDOT engineers for a comprehensive understanding in evaluating proposed roadside features and/or improving the safety performance of the current system. The modeling and simulation work, along with research findings, will be presented at technical conferences and submitted for publication in technical journals to help researchers and DOT engineers nationwide with similar needs. The research results of this project will be distributed to the public through this report, which will be made available by NCDOT.

References

1. AASHTO (2011). *Roadside Design Guide*, 4th edition, American Association of State Highway and Transportation Officials, Washington, D.C.
2. Atahan, A.O. (2002). "Finite element simulation of a strong-post W-beam guardrail system." *Simulation*, 78(10), 587-599.
3. Atahan, A.O. (2003). "Impact behaviour of G2 steel weak-post W-beam guardrail on nonlevel terrain." *International Journal of Heavy Vehicle Systems*, 10(3), 209-223.
4. Atahan, A.O. (2007). "Crashworthiness analysis of a bridge rail-to-guardrail transition." *Accident Analysis and Prevention*, in press.
5. Atahan, A.O., Cansiz, O.F. (2005). "Crashworthiness analysis of a bridge rail-to-guardrail transition." *Finite Elements in Analysis and Design*, 41, 371-396.
6. Bligh, R., Miaou, S.P., Lord, D., Cooner, S. (2006). "Median barrier guidelines for Texas." *Report 0-4254-1*, Texas Transportation Institute, College Station, TX.
7. Bligh, R.P., Abu-Odeh, A.Y., Hamilton, M.E., Seckinger, N.R. (2004). "Evaluation of roadside safety devices using finite element analysis." *Report 0-1816-1*, Texas Transportation Institute, College Station, TX.
8. Bligh, R.P., Mak, K.K. (1999). "Crashworthiness of roadside features across vehicle platforms." *Transportation Research Record*, 1690, 68-77.
9. BMI-SG (2004). "Improved guidelines for median safety." *NCHRP 17-14(2) Draft Report of Analysis Findings*, Transportation Research Board, National Research Council, Vienne, VA..
10. Donnell, E.T., Harwood, D.W., Bauer, K.M., Mason, J.M., Pietrucha, M.T. (2002). "Cross-median collisions on Pennsylvania interstates and expressways." *Transportation Research Record*, 1784, 91-99.
11. Dunlap, D.F. (1973). "Barrier-Curb Redirection Effectiveness," *Highway Research Record 340*, HRB, National Research Council, Washington, DC.
12. Fang, H., Li, N., Tian, N., (2010). "Median barrier placement on six-lane, 46-foot median divided freeways." *Final Report NCDOT 2009-04*, North Carolina Department of Transportation, Raleigh, NC.
13. Ferdous, M.R., Abu-Odeh, A., Bligh, R.P., Jones, H.L., Sheikh, N.M. (2011). "Performance limit analysis for common roadside and median barriers using LS-DYNA." *International Journal of Crashworthiness*, 16(6), 691-706.
14. Findley, D.J., Cunningham, C.M., Schroeder, B.J., Vaughan, C.L., Fowler, T.J. (2012). "Structural and safety investigation of statewide performance of weathered steel beam guardrail in North Carolina" *Transportation Research Record: Journal of the Transportation Research Board*, 2309, 63-72.
15. Gabler, H.C., Gabauer, D.J. (2006). "Safety audit of fatalities and injuries involving guide rail." *Final Report FHWA-NJ-2007-001*, Virginia Tech, Blacksburg, VA.
16. Gabler, H.C., Gabauer, D.J., Bowen, D. (2005). "Evaluation of cross median crashes." *Final Report FHWA-NJ-2005-004*, Rowan University, Glassboro, NJ.
17. Gowat, R.C., Gabauera, D.J. (2013). "Secondary Collisions Revisited: Real-World Crash Data and Relationship to Crash Test Criteria." *Traffic Injury Prevention*, 14(1), 46-55.

18. Hampton, C., Gabler, H. (2013). "Development of a missing post repair guideline for longitudinal barrier crash safety." *Journal of Transportation Engineering*, 139(6), 549–555.
19. Hampton, C.E., Gabauer, D.J., Gabler, H.C. (2010) "Limits of acceptable rail-and-post deflection in crash-damaged strong-post W-beam guardrail" *Transportation Research Record: Journal of the Transportation Research Board*, 2195, 95-105.
20. Hiser, N.R., Reid, J.D. (2005). "Modeling slip base mechanisms." *International Journal of Crashworthiness*, 10(5), 463-472.
21. Hiss Jr, J.G.F., Bryden, J.E. (1992). "Traffic barrier performance." *Report 155*, New York State Department of Transportation, Albany, NY.
22. Hu, W., Donnell, E.T. (2010) "Median barrier crash severity: some new insights" *Accident Analysis & Prevention*, 42(6), 1697-1704.
23. Kan, C.D., Marzougui, D., Bahouth, G.T., Bedewi, N.E. (2001). "Crashworthiness evaluation using integrated vehicle and occupant finite element models." *International Journal of Crashworthiness*, 6, 387-398.
24. Lewis, B.A. (2004). "Manual for LS-DYNA soil material model 147." *FHWA-HRT-04-095*, U.S. Department of Transportation, Federal Highway Administration, McLean, VA.
25. LSTC (2007). "LS-DYNA keyword user's manual - version 971." Livermore Software Technology Corporation (LSTC), Livermore, CA.
26. Lynch, J.M., Crowe, N.C., Rosendahl, J.F. (1993). "Interstate across median accident study: a comprehensive study of traffic accidents involving errant vehicles which cross the median divider strips on North Carolina interstate highways." *1993 AASHTO Annual Meeting Proceedings*, Publisher American Association of State Highway and Transportation Officials, 125-133.
27. Mackerle, J. (2003). "Finite element crash simulations and impact-induced injuries: an addendum. A bibliography (1998–2002)." *The Shock and Vibration Digest*, 35(4), 273-280.
28. Mak, K.K., Bligh, R.P. (2002). "Assessment of NCHRP Report 350 test conditions." *Transportation Research Record* 1797, 38-43.
29. Mak, K.K., Sicking, D.L. (2003). "NCHRP Report 492 roadside safety analysis program (RSAP) – engineer's manual." *Transportation Research Board*, 7-28.
30. Marzougui, D., Bahouth, G., Eskandarian, A., Meczkowski, L., Taylor, H. (2000). "Evaluation of portable concrete barriers using finite element simulation." *Transportation Research Record*, 1720, 1-6.
31. Marzougui, D., Mahadevaiah, U., Kan, C.D., Opiela, K. (2009). "Analyzing the effects of cable barriers behind curbs using computer simulation." *NCAC 2009-W-008*, The National Crash Analysis Center, George Washington University.
32. Marzougui, D., Mohan, P., Kan, C.D., Opiela, K.S. (2007). "Evaluation of rail height effects on the safety performance of W-beam barriers." *2007 TRB Annual Meeting*, Washington, D.C.
33. Marzougui, D., Mohan, P., Kan, C.D., Opiela, K.S. (2012). "Assessing options for improving barrier crashworthiness using finite element models and crash simulations." *Final Report NCAC-2012-W-008*, National Crash Analysis Center, George Washington University, Washington, D.C.

34. Marzougui, D., Zink, M., Zaouk, A.K., Kan, C.D., Bedewi, N.E. (2004). "Development and validation of a vehicle suspension finite element model for use in crash simulations." *International Journal of Crashworthiness*, 9(6), 565-576.
35. MASH (2009). "Manual for assessing safety hardware (MASH)." American Association of State Highway and Transportation Officials (AASHTO), Washington, D.C.
36. Miaou, S.P., Bligh, R.P., Lord, D. (2005). "Developing guidelines for median barrier installation: benefit-cost analysis with Texas data." *Transportation Research Record*, 1904, 3-19.
37. Mohan, P., Marzougui, D., Kan, C.D. (2007). "Validation of a single unit truck model for roadside hardware impact." *International Journal of Vehicle Systems Modelling and Testing*, 2(1), 1-15.
38. Murray, Y.D. (2007). "User manual for LS-DYNA concrete material model 159." *FHWA-HRT-05-062*, U.S. Department of Transportation, Federal Highway Administration, McLean, VA.
39. Murray, Y.D., Reid, J.D., Faller, R.K., Bielenberg, B.W., Paulsen, T.J. (2005). "Evaluation of LS-DYNA wood material model 143." *FHWA-HRT-04-096*, U.S. Department of Transportation, Federal Highway Administration, McLean, VA.
40. NCAC (web1). "NCAC finite element models." <<http://www.ncac.gwu.edu/vml/models.html>>.
41. NCAC (web2). "NCAC publications." <<http://www.ncac.gwu.edu/filmlibrary/publications.html>>.
42. NCHRP 22-21 (2011). "Project 22-21: median cross-section design for rural divided highways." <<http://apps.trb.org/cmsfeed/TRBNetProjectDisplay.asp?ProjectID=694>>.
43. NCHRP 22-22 (2010). "Project 22-22: placement of traffic barriers on roadside and median slopes." <<http://apps.trb.org/cmsfeed/TRBNetProjectDisplay.asp?ProjectID=695>>.
44. NCHRP 22-27 (2012). "Project 22-27: roadside safety analysis program (RSAP) update." <<http://apps.trb.org/cmsfeed/TRBNetProjectDisplay.asp?ProjectID=2517>>.
45. Nicol, D. A. (2010) "Roadside design: steel strong post W-beam guardrail." *Memorandum 051710*, U.S. Department of Transportation, Federal Highway Administration, McLean, VA.
46. Ochoa, C.M., Ochoa, T.A. (2011) "Guardrail optimization for rural roads." *Transportation Research Board of the National Academies*, 2203, 71-78.
47. Ohio DOT (2013). "Guidelines for the Installation and Maintenance of Roadside Safety Hardware." Roadside Safety Field Guide, Federal Highway Administration, U.S. Department of Transportation.
48. Olson, R.M., Weaver, G.D., Ross Jr., H.E., Post, E.R. (1974). "Effect of Curb Geometry and Location on Vehicle Behavior." *NCHRP Report 150*, TRB, National Research Council, Washington, D.C.
49. Orengo, F., Ray, M.H., Plaxico, C.A. (2003). "Modeling tire blow-out in roadside hardware simulations using LS-DYNA." *IMECE2003-55057*, 2003 ASME International Mechanical Engineering Congress & Exposition, Washington, D.C.
50. Patzner, G.S., Plaxico, C.A., Ray, M.H. (1999). "Effects of post and soil strength on performance of modified eccentric loader breakaway cable terminal." *Transportation Research Record*, 1690, 78-83.
51. Plaxico, C.A. (2002). "Design guidelines for the use of curbs and curb/guardrail combinations along high-speed roadways." Dissertation, Civil and Environmental Engineering, Worcester Polytechnic Institute.

52. Plaxico, C.A., Hackett, R.M., Uddin, W. (1997). "Simulation of a vehicle impacting a modified thrie-beam guardrail." *Transportation Research Record*, 1599, 1-10.
53. Plaxico, C.A., Mozzarelli, F., Ray, M.H. (2003). "Tests and simulation of a w-beam rail-to-post connection." *International Journal of Crashworthiness*, 8(6), 543-551.
54. Plaxico, C.A., Patzner, G.S., Ray, M.H. (1998). "Finite element modeling of guardrail timber posts and the post-soil interaction." *Transportation Research Record*, 1647, 139-146.
55. Plaxico, C.A., Ray, M.H., Hiranmayee, K. (2000). "Impact performance of the G4(1W) and G4(2W) guardrail systems: comparison under NCHRP Report 350 test 3-11 conditions." *Transportation Research Record*, 1720, 7-18.
56. Plaxico, C.A., Ray, M.H., Weir, J.A., Orengo, F., Tiso, P., McGee, H., Council, F., Eccles, K. (2005). "Recommended Guidelines for Curb and Curb-Barrier Installations." *NCHRP Report 537*, Transportation Research Board, National Research Council, Washington, D.C.
57. Ray, M.H. (1996a). "Repeatability of full-scale crash tests and criteria for validating simulation results." *Transportation Research Record*, 1528, 155-160.
58. Ray, M.H. (1996b). "Use of finite element analysis in roadside hardware design." *Transportation Research Circular*, 453, 61-71.
59. Ray, M.H., McGinnis, R.G. (1997). "Guardrail and median barrier crashworthiness: synthesis of highway practice." Transportation Research Board, Washington, D.C.
60. Ray, M.H., Oldani, E., Plaxico, C.A. (2004). "Design and analysis of an aluminum F-shape bridge railing." *International Journal of Crashworthiness*, 9(4), 349-363.
61. Ray, M.H., Patzner, G.S. (1997). "Finite element model of modified eccentric loader terminal (MELT)." *Transportation Research Record*, 1599, 11-21.
62. Ray, M.H., Weir, J., Hopp, J. (2003). "In-service performance of traffic barriers." *NCHRP Report 490*, Transportation Research Board, National Research Council, Washington, D.C.
63. Ray, M.H., Weir, J.A. (2001). "Unreported collisions with post-and-beam guardrails in Connecticut, Iowa, and North Carolina." *Transportation Research Record*, 1743, 111-119.
64. Reid, J. D. (1998). "Admissible modeling errors or modeling simplifications?" *Finite Elements in Analysis and Design*, 29, 49-63.
65. Reid, J.D. (1996). "Towards the understanding of material property influence on automotive crash structures." *Thin-Walled Structures*, 24, 285-313.
66. Reid, J.D. (2004). "LS-DYNA simulation influence on roadside hardware." *Transportation Research Record*, 1890, 34-41.
67. Reid, J.D., Bielenberg, B.W. (1999). "Using LS-DYNA simulation to solve a design problem: bullnose guardrail example." *Transportation Research Record*, 1690, 95-102.
68. Reid, J.D., Coon, B.A., Lewis, B.A., Sutherland, S.H., Murray, Y.D. (2004). "Evaluation of LS-DYNA soil material model 147." *FHWA-HRT-04-094*, U.S. Department of Transportation, Federal Highway Administration, McLean, VA.
69. Reid, J.D., Hiser, N.R. (2004). "Friction modelling between solid elements." *International Journal of Crashworthiness*, 9(1), 65-72.
70. Reid, J.D., Hiser, N.R. (2005). "Detailed modeling of bolted joints with slippage." *Finite Elements in Analysis and Design*, 41, 547-562.

71. Reid, J.D., Kuipers, B.D., Sicking, D.L., Faller, R.K. (2009). "Impact performance of W-beam guardrail installed at various flare rates." *International Journal of Impact Engineering*, 36, 476-485.
72. Reid, J.D., Marzougui, D. (2002). "Improved truck model for roadside safety simulations: Part I - structural modeling." *Transportation Research Record*, 1797, 53-62.
73. Ross Jr, H.E., Sicking, D.L. (1984). "Guidelines for placement of longitudinal barriers on slopes." *Transportation Research Record*, 970, 3-9.
74. Ross Jr, H.E., Sicking, D.L., Zimmer, R.A., Michie, J.D. (1993). "Recommended procedures for the safety performance evaluation of highway features." *NCHRP Report 350*, Transportation Research Board, National Research Council, Washington, D.C.
75. Schrum, K.D., Lechtenberg, K.A., Bielenberg, R.W., Rosenbaugh, S.K., Faller, R.K., Reid, J.D., Sicking, D.L., (2013). "Safety performance evaluation of the non-blocked midwest guardrail system (MGS)." Midwest Roadside Safety Facility. TRP-03-262-12.
76. Thiele, J.C., Lechtenberg, K.A., Reid, J.D., Faller, R.K., Sicking, D.L., Bielenberg, R.W. (2009). "Performance limits for 6-in. (152-mm) high curbs placed in advance of the MGS using MASH vehicles Part II: Full-scale crash testing." *MwRSF Report TRP-03-221-09*, Midwest Roadside Safety Facility (MwRSF), Nebraska Transportation Center, Lincoln, Nebraska.
77. Thiele, J.C., Reid, J.D., Lechtenberg, K.A., Faller, R.K., Sicking, D.L., Bielenberg, R.W. (2010). "Performance limits for 6-in. (152-mm) high curbs placed in advance of the MGS using MASH vehicles Part III: Full-scale crash testing (TL-2)." *MwRSF Report TRP-03-237-10*, Midwest Roadside Safety Facility (MwRSF), Nebraska Transportation Center, Lincoln, Nebraska.
78. Tiso, P., Plaxico, C., Ray, M. (2002). "Improved truck model for roadside safety simulations: Part II - suspension modeling." *Transportation Research Record*, 1797, 63-71.
79. Whitworth, H.A., Bendidi, R., Marzougui, D., Reiss, R. (2004). "Finite element modeling of the crash performance of roadside barriers." *International Journal of Crashworthiness*, 9(1), 35-43.
80. Zaouk, A.K., Bedewi, N.E., Kan, C.D., Marzougui, D. (1997). "Development and evaluation of a C-1500 pickup truck model for roadside hardware impact simulation." *FHWA-RD-96-212*, Federal Highway Administration, Washington, D.C.
81. Zaouk, A.K., Marzougui, D., Bedewi, N.E. (2000a). "Development of a detailed vehicle finite element model, Part I: methodology." *International Journal of Crashworthiness*, 5(1), 25-36.
82. Zaouk, A.K., Marzougui, D., Kan, C.D. (2000b). "Development of a detailed vehicle finite element model, Part II: material characterization and component testing." *International Journal of Crashworthiness*, 5(1), 37-50.
83. Zhu, L., Reid, J.D., Faller, R.K., Sicking, D.L., Bielenberg, R.W., Lechtenberg, K.A., Benner, C.D. (2009). "Performance limits for 152-mm (6 in.) high curbs placed in advance of the MGS using MASH-08 vehicles Part I: Vehicle-curb testing and LS-DYNA analysis." *MwRSF Report TRP-03-205-09*, Midwest Roadside Safety Facility (MwRSF), Nebraska Transportation Center, Lincoln, Nebraska.
84. Zweden, J.V., Bryden, J.E. (1977). "In-service performance of highway barriers." *Report NYSDOT-ERD-77-RR51*, New York State Department of Transportation, Albany, NY.